ABSTRACT

DECRANE, STACY NICOLE. Quantification and Improvement of Endotoxin Removal in BTEC's Downstream Process for Green Fluorescent Protein Production. (Under the direction of Dr. Gary Gilleskie).

Endotoxin contamination is of major concern for any biopharmaceutical process, especially when the protein is produced in gram-negative bacteria, such as the commonly used *Escherichia coli* (*E. coli*). The outer membrane of a typical *E. coli* cell has approximately two million of these toxins, which cause immune reactions including fever if injected into the body. The biological effects of endotoxin have resulted in the United States Food and Drug Administration specifying limitations on the amount allowed in any injectable product. This topic is of interest to the Biomanufacturing Training and Education Center (BTEC) because *E. coli* is used in its process to express green fluorescent protein (GFP), which is used as a model biopharmaceutical in a number of courses. Several unit operations currently used to purify GFP such as chromatography and filtration are known to remove endotoxin. The purpose of this work was to determine the endotoxin concentration throughout the intermediate-scale downstream process at BTEC and to suggest possible process improvements to reduce endotoxin levels in the final product. The chromogenic kinetic *Limulus* Amebocyte Lysate assay was characterized and used for quantifying endotoxin. It was found that the first chromatography step in the process, which uses Q Sepharose Fast Flow anion exchange resin, was able to remove more than 99% of the endotoxin, which is not attributed to anticipated charge separation, but rather size exclusion of endotoxin aggregates from the beads, consequently limiting endotoxin binding to only the surface of the beads. Additionally, endotoxin removal in the lysate clarification process was improved 10-fold compared to the current process by removing the centrifugation step and decreasing the pore size of the filter membrane. Finally, the elution gradient for the polishing step with hydrophobic interaction chromatography was altered to increase resolution between the endotoxin and GFP peaks, further reducing endotoxin levels in the final product.

Quantification and Improvement of Endotoxin Removal in BTEC's Downstream Process for Green Fluorescent Protein Production

by
Stacy Nicole DeCrane

A thesis submitted to the Graduate Faculty of
North Carolina State University
in partial fulfillment of the
requirements for the degree of
Master of Science

Biomanufacturing

Raleigh, North Carolina

2015

APPROVED BY:

_____
Dr. Gary Gilleskie
Committee Chair

_____ _____
Dr. Nathaniel Hentz Dr. Baley Reeves

DEDICATION

This thesis is dedicated to my friends and family who supported me throughout graduate school.

BIOGRAPHY

Stacy DeCrane is from Bloomington, Illinois and received her Bachelor of Science in Chemical Engineering from Kettering University in Michigan. Her four-year co-op at Argonne National Laboratory inspired her love of research, and courses for her Biochemistry minor inspired her to apply her chemical engineering knowledge in a more biology-oriented field. Her engineering, research, and biochemistry interests melded into pursuing a career in biopharmaceutical process development, which began with attending North Carolina State University to obtain her Master of Science in Biomanufacturing. This thesis work as well as her internship at Novartis Vaccines secured her interest in downstream processes development, which she will pursue further in her full time position at KBI BioPharma starting in July 2015.

ACKNOWLEDGMENTS

First, a big thank you goes to my committee, Dr. Gary Gilleskie, Dr. Nathaniel Hentz, and Dr. Baley Reeves for their guidance and support over the last two years. Thank you to the analytical staff, Brian Mosley and Becky Kitchener, for their advice and training. Thanks to Eric Safarz and Nathan Blackwell, who kept me well-stocked with supplies and buffers. I want to thank all of the laboratory staff, especially Michele Ray, John Taylor, LaShonda Herndon, and Lauren Liles, who trained me on using the downstream equipment and provided me with all of the information I needed to run the processes.

Thanks to all of my friends, both within the program as well as outside of BTEC, who supported me throughout these stressful years. Finally, thank you to my family for their continued support.

TABLE OF CONTENTS

LIST OF TABLES

LIST OF FIGURES

CHAPTER 1: Introduction and Background

1.1. Introduction

Biopharmaceuticals are complex large molecule drugs that are produced in biological systems rather than by traditional chemical synthesis methods utilized by small molecule drug manufacturers. Many protein therapeutics on the market are recombinant, meaning that the gene coding for the protein is genetically engineered into a host cell, which over-expresses the protein of interest during upstream manufacturing. In downstream manufacturing, the product is then separated from impurities introduced by the host cell and the rest of the process as well as product variants in order to obtain a drug product that is safe and effective for patients. Because proteins are naturally degraded in the stomach and intestines, biopharmaceuticals are normally delivered as subcutaneous or intravenous injections rather than by oral administration. As the drug product typically has direct access to the bloodstream, the removal of harmful impurities such as DNA, virus, and host cell proteins (HCPs) is vital and consequently highly regulated. The United States Food and Drug Administration (FDA) is the regulatory body in the United States that ensures that drug products are safe and effective. While the FDA and the World Health Organization have guidance documents that offer certain industry standard recommendations for maximum impurity levels,[1–3] it is the responsibility of each manufacturer to prove the safety of the drug during preclinical and clinical trials.

With the exception of whole microorganisms or cells, endotoxin is the only impurity with a specification limit required by the United States Pharmacopeia (USP), making it a major concern in biopharmaceutical manufacturing processes. Endotoxin falls within a class of molecules called pyrogens, which are known to induce fever when injected into humans. More severe reactions such as shock, tissue injury, or even death could result if the patient is exposed to high amounts of endotoxin. It is typically measured in units of activity, in which one endotoxin unit (EU) typically equates to 120 pg of endotoxin.[4] Meeting the threshold of 5 EU/kg body weight/hour[5] has historically been a challenge for the pharmaceutical industry.[6]

Endotoxins are lipopolysaccharide (LPS) molecules that make up ¾ of the outer cell

membrane of gram-negative bacteria,[6] such as *Escherichia coli* (*E. coli*), and almost 30% of biopharmaceuticals are produced using this expression system.[7] The FDA describes the importance of impurity profiling during process development of a pharmaceutical in its guidance document on development and manufacture of drug substances: "it is important to understand the formation, fate (whether the impurity reacts and changes its chemical structure), and purge (whether the impurity is removed by, for example, crystallization, extraction), as well as their relationship to the resulting impurities that end up in the drug substance." As endotoxin concentration of the drug product is typically a critical quality attribute, understanding its removal throughout the downstream process is important to design quality into the process, and designing robust endotoxin removal steps is crucial in meeting specifications.

The green fluorescent protein (GFP) production process at the Golden LEAF Biomanufacturing Training and Education Center (BTEC) is used as a model for an *E. coli*-based biopharmaceutical production process. Intermediate-scale and large-scale versions of the process are used to teach fundamental concepts, process development methodologies, and manufacturing operations in both upstream and downstream biopharmaceutical processes. The purpose of this project is to create an impurity profile for endotoxin throughout the intermediate-scale downstream process and suggest possible process improvements in order for a reasonable "dose" of GFP drug product to more consistently meet the required endotoxin specification.

1.2. Endotoxin Physical and Chemical Properties

Endotoxin molecules are amphiphilic, containing a hydrophilic polysaccharide head and a hydrophobic lipid A tail.[8] These are linked by a core region that is phosphorylated, giving endotoxin its negative charge when present in solutions with pH greater than its isoelectric point (pI) of 2.[9] The structure of an endotoxin monomer is shown in Figure 1.1.

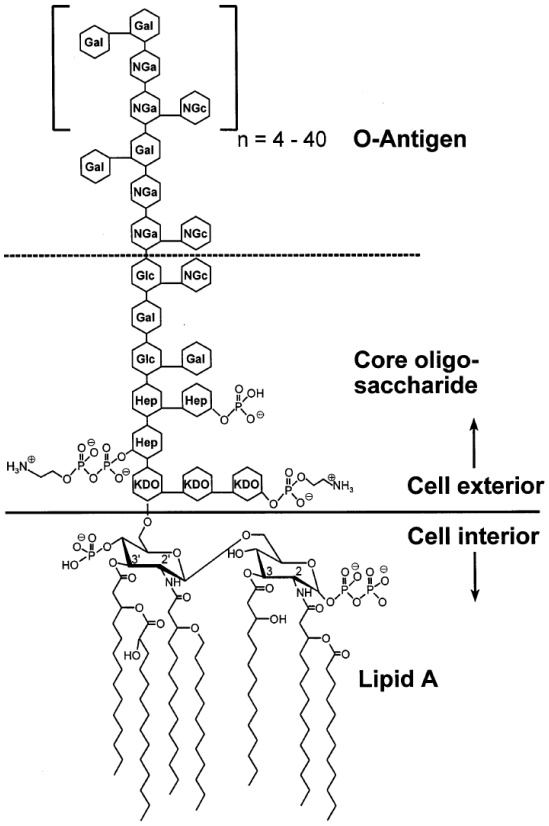

Figure 1.1. Schematic view of the chemical structure of endotoxin from *E. coli* O111:B4.[6]

Endotoxin monomers vary in mass from 10-20 kDa depending on the length of the polysaccharide chain.[8] However, in aqueous solutions, the hydrophobic lipid A portions come together to form stable micelles and vesicles, which can have molecular weights of more than 1,000 kDa.[6] These interactions are aided by bivalent cations such as Ca^{2+} and Mg^{2+}, which form bridges between phosphorylated groups on neighboring endotoxin molecules. Aggregation is hindered by the addition of ethylenediaminetetraacetic acid (EDTA), which chelates the bivalent cations and prevents this bridging.[6] Jang et al. used size exclusion chromatography to show that endotoxin in cell lysate exists partially in more aggregated form (>200 kDa) and partially as monomers or small micelles.[10] The various aggregation states of endotoxin are shown in Figure 1.2.

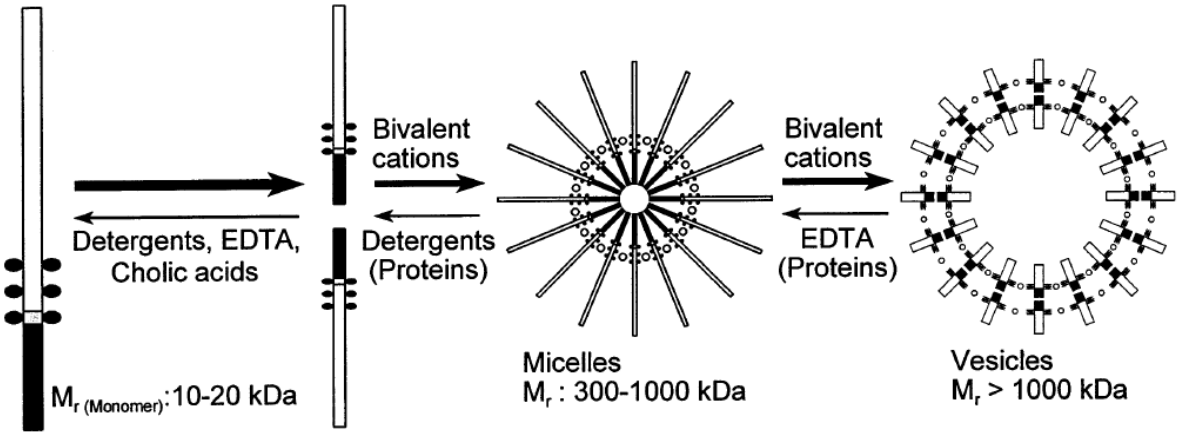

Figure 1.2. Structure of endotoxin aggregates in aqueous solutions of different composition. The left diagram represents the endotoxin monomer; (open square) and (grey square) are hydrophilic sites, (black square) is lipophilic, (black circle) represent charged functional groups, (open circle) bivalent cations, such as Ca^{2+} and Mg^{2+}.[6]

The shape of endotoxin aggregates are not always as symmetrical as depicted in Figure 1.2. Isolated endotoxin has been shown to take various macrostructures such as snake-like, donut-like, rod-like, or flat sheet forms, some of which are shown in Figure 1.3 along with their dependency on the shape of the lipid part of the endotoxin.[11]

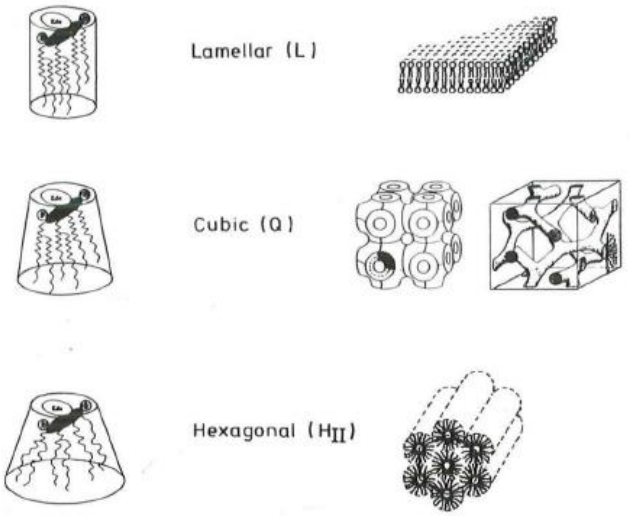

Figure 1.3. Correlation between the molecular shape of lipids and the three-dimensional supramolecular structures they form.[11]

Endotoxins are extremely pH and temperature stable. Depyrogenation procedures used for glassware and other laboratory equipment requires temperatures in excess of 250°C for 30 minutes or 180°C for 3 hours or treatment with solutions with greater than 0.1 M acid or base.[8]

1.3. Endotoxin Removal Techniques

Pharmaceutical manufacturers take measures to prevent active endotoxin from ever entering the process. They use raw materials certified to contain very low amounts of endotoxin, purify water used in the process to remove endotoxin contamination, and/or inactivate endotoxin that may be present on glassware or other product contact surfaces. Even with these precautions, endotoxin is inevitably a concern, and its presence in some processes, especially those with gram-negative bacteria expression system, is unavoidable. The harsh conditions required for inactivating endotoxin are not feasible in the presence of biopharmaceutical products. Thus, in order to meet the required specification, removal techniques are required to ensure that the product meets the required specification.

Chromatographic techniques with positively-charged adsorbents are often used to remove endotoxin from protein solutions.[12] These anion exchange chromatography steps are typically operated in flowthrough mode, where the endotoxin and other negatively-charged impurities bind and the positively-charged product flows through for further processing. However, care must be taken to properly formulate the load to an optimal pH and ionic strength that will help to minimize product loss due to binding to the ligands as well as minimize the interactions between proteins and endotoxin. More selective adsorption techniques have been developed using other ligands such as polymixin B, histidine, histamine, poly(ethyleneimine),[6] chitosan, and aminated poly(γ-methyl L-glutamate),[13] but the use of a purification step solely for endotoxin removal would only be used in extreme cases as it would involve extra equipment, validation time, processing time, documentation review, and product yield loss. Ideally, a protein purification process could be optimized during process development to reduce endotoxin levels to below the specified limit without the use of an additional unit operation implemented solely for endotoxin removal.

Because of the high aggregation states in aqueous solutions, endotoxin can be removed from water or other small molecules using flowthrough ultrafiltration with a 10 kDa molecular weight cut-off (MWCO) membrane. If a high enough MWCO is used such that a protein product can permeate the membrane, ultrafiltration can also be used to remove large endotoxin aggregates from a biological protein preparation.[8] With this technique, the product is the filtrate and large molecules, such as endotoxin aggregates are retained, thus being removed from the product. In one study, endotoxin was spiked into water, 0.9% NaCl, or even 5 mM EDTA and filtered through various pore size membranes.[14] When each of these solutions was filtered with a 10 MWCO membrane, the endotoxin concentration in the filtrate was below the limit of detection, corresponding to more than 99.99% of the endotoxin being removed from the solution. However, the ultrafiltration step typically used in therapeutic protein manufacturing processes for final product concentration and formulation is operated such that the protein is retained. Since endotoxin aggregates are also retained by ultrafiltration membranes, the product would remain unseparated from the majority of the endotoxin. Complete permeation of the endotoxin through the 10 kDa membrane in the aforementioned experiments was only observed when the endotoxin solution contained detergents such as 2% sodium cholate with 5 mM EDTA or 1% deoxycholate.[14] The addition of detergents and EDTA in order to disaggregate endotoxin to permeate an ultrafiltration membrane would not be ideal for pharmaceutical manufacturers nor as these compounds would subsequently have to be removed.

Two-phase aqueous extraction, non-selective hydrophobic interaction chromatography, size exclusion chromatography, sucrose gradient centrifugation, and Triton-X-114 phase separation have all been used in the separation of endotoxin from product in biological preparations.[8] The efficiency of each of these techniques are highly dependent on the properties of the target protein and their implementation into a large-scale manufacturing process may not be practical.

1.4. Endotoxin Detection and Quantification

Due to the immune response and subsequent fever caused when endotoxins are

injected, the rabbit pyrogen test was developed in the 1920s[15] and was required by law to test the pyrogenicity of material for parenteral use.[16] For this method, rabbits are injected with the drug product and monitored for any rise in temperature. This method is expensive and time-consuming, and has since been largely replaced with the *Limulus* Amoebocyte Lysate (LAL) assay.[15] LAL is prepared from extracts of blood from *Limulus polyphemus*, the horseshoe crab, which contains the protein coagulogen.[18] In the presence of endotoxins, a cascade of enzymatic reactions causes the cleavage of coagulogen, creating an insoluble product, coagulin, which forms a gel clot if endotoxin levels are high enough. This discovery led first to the development of the LAL gel-clot assay, which involves the detection of a gel clot in a test tube incubated at 37°C if the sample contains more endotoxin than the sensitivity of the assay.[15] To obtain semi-quantitative data for endotoxin concentration in samples using this assay, hour-long incubation times for multiple iterations of dilutions are often required, making the assay time-consuming and tedious.

In 1977, researchers at Kyoto University published their findings that the same enzymatic reactions can be used to cleave the peptide (α-N-benzoyl)-Ile-Glu-Gly-Arg- bound to p-nitroanilide (PNA).[19] The peptide-PNA molecule is colorless, but after cleavage with the peptide, PNA alone is yellow, allowing the extent of the reaction to be measured using the absorbance at 405 nm. Thus, the LAL assay was adapted to accommodate this faster and more quantitative endotoxin detection method utilizing color. In order to prevent interference from a gel clot and allow the peptide-PNA chromogenic substrate to be preferentially cleaved in this version of the assay, coagulogen concentration was reduced in the LAL reagent.[18] Endotoxin acts as a catalyst in the reaction, so higher endotoxin concentration results in a faster reaction and faster change in color. A visual summary of the reaction principle for the chromogenic LAL assay is shown in Figure 1.4 below.

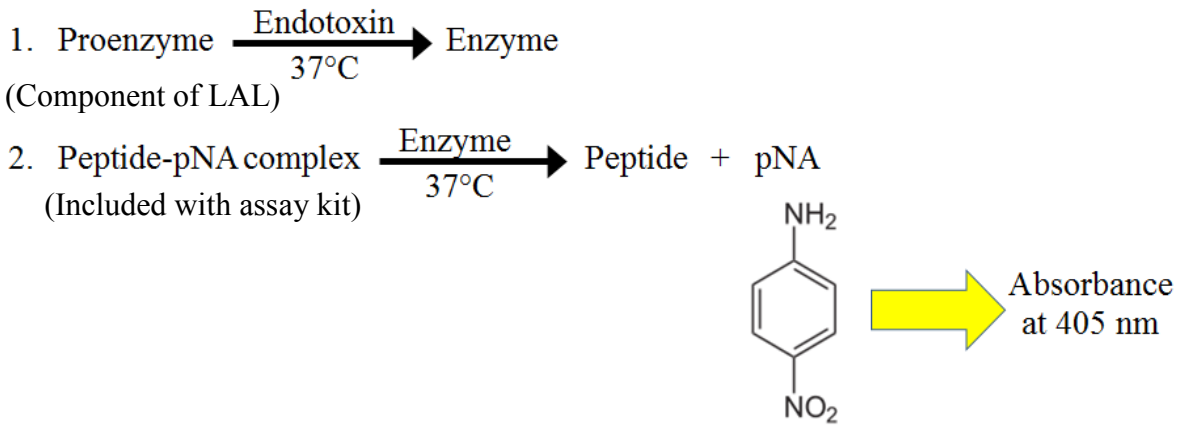

Figure 1.4. Reaction used for endotoxin detection using the chromogenic kinetic LAL assay.

Endotoxin quantification using the chromogenic kinetic LAL assay can either be performed using the endpoint or kinetic methods.[18] With the endpoint method, the reaction is stopped using acetic acid after a certain incubation time and a standard curve is constructed using the A_{405} of standards with known endotoxin concentrations. For the kinetic method, the A_{405} is measured periodically over an incubation time. The amount of time required to reach a certain optical density (OD) is called the onset time and is used in a standard curve with known endotoxin standards. An example of kinetic results from the chromogenic assay with five endotoxin standards and a negative control is shown in Figure 1.5. The chosen onset OD of 0.15 is shown to demonstrate how the onset time decreases with increasing endotoxin concentration.

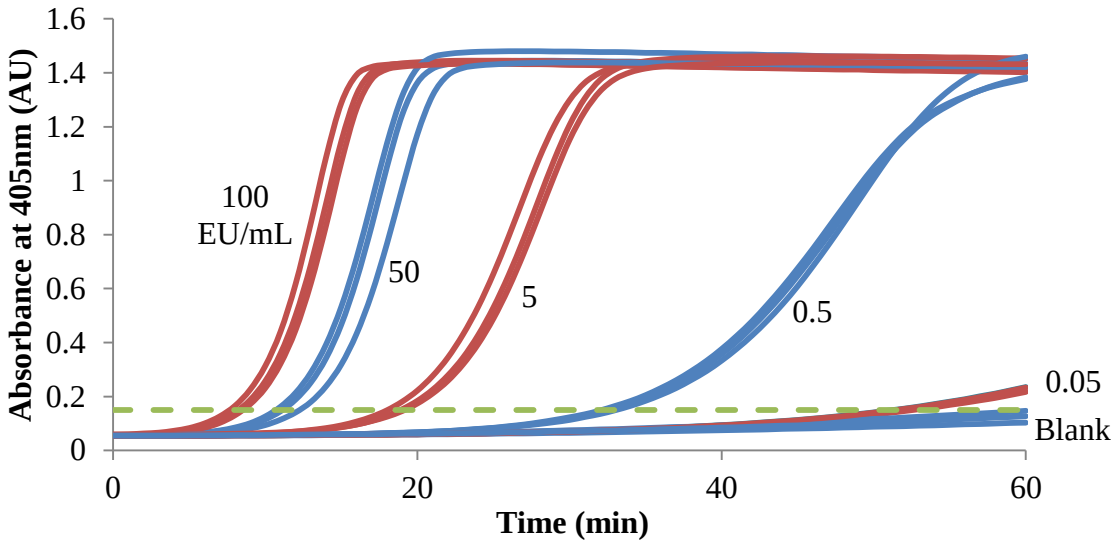

Figure 1.5. Trace of absorbance of 405 nm versus time for standards of known endotoxin concentration used in the kinetic chromogenic LAL assay.

1.5. Green Fluorescent Protein

GFP was originally found in the jellyfish *Aequorea victoria*, where it accompanies the chemiluminescent protein, aequorin.[20] In 2008, Osamu Shimomura, Martin Chalfie, and Roger Tsien were awarded the Nobel Prize in Chemistry for its discovery and development because it has many useful applications in scientific research.[21] Although GFP has no therapeutic value, it is used as a model protein therapeutic in many processes at BTEC because its fluorescence under ultraviolet (UV) light is easy to see and quantify.

GFP is composed of 238 amino acids arranged in an 11-stranded β-barrel with an α-helix in the center containing the chromaphore, which is formed from a reaction of three amino acids, Ser-Tyr-Gly, in positions 65-67 of the amino acid sequence.[20] The structure is shown in Figure 1.6.

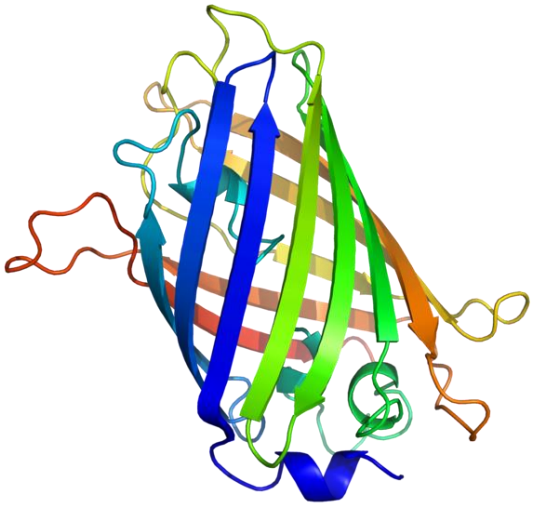

Figure 1.6. Three-dimensional structure of GFP.[22]

BTEC staff genetically engineered *Escherichia coli* (*E. coli*) strain BL21(DE3) to contain the gene coding for GFPuv, a more fluorescent mutant of the GFP protein, using a pET17gfpuv vector.

CHAPTER 2: Materials and Methods

2.1. *E. coli* Fermentation and GFP production

The fermentation broth used for downstream processing at BTEC is produced from different batches for a variety of reasons. Consequently, the fermentation media composition, inoculum scale-up procedure, feeding strategies, control strategies, and final production volume are not always consistent. Although some of the starting material for experiments in this project originated from other fermentation procedures, the majority of the fermentation broth was produced as follows.

Three vials of bacterial working cell bank were used to inoculate 400 mL of pre-warmed media in a 2 L sterile shake flask. Media used for the upstream process had a composition of approximately 1 g/L NH_4Cl, 6 g/L Na_2HPO_4, 3 g/L KH_2PO_4, 25 g/L Bacto Yeast Extract, 150 g/L tryptic soy broth, 50 mg/L ampicillin, 30 g/L dextrose, and 1 mL antifoam 204 for every 3 L of media.[23] The inoculum was incubated in a New Brunswick Scientific 12500 series incubator shaker at 37°C at 250 rpm for approximately 7 hours. Ten 2 L shake flasks with 400 mL of pre-warmed media were each inoculated with 10 mL of the previous shake flask. After incubating at 37°C at 250 rpm for 12-16 hours, all ten shake flasks were pooled and used to inoculate a sterilized 300 L Sartorius bioreactor containing 280 L of media. During fermentation, pH was controlled to 6.8 ± 0.2 with a dead-band of 0.05 by addition of 6 N NH_4OH and 3 N HCl. The pO_2 was maintained at 30% through cascade control of agitation (100 to 400 rpm), aeration (1 vessel volume per minute), and oxygen ratio in the sparge air (0 – 40%). Temperature was maintained at 37°C and back pressure at 5 psi. When the optical density reached 20-25 and glucose concentration reached 8-10 g/L (approximately 7 hours of fermentation), GFP production was induced by the addition of 1 L of 100 g/L isopropyl β-D-1-thiogalactopyranoside (IPTG) solution, and pH control was adjusted to maintain a pH of 7.0. Either 6 hours after induction or the morning after, depending on the reactor, the broth was cooled to 10°C and then emptied into a portable vessel.[24]

2.2. Intermediate-scale Downstream Process at BTEC

An overview of the intermediate-scale downstream process is shown in Figure 2.1, beginning with harvest of the fermentation broth and wash of cell paste (centrifugation). Because GFP is produced intracellularly, lysis of the *E. coli* cells is required (homogenization). Clarification of the lysate involves another centrifugation step followed by 0.45 μm filtration. GFP purification includes an anion exchange chromatography (AEC) capture step followed by a hydrophobic interaction chromatography (HIC) polishing step. The GFP is then formulated by concentrating and exchanging the buffer using an ultrafiltration (UF) / diafiltration (DF) step. This purification process was originally developed using the ratio of GFP concentration to total protein concentration as a measure of purity. This work focuses on measuring the resulting endotoxin removal in the process.

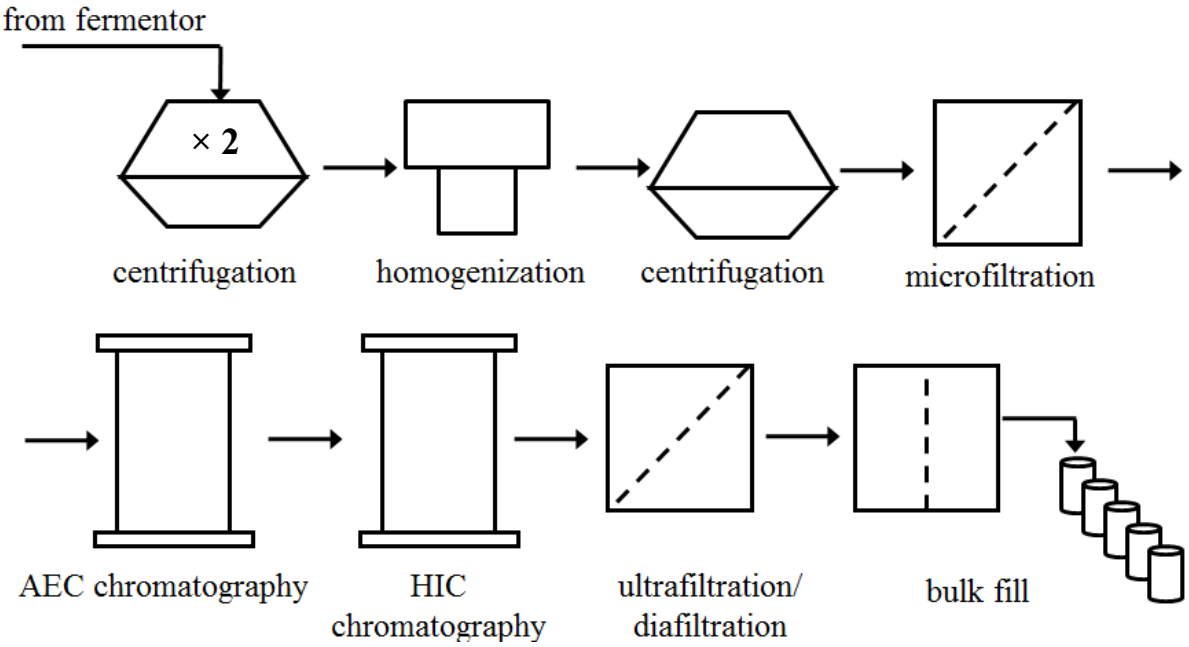

Figure 2.1. Process flow diagram of the intermediate-scale downstream GFP processing.[25]

2.2.1. *E. coli* Recovery from Fermentation Broth

Disc-stack centrifuges are often used in bioprocessing to continuously flow cell slurry

to a spinning bowl, which concentrates the solids inside the bowl and allows clarified liquid to continuously flow out. These centrifuges are often equipped to automatically discharge concentrated solids periodically, allowing for higher volumes to be processed without accumulating solids beyond the recommended solids capacity, which is generally 50% of the bowl volume.

Cells from either a 30 L or 300 L GFP fermentation broth were separated from the spent liquid media using a Westfalia CTC1 Whisperfuge disc-stack centrifuge, which has a bowl volume (V_{bowl}) of 1 L and a sigma value of 1900 m^2. The Whisperfuge was operated at a rotation rate that produced 12,000 times the force of gravity and under 10-15 psi backpressure. Fermentation broth was fed to the centrifuge at a rate of 1 L/min using a Watson Marlow 620S pump. Since the Whisperfuge does not have the automatic solids discharging capability, the bowl was manually disassembled and solids removed when the bowl reached approximately half full with cells. The maximum volume of cell slurry (V_{max}) that could be fed to the centrifuge was calculated using the following equation:

$$V_{max} = \frac{(V_{bowl}) * (solids\ capacity)}{\%\ solids}$$

where % solids was measured by centrifuging 50 µL of mixed cell slurry in a Sartorius Stedim Biotech VoluPac tube using an Eppendorf Bench Top Centrifuge 5418 with rotor FA-45-18-11 at 14,000 rpm for 5 minutes. A typical fermentation broth has 8% solids, which corresponds to a maximum of 6.25 L fed to the centrifuge prior to disassembling and scraping out the cells when assuming a 50% solids capacity.

Recovered cells required washing in order to remove as much of the spent media components as possible. Without a wash step, the ionic strength of the lysate may be too high for the subsequent ion exchange step to bind the product as intended. To wash the cell paste, 1 kg of cell paste was combined with 10 L of 50 mM Tris (2-amino-2-hydroxymethyl-propane-1,3-diol) buffer adjusted to pH 8.0 and mixed for 30-60 minutes with a magnetic stir bar. The resuspended cells were then poured into 1 L bottles and centrifuged at 8500 rpm in the fixed angle rotor, SLC-6000 F8-6x 1000y mL, in a Thermo Scientific Sorvall Evolution RC floor

centrifuge for 10 minutes at 18°C. The supernatant was decanted and the washed cell paste was collected for further processing.

2.2.2. Cell Lysis and Lysate Clarification

Because the GFP is contained within the *E. coli* cells, the bacterial membrane must be disrupted in order to release the product into the liquid. For the GFP downstream process, high pressure homogenization is used to lyse the cells as they come into contact with the valve at high pressures and high shear forces as well as due to the sudden pressure drop after the valve. Depending on cell robustness, homogenizer pressure, and valve type, one pass through the homogenizer may not sufficiently lyse all of the cells, so multiple passes of the feed may be used to maximize product recovery.

To prepare for cell lysis, 1 kg of washed cell paste was mixed with 10 L of 50 mM Tris, pH 8.0 for 30-60 minutes with a magnetic stir bar. This slurry was fed at a rate of 10 L/hr for two passes through a Niro Soavi Type NS1001homogenizer at 900 bar to obtain lysate, which contains the GFP in the liquid. To remove large cell debris remaining after homogenization, lysate was poured into 1 L bottles and centrifuged at 8500 rpm in a Thermo Scientific Sorvall Evolution RC floor centrifuge for 2 hours at 18°C. The supernatant was then filtered through a Sartorius Stedium Biotech Sartobran P 0.45 μm capsule filter with a 0.65 μm pre-filter using a Watson Marlow 520 peristaltic pump operating at 80 rpm. The filtrate was referred to as intermediate-scale clarified lysate.

2.2.3. Anion Exchange Chromatography

The first step in purifying GFP from impurities present in the clarified lysate is AEC. The specific resin used for this process is GE Life Sciences Q Sepharose Fast Flow (FF). Properties of this resin are shown in Table 2.1.

Table 2.1. Properties of Q Sepharose FF Resin.

Property	Description
Base	Cross-linked agarose
Ligand	Quaternary amine ($-CH_2N^+(CH_3)_3$)
Average Bead Diameter	90 μm
Exclusion Limit	4,000 kDa

During chromatography, numerous parameters are monitored at the column outlet including UV absorbance at 280 nm and 395 nm as well as the conductivity of the solution leaving the column. Proteins exhibit an absorption maximum at approximately 280 nm due to the presence of aromatic amino acids such as tryptophan, phenylalanine, and tyrosine. In addition, GFP has an additional excitation adsorption maxima at 395 nm,[20] so A_{395} is measured to give a more specific measure of GFP eluting from the column. The conductivity measures the ionic strength of the buffer flowing through the column, which provides a check to ensure the correct buffers are being used and mixed properly in each step of the chromatography run. The traces of these three measurements are shown for a typical intermediate-scale AEC run in Figure 2.2.

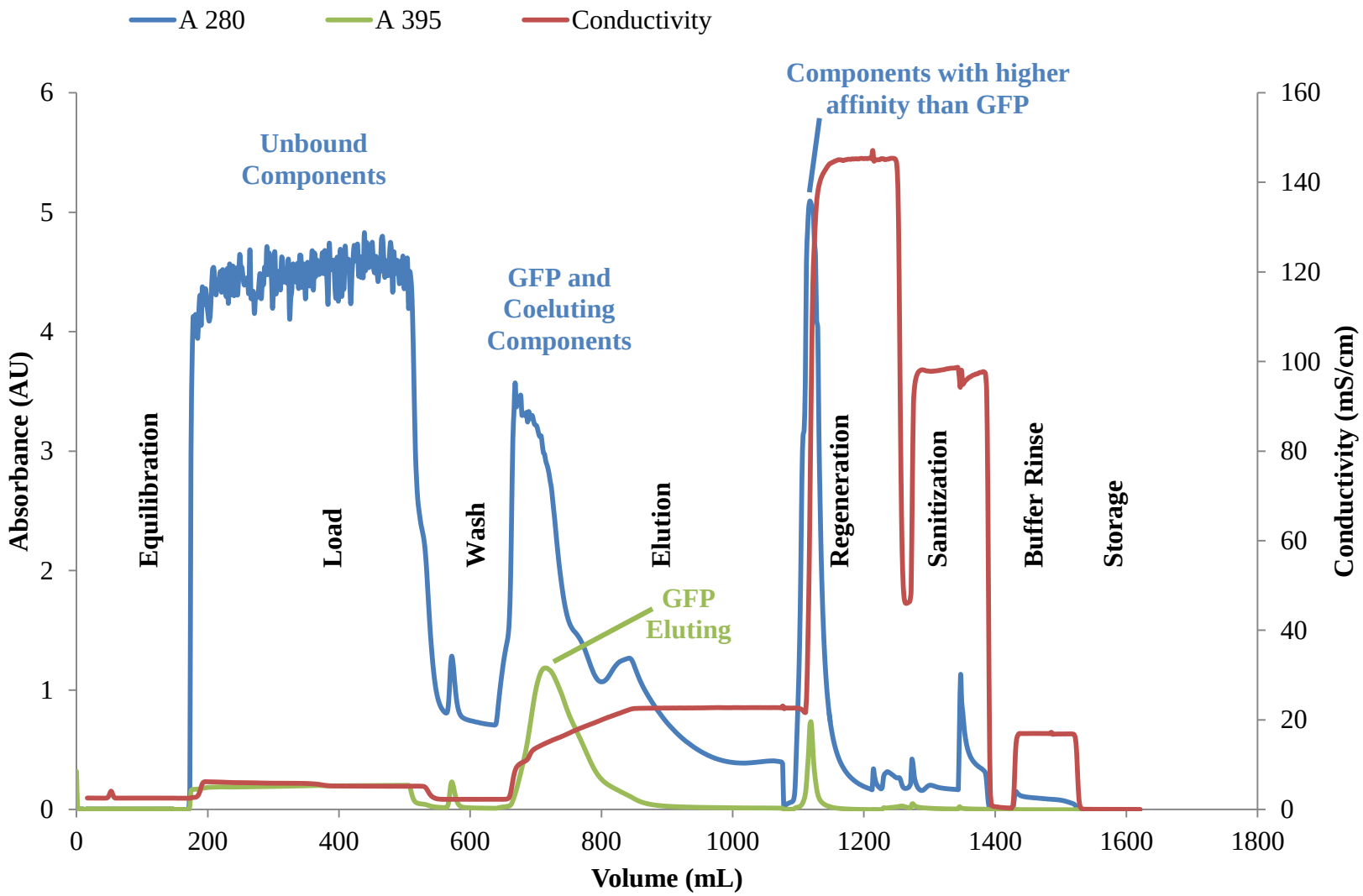

Figure 2.2. Typical AEC chromatogram for the GFP intermediate-scale process.

For the GFP capture chromatography step, a constant flow rate of 10 mL/min was used in a 1.5 cm Pall LRC column packed to a column volume (CV) of 45.4 mL with Q Sepharose Fast Flow resin. The method for solution inputs, monitoring, and sample collection was programmed using UNICORN 5.11 or 5.31 software to operate a GE ÄKTAexplorer 100. The method is described in Table 2.2, which gives the solution and amount required for each of the steps labeled in Figure 2.2.

Table 2.2. Description of the Method Used for the Current AEC Process.

Step	Amount	Solution
Equilibration	3 CVs	50 mM Tris, pH 8.0
Load	~700 g GFP	Clarified lysate
Wash	3 CVs	50 mM Tris, pH 8.0
Elution	4 CVs	0.1 M NaCl to 0.2 M NaCl in 50 mM Tris, pH 8.0
	6 CVs	0.2 M NaCl in 50 mM Tris, pH 8.0
Regeneration	3 CVs	2 M NaCl
Sanitization	3 CVs	0.5 M NaOH
Buffer Rinse	3 CVs	0.5 M Tris, pH 8.0
Storage	3 CVs	20% ethanol in water

The equilibration step of chromatography was necessary to replace the storage buffer in the column with a buffer of similar ionic strength and pH to that of the load. Following equilibration, the clarified lysate was loaded onto the column. Because the pI of GFP is 5.78[26] and the clarified lysate was in a buffer at pH 8.0, GFP had a net negative charge and bound to the Q Sepharose resin along with other negative molecules present in the clarified lysate. Load volume was typically calculated based on the GFP concentration in the clarified lysate as determined by the direct fluorescence assay described in section 2.5.1 and a GFP load mass of 700 mg. The liquid effluent from the column during the load step, referred to as the load flowthrough sample, was collected. Although the A_{395} in Figure 2.2 increased slightly during the load step, the load flowthrough fraction was found to contain negligible GFP when tested with the fluorescence assay. This suggests that essentially all of the GFP that was loaded to the column bound to the resin, which was confirmed by the green observed in the top half of the

column throughout this step as shown in Figure 2.3. For all of the intermediate-scale AEC runs, the A_{280} of the solution leaving the column during this step exceeded the upper range for the UV spectrophotometer, indicating a large amount of positively-charged proteins and/or other components that absorb UV light at 280 nm were unable to bind to the resin and were successfully separated from the GFP.

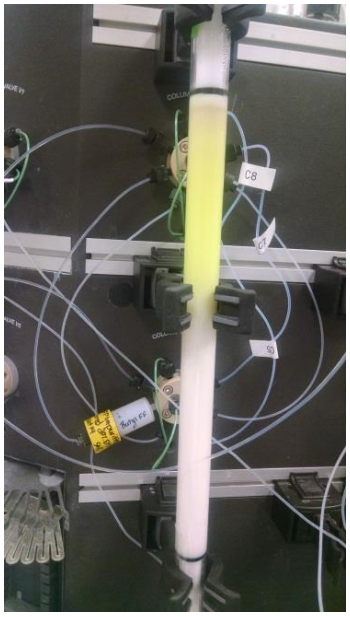

Figure 2.3. GFP bound to the resin at the end of the load step of AEC.

After the calculated volume of clarified lysate was loaded onto the column, a wash step was executed in order to purge unbound proteins from the column.

High charge-density salt ions such as Cl^- are used to recover proteins that have bound to the resin. When salt is added to the column, it replaces larger, lower charge-density molecules, which then are forced to flow down the column until they either replace a more loosely-bound protein or, if no binding site is available, elute from the column. Slowly increasing the concentration of salt used in the elution step allows the least strongly-bound components to elute from the column first, while the molecules with higher affinity for the resin elute later. This elution method, called a linear salt gradient, effectively separates bound molecules based on their pI or net charge. For the salt gradient in the current intermediate-scale AEC step,

pumps A and B on the ÄKTAexplorer system were used to mix 50 mM Tris, pH 8.0 with 1 M NaCl in order to obtain a linear salt gradient from 0.1 M NaCl in 50 mM Tris to 0.2 M NaCl over 4 CVs, after which the concentration remained at 0.2 M for the subsequent 6 CVs. As shown by the A_{395} curve in Figure 2.2, GFP elutes during this step. The eluate was automatically collected in 12 mL fractions throughout this step.

Resins are manufactured to be stable over many chromatography runs. Thus, after the product has eluted, all bound components must be removed, the column must be sanitized, and the column must be properly stored in between runs. 2 M NaCl was used to regenerate the resin. As shown in Figure 2.2, the A_{280} of this step is high, indicating the removal of many proteins. This fraction was collected separately for further testing.

To ensure that any microorganisms that could be present in the column were killed prior to storage, a sanitization step with 0.5 M NaOH was executed. After 2.9 CVs of 0.5 M NaOH solution was fed to the column, the column was held for 45 minutes. The flowthrough from the sanitization step was occasionally collected and tested, though it was hypothesized to have minimal contaminants as most molecules should detach from the resin during the regeneration step. Because a solution with such a high pH was used, a high capacity buffering solution was needed to neutralize the pH in the column. This was accomplished with 0.5 M Tris, pH 8.0 in the buffer rinse step. Finally, 20% ethanol was used to flush out all the buffer and put the column into a solution in which it could be stored to prevent microbial growth. Typically, all samples collected were tested for GFP and endotoxin using the methods described in section 2.3. The nine fractions that contained the most GFP according to the direct fluorescence assay were pooled and used for further processing.

2.2.4. Hydrophobic Interaction Chromatography

The second purification step in the GFP downstream process is hydrophobic interaction chromatography, which separates proteins and other molecules by exploiting differences in hydrophobicity. The column used for this step was a 5 mL prepacked HiTrap Butyl Sepharose 4 Fast Flow, whose beads are made of cross-linked agarose containing butyl ligands (-$O(CH_2)_3CH_3$). When hydrophobic ligands and proteins are exposed to pure water, the water molecules arrange themselves in a highly-ordered structure around the hydrophobic molecules

due to their inability to form hydrogen bonds in that region. When salts or organic solvents are added, hydrophobic interactions are enhanced such that the hydrophobic regions on the proteins are able to bind to the hydrophobic ligands on the beads.[27] Thus, in order to bind molecules to the butyl resin, the proteins must be loaded at high salt concentration. In order to elute the molecules off the resin in order of least affinity (most hydrophilic) to highest affinity (most hydrophobic), a linear gradient of decreasing salt concentration was used.

For the GFP process, the AEC eluate was diluted 2-fold with 4 M $(NH_4)_2SO_4$ in order to obtain a load solution at a concentration of 2 M $(NH_4)_2SO_4$. The concentration of GFP in this mixture was measured with the direct fluorescence assay in order to determine the load volume required to load approximately 72 mg of GFP onto the column. The method used is described in Table 2.3.

Table 2.3. Description of the Method Used for the Current HIC Process.

Step	Amount	Solution
Equilibration	3 CVs	2 M $(NH_4)_2SO_4$
Load	72.2 g GFP	AEC eluate in 2 M $(NH_4)_2SO_4$
Wash	3 CVs	2 M $(NH_4)_2SO_4$
Elution	4 CVs	2 M $(NH_4)_2SO_4$ to 0 M $(NH_4)_2SO_4$ in 50 mM Tris, pH 8.0
	6 CVs	50 mM Tris, pH 8.0
Regeneration	3 CVs	50 mM Tris, pH 8.0
Sanitization	3 CVs	0.5 M NaOH
Buffer Rinse	3 CVs	0.5 M Tris, pH 8.0
Storage	3 CVs	20% ethanol in water

Elution fractions were collected in 2 mL aliquots. A typical chromatogram is shown in Figure 2.4. The A_{280} during the load step in this HIC run was approximately 0.4 absorbance units, suggesting that the HIC step was able to purify GFP from some components that were not hydrophobic enough to bind to the HIC column at 2 M $(NH_4)_2SO_4$.

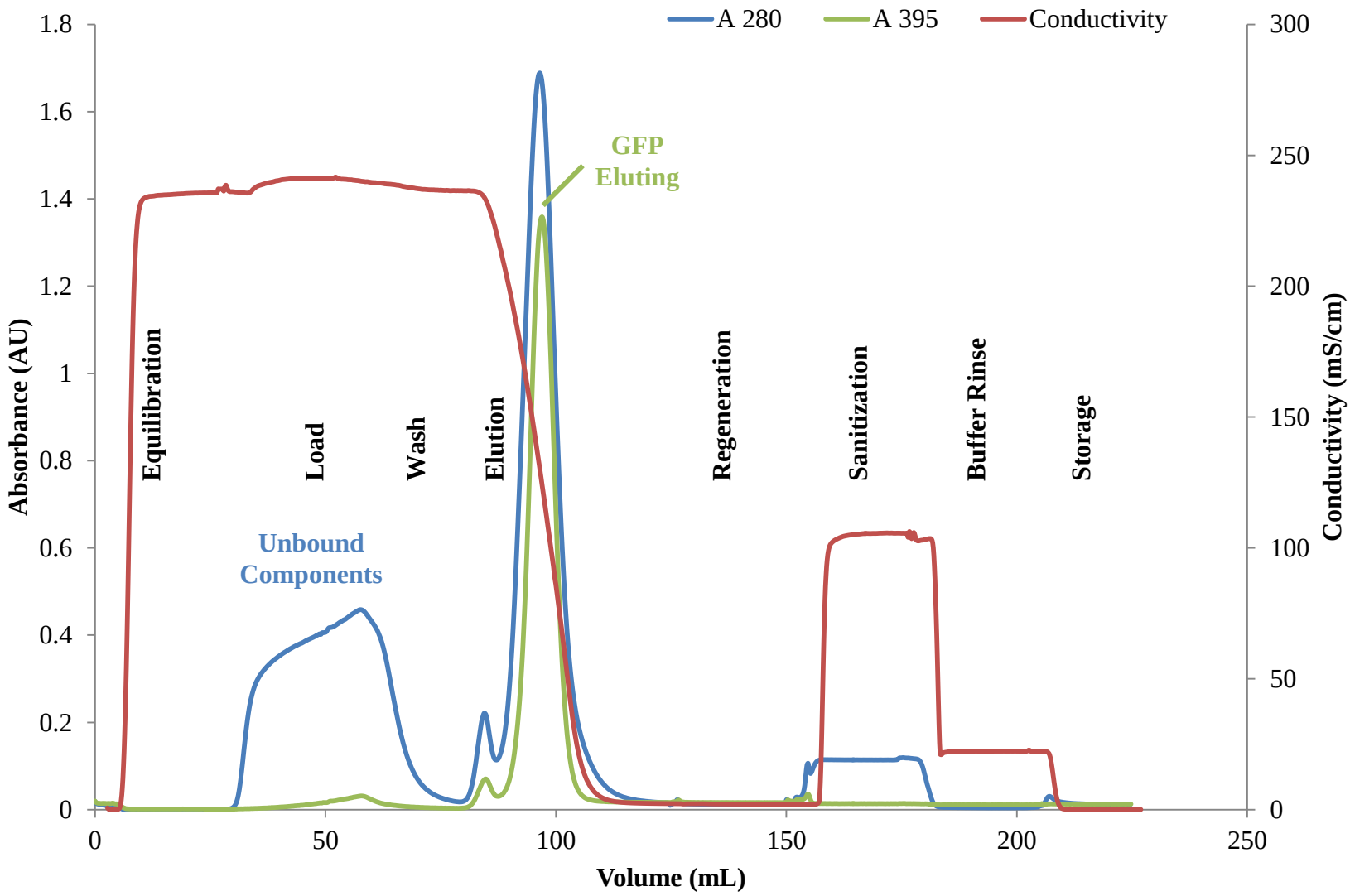

Figure 2.4. Typical HIC chromatogram for the GFP intermediate-scale process.

2.2.5. Ultrafiltration and Diafiltration

A 10 kDa MWCO membrane is used for the final concentration and buffer exchange step in the GFP downstream process. Because endotoxin monomers are 10-20 kDa and aggregates are much larger, it was not expected to provide significant endotoxin clearance. This hypothesis is supported by a study which showed that less than 0.01% of endotoxin was removed from a solution of water with 0.9% NaCl or 5 mM EDTA.[14] Thus, this was not a critical unit operation for endotoxin removal and was not studied in this work.

2.3. Studies on Individual Unit Operations

In addition to evaluating endotoxin levels in the standard intermediate-scale process, more focused studies on individual unit operations that are part of the processes were performed. Experimental details are given in the subsequent sections.

2.3.1. Homogenization Experiments

Critical process parameters for homogenization include pressure and number of times the same material passes through the homogenizer. Three batches of 2.2 L resuspended cell paste slurry were prepared to study the impact of pressure and passes on endotoxin release during homogenization. Pressures of 300, 600, and 900 bar were used with five passes executed at each pressure. Samples were collected prior to homogenization as well as after each pass. 1 mL of each sample was centrifuged in an Eppendorf tube at 14,000 rpm for 15 minutes using an Eppendorf Bench Top Centrifuge 5418 with rotor FA-45-18-11. The supernatants generated were decanted and filtered through a Fisherbrand 0.45 μm syringe filter. Each filtrate was tested for endotoxin concentration.

The amount of GFP released as a result of homogenizing from one to five passes at pressures of 300 or 900 bar was determined using the direct fluorescence assay for centrifuged lysate samples with a similar experiment.

2.3.2. Preliminary Clarification Experiments

To explore the effect of filtration on endotoxin removal, some small-scale experiments were performed. The 1.5 L of 5 pass homogenized material at each of the three pressures left from homogenization experiments described in section 2.3.1 were centrifuged and filtered

separately using the standard intermediate-scale process described in section 2.2.2. For additional filtration experiments, approximately 30 mL samples collected after each pass of 900 bar homogenization were centrifuged at 3500 rpm for 5.5 hours in a Thermo Scientific Sorvall Legend XTR centrifuge, and filtered through 0.45 µm Nylon Fisherbrand syringe filters. These processing conditions proved to be statistically the same as the typical intermediate-scale clarification process with respect to endotoxin concentration (data not shown). All of these samples were tested for endotoxin concentration as described in section 2.5.2 before and after filtration.

2.3.3. Additional Clarification Experiments

To determine the effect of filter pore size on endotoxin clearance, intermediate-scale centrifuged lysate generated according to section 2.2.2 was filtered using syringe filters of differing pore size:

- Fisherbrand 0.45 µm nylon 33 mm
- Fisherbrand 0.22 µm PVDF 13 mm
- Fisherbrand 0.2 µm nylon 25 mm
- Whatman Anotop 25 0.1 µm inorganic membrane 25 mm

The centrifuged lysate and all filtrates were tested for endotoxin and GFP concentration according to the analytical procedures described in section 2.5.

To determine the effect of hold time on endotoxin removal, the same centrifuged lysate used for the filter pore size study was held at 2-8°C. Every few days, some of the material was filtered through a Fisherbrand 0.45 µm nylon 33 mm syringe filter and some through a Fisherbrand 0.2 µm nylon 25 mm syringe filter. The pre-filtration sample and both filtered samples were generally immediately tested for endotoxin concentration on the day of generation to minimize any effect of sample age on the assay performance.

To determine the effect of the centrifugation step, another batch of intermediate-scale lysate material was generated, and 1 L was kept at 2-8°C for a hold time study involving filtration of lysate without centrifugation. Since this material had significantly more solids, filtrate could not be obtained from syringe filters, and more surface area was required. Every

few days after lysate generation, some of the lysate was pumped with a Watson Marlow 520 peristaltic pump operating at 5 rpm through a Millipore Opticap XL 4 Capsule filter with Durapore 0.22 μm media and some through a Sartorius Stedium Biotech Sartobran P 0.45 μm filter until 5-10 mL of each filtrate was collected. Endotoxin concentration was also tested for these samples immediately after sample generation.

2.4. Large-scale Clarification Process

For large-scale processing of GFP, cell paste was obtained from the fermentation broth from the 300 L bioreactor described in section 0 using an Alfa Laval LAPX 404 disc stack centrifuge fed at 120 L/h, rotating to exert approximately 11,000 times the force of gravity, and automatic solids discharge cell paste was collected in a carboy or bag.[28] After resuspending the solids in 50 mM Tris, pH 8.0 for washing and then centrifuging according to the same procedure, the washed cells were stored at 2-8°C. When ready to homogenize, the cell paste was resuspended with 10 L of 50 mM Tris, pH 8.0 for every 1 L of cell paste.

The resuspended cells were then homogenized using the GEA Niro Inc. homogenizer at a pump speed of 80% and a pressure of 900 bar.[29] The one-pass lysate was sometimes held for a period of a week or more prior to executing the second homogenization pass under the same conditions. This lysate was also sometimes held for a week or more prior to clarification.

For clarification of the lysate, a Millipore FIS-1441 Tangential Flow Filtration Unit was used with a Spectrum Laboratories, Inc. KrosFlo 0.2 μm modified polyethersulfone hollow fiber filter with a surface area of 2.6 m^2. The flow rate of the lysate fed to the unit was maintained at 10 L/min, and the clarified lysate permeated the membrane at approximately 2 L/min.

2.5. Analytical Methods

2.5.1. GFP Direct Fluorescence Assay

To quantify the concentration of GFP in the various downstream samples, a plate-based fluorescence assay was used to compare the fluorescence of the sample with a standard curve

prepared from a known standard of 1 g/L GFP.

In the first row of a Corning black polystyrene flat-bottom 96-well microplate, the standard (in duplicate) or sample was diluted 1:10 with 50 mM sodium phosphate buffer at pH 7.2.[30] A 2-fold serial dilution was then prepared in the following six rows, mixing with a multi-channel pipettor. The final row contained only 50 μL of the buffer as negative controls and blanks. The plate was placed into a BioTek Instruments Synergy4 plate reader and the fluorescence (excitation 380/20, emission 508/20) of each well was read using Gen5 1.10 software. The averages of the fluorescence measurements for the replicates of each standard were taken and the average blank value was subtracted from the standards and every sample well. The fluorescence measurements of the background-subtracted standards were graphed versus the known concentration of GFP, to create a standard curve similar to Figure 2.5. This equation was then used to calculate the concentration of GFP in wells containing unknown samples, and the concentration was multiplied by the dilution factor of that well. The concentrations of GFP in the three least diluted wells that fall into the standard curve were averaged to obtain the estimated GFP concentration of each unknown sample.

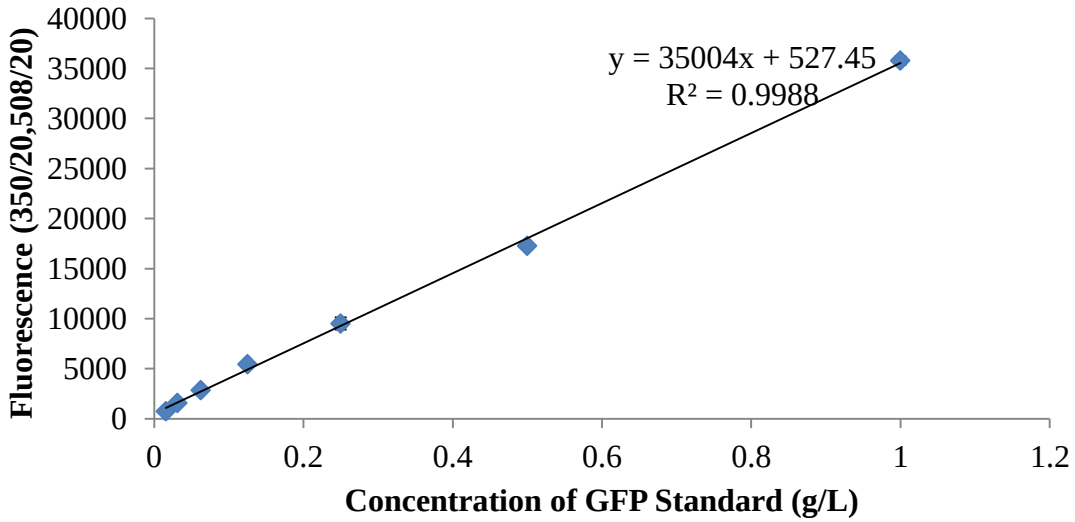

Figure 2.5. Typical GFP fluorescence standard curve using the direct fluorescence assay.

2.5.2. Chromogenic Kinetic LAL Assay

For the endotoxin quantification assay, whose theory is described in section 1.4, Pyrochrome reagent, Glucashield buffer, endotoxin-free LAL Reagent Water (LRW), and control standard endotoxin (CSE) were obtained from Associates of Cape Cod, Inc. and stored at 2-8°C until use. The CSE in the vial was reconstituted in 2 mL of LRW to achieve a final concentration of 100 EU/mL. This solution was diluted 1:2 to obtain a 50 EU/mL standard, which was 10-fold serially diluted to obtain 5 EU/mL, 0.5 EU/mL, and 0.05 EU/mL standards. Samples from the GFP downstream process required dilution as they generally contained more endotoxin than 100 EU/mL and/or contained components that interfered with the assay performance. Typically, 100-fold serial dilutions with LRW were made to achieve concentrations within the standard curve. Most samples required a 1:10,000 dilution, but lysate and clarified lysate samples often had to be diluted as much as 1:1,000,000. One vial of ChromoLAL or Pyrochrome reagent was reconstituted in 3.2 mL of Glucashield buffer, mixed gently, and kept at 2-8°C until used.

Either 50 or 100 µL of each sample and standard was plated in triplicate on a Corning Life Sciences Pyroplate, a 96-well endotoxin and glucan-free microplate. Whichever volume of sample was used, the equivalent volume of reconstituted reagent was dispensed and mixed with the sample using a multichannel pipettor. The plate was then put into a BioTek Instruments Synergy4 plate reader pre-warmed to 37°C to begin data collection using Gen5 1.10 software. The plate reader first shook the plate for 15 seconds to further mix the sample with the reagent. Then, the absorbance of each well at 977 nm was read in order to determine the pathlength, which is proportional to the volume of the liquid in the well. Every minute thereafter, for 60 or 75 minutes, the absorbance at 405 nm was measured to track the course of the enzymatic reaction. After the kinetic readings were taken, the pathlength was again measured.

The software automatically calculated the time at which the A_{405} reached 0.15, or onset time, for each well. Although the plate only took absorbance readings once per minute, the software linearly interpolated the readings in order to obtain a more accurate estimate of when the well likely reached this absorbance depending on the change in absorbance over that

minute. These data were used for all further analysis. The average of onset time in the triplicate wells was calculated for each standard, and a log-log plot similar to Figure 2.6 was constructed to create the standard curve equation used to calculate endotoxin concentration in the diluted unknown samples. The average and standard deviation of these endotoxin concentrations were calculated and multiplied by the dilution factor to get the endotoxin concentration in the original sample.

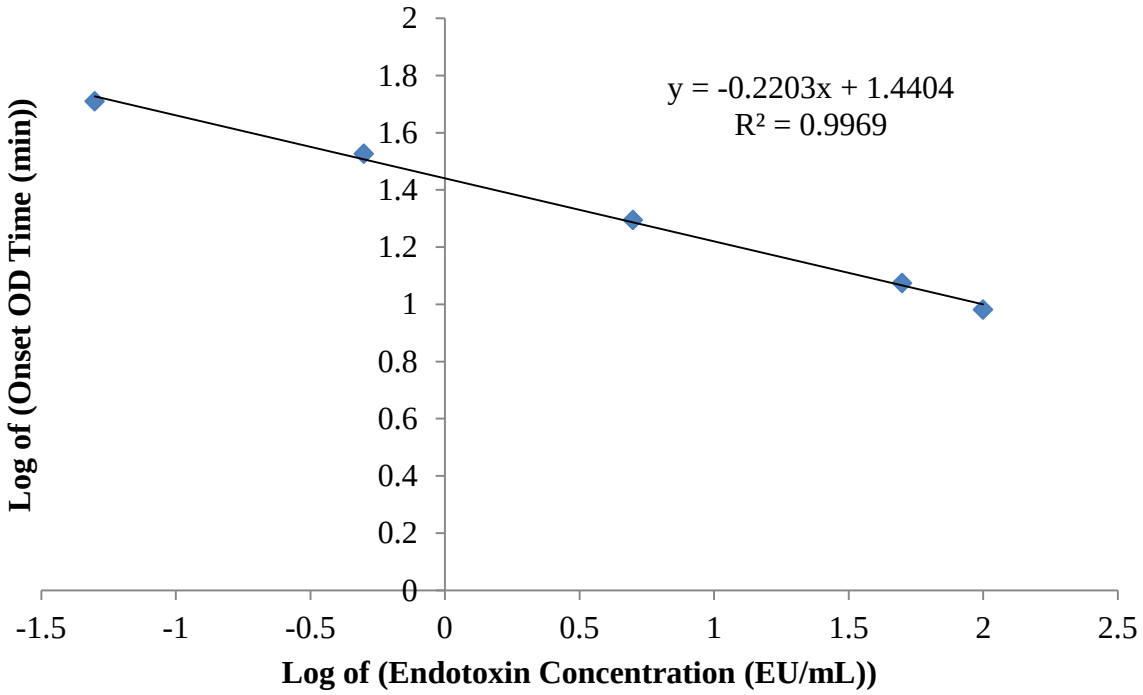

Figure 2.6. Typical endotoxin standard curve using the chromogenic kinetic LAL assay.

CHAPTER 3: Chromogenic Kinetic LAL Assay Characterization

3.1. Introduction

Prior to being used in development or manufacturing, the ability of an assay to produce reliable data using the protocols and samples to be analyzed must be proven. Specifically for assays which aim to quantify impurities, the International Conference on Harmonisation (ICH) document Q2(R1) gives guidance on assay parameters to be tested to perform a full validation as well as some recommendations on how to test them.[31] These parameters include specificity, linearity, range, accuracy, precision, detection and quantitation limits, and robustness. The parameters that were studied are defined in subsequent sections along with the associated experimental designs, results, and conclusions found during a partial assay validation for the chromogenic kinetic LAL assay. Validation parameter criteria were found specifically for the chromogenic kinetic LAL assay in the USP 35 ‹85›, Bacterial Endotoxin Test.[32]

3.2. Accuracy

According to the USP, the percent recovery of spiked endotoxin needs to be between 50 and 200% in order for the chromogenic kinetic assay to be considered accurate.[32] First, LRW was spiked with 5 EU/mL using various dilution schemes other than that used to create the standard curve sample. In order to meet USP specifications, the endotoxin concentration of these spikes should be between 2.5 and 10 EU/mL. The amount of endotoxin recovered from 5 EU/mL spikes are shown in Figure 3.1 with the USP specification requirements shown with red lines.

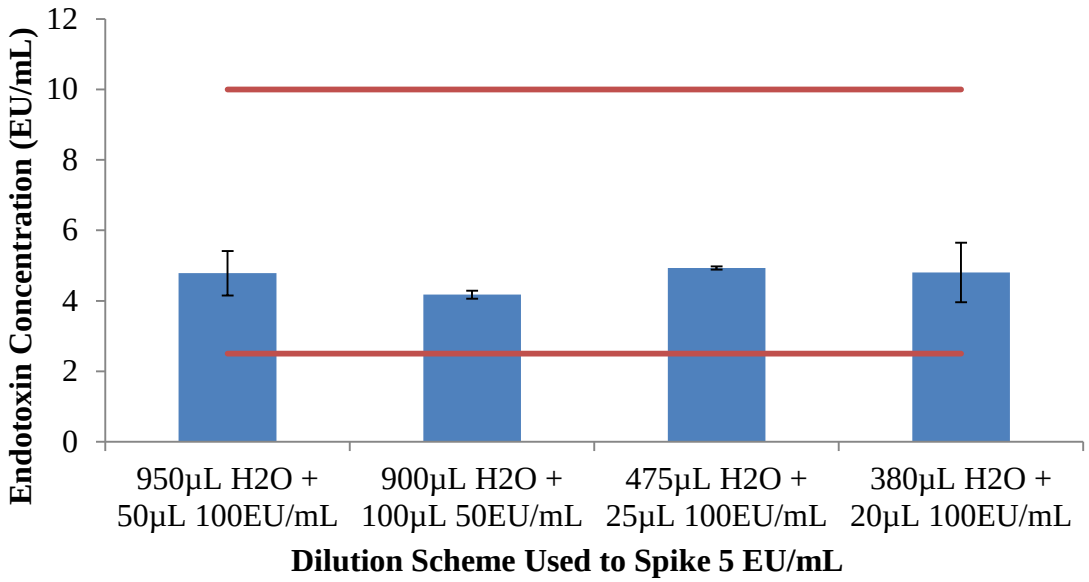

Figure 3.1. Recovery 5 EU/mL in LRW spike using four different dilution schemes. USP specification for assay accuracy, 50% (2.5 EU/mL) to 200% (200 EU/mL) are shown with red lines.

All of these spikes were within the USP requirement. Accuracy was then tested by spiking 5 EU/mL into a clarified lysate sample as well as a more pure AEC eluate sample. The results of this spiking study are shown in Table 3.1.

Table 3.1. 5 EU/mL spike into two process samples.

	Concentration of Endotoxin (EU/mL)		Average Difference (with-without spike, EU/mL)	% of 5 EU/mL Spike Recovery
	Without Spike	With Spike		
Clarified Lysate	3.89	8.51	4.49	90%
	3.53	7.89		
AEC Eluate Fraction A9	0.15	8.06	6.94	139%
	0.18	6.16		

Both of the spiked samples fell within the 50 to 200% recovery, indicating that the assay is accurate even in a sample containing many impurities.

3.3. Linearity and Range

The linearity parameter in assay validation refers to obtaining measurements that are directly proportional to the concentration of the component to be analyzed. According to USP ‹85›, the correlation coefficient of the standard curve, r, for the chromogenic kinetic assay must be greater than 0.98.[32] The correlation coefficient for the standard curve for every plate tested with this assay is graphed in Figure 3.2.

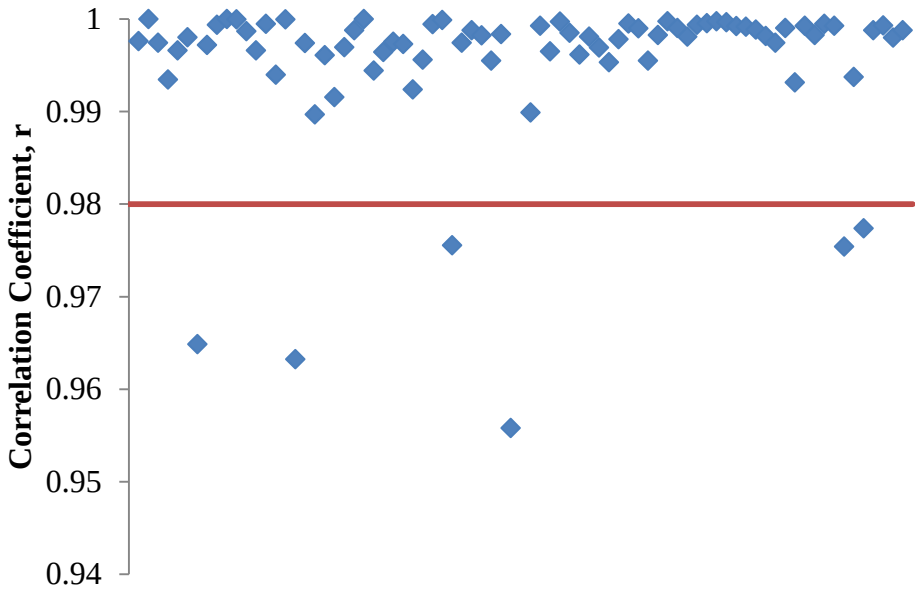

Figure 3.2. Correlation coefficients for all standard curves.

For 72 out of the 78 experiments, the correlation coefficient of the standard curve met the acceptance criterion. For some of the standard curves tested at the beginning, the 0.05 EU/mL samples did not reach the onset OD in the 60 minute time incubation time initially set. Consequently, incubation time was extended to 75 minutes to achieve this lower range. An upper range extension to 800 EU/mL was attempted, but the point did not appear to fall within the rest of the linear trend as shown in Figure 3.3, so the upper range limit was maintained at 100 EU/mL.

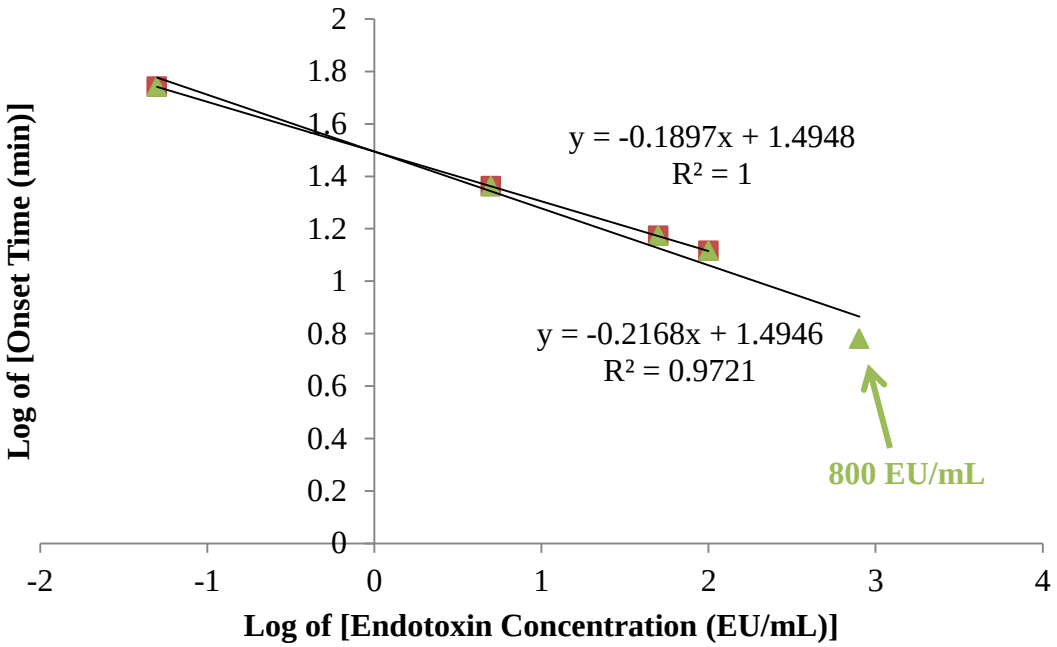

Figure 3.3. Linear regression analysis of extending the range to higher endotoxin concentration, where the top equation represents the standard curve and high correlation (R^2=1) without the 800 EU/mL standard and the bottom equation represents the standard curve and decreased correlation (R^2=0.9721) with the 800 EU/mL standard.

3.4. Precision

Precision "expresses the closeness of agreement (degree of scatter) between a series of measurements obtained from multiple sampling of the same homogeneous sample under prescribed conditions."[31] One measure of precision is the variability between triplicate wells of the same sample on the same plate, or repeatability. For each standard curve sample on each plate, the average and standard deviation of the onset time were calculated in order to obtain the coefficient of variation (CoV), which is defined as the ratio of the standard deviation to the average. A histogram of all the CoVs for the onset time of all standard curve points is shown in Figure 3.4, with all CoVs falling below 2.5% represented by the first bar, all CoVs between 2.5% and 5% represented by the second bar, etc.

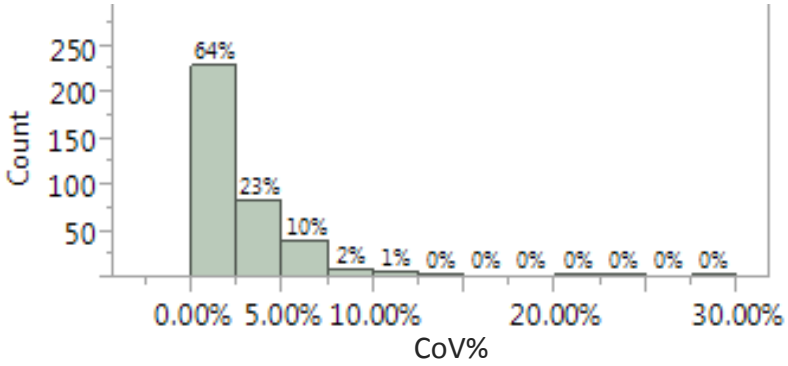

Figure 3.4. Histogram of CoV% for onset time of all standard curve points.

Figure 3.4 shows that most of the data had a CoV of less than 5% and almost all of the data was within 10% CoV. This gives an idea of the variability of standards that can be expected when testing the same dilution of the same sample on the same plate, or repeatability.

However, these standards only have endotoxin in very pure water and may not represent the variability expected when testing samples from the GFP process. During experimentation, it was observed that the repeatability of the assay may be dependent on the sample itself. In these experiments, the CoV for lysate samples were on average significantly different compared to the CoV for filtered samples. A statistical analysis of these samples is shown in the box plot in Figure 3.5.

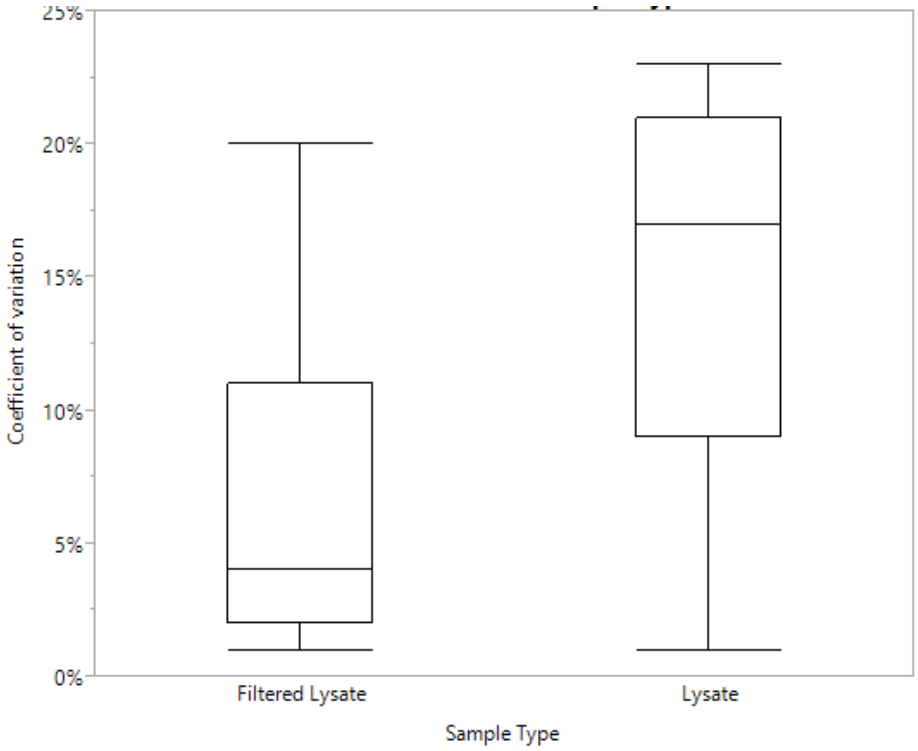

Figure 3.5. Boxplot showing the difference in CoVs between lysate and filtered lysate during two experiments.

Although some outliers cover the range of CoVs, Figure 3.5 shows that the CoV for a lysate sample is typically much higher than that of a filtered lysate sample. Therefore, when considering acceptance criteria for the variation within each sample, it may be important to become familiar with typical CoVs for samples of similar composition.

3.5. Robustness

3.5.1. Effect of Time

To determine the time frame in which a sample must be tested after its generation, two lysate samples were tested on the day of generation as well as 10, 21, and 30 days later. The samples were stored at 2-8°C and mixed thoroughly prior to testing with the chromogenic kinetic LAL assay. Mixing was required to disperse settled particulate so that a homogenous sample could be used for testing. The results are shown in Table 3.2.

Table 3.2. Time Study of Homogenization Samples.

	Days after homogenization sample was tested	Concentration of endotoxin in sample (mg/mL)	Standard deviation (mg/mL)
Lysate, 900 bar, 2 passes	0	0.97	0.00
	10	1.34	0.14
	21	3.59	0.18
	30	>12	
Lysate, 900 bar, 3 passes	0	1.29	0.24
	10	0.73	0.13
	21	3.11	0.05
	30	>12	

In general, Table 3.2 shows a general increase in the apparent concentration of endotoxin with hold time of the sample. When testing the samples 21 days after generation, the concentration of endotoxin in both samples appeared to increase to over 3 mg/mL (270% or 141%). After 30 days, the samples diluted with the same dilution scheme no longer fell within the standard curve, indicating that they contained over 12 mg/mL of endotoxin. A similar pattern was observed for purified GFP samples. One possible reason for this phenomenon is that the endotoxin aggregates over time, forming large micelles and vesicles. Since the aggregates are the active form of endotoxin,[33] the aggregates that form over time would cause the sample to appear to contain more endotoxin than it did at an earlier time point, which was presumably in a less aggregated state. These data show the importance of maintaining consistency of age of sample tested in order to ensure comparability between experiments. After obtaining these time study data, samples were typically tested on the day of their generation.

3.5.2. Placement of Samples on Plate

For samples or standards that had high onset time CoV, the source of variation was often investigated. For many of these samples during the first few experiments, it was observed that the wells located in the outer wells of the plate almost always had an onset time that was lower than inner wells containing the same sample. A study was performed to determine if this change in onset OD was correlated with a greater reduction of volume of liquid in the outer

wells due to incubation at 37°C for the duration of the assay. The pathlength was determined by the software after measuring the absorbance at 960 nm of each well before and after the kinetic reads. These measurements gave estimates of the relative volume of liquid in the wells, and the difference in the pathlength was calculated to estimate the relative change in volume of liquid in the wells. Figure 3.6 shows this loss in pathlength for a typical 96-well plate using color scaling to illustrate wells with high difference in pathlength (red) compared to wells with smaller pathlength changes (green).

	1	2	3	4	5	6	7	8	9	10	11	12
A	0.055	0.048	0.052	0.049	0.051	0.052	0.049	0.053	0.049	0.052	0.052	0.058
B	0.048	0.045	0.042	0.038	0.049	0.042	0.036	0.038	0.038	0.042	0.041	0.047
C	0.045	0.042	0.037	0.034	0.049	0.048	0.035	0.032	0.032	0.035	0.039	0.054
D	0.045	0.037	0.037	0.036	0.033	0.032	0.03	0.032	0.031	0.033	0.035	0.041
E	0.035	0.03	0.027	0.024	0.022	0.025	0.03	0.03	0.031	0.031	0.034	0.041
F	0.051	0.039	0.033	0.031	0.03	0.03	0.028	0.027	0.025	0.027	0.031	0.038
G	0.048	0.04	0.038	0.035	0.043	0.03	0.018	0.015	0.021	0.02	0.021	0.029
H	0.052	0.04	0.05	0.035	0.03	0.034	0.042	0.045	0.047	0.042	0.05	0.032

Figure 3.6. Loss in pathlength in each well of a 96-well plate over the 60 minute assay. Data is in units of centimeters.

As shown in Figure 3.6, rows A and H as well as columns 1 and 12 show significantly higher loss in pathlength compared to the inner wells of the plate. This is likely due to the increased difficulty in heating wells at the center of the plate. With the outside wells more exposed to the warm air, more water evaporates from these wells causing the more significant decrease in well volume. Consequently, reactants in the wells become more concentrated, which likely speeds up the reactions and causes the absorbance to reach the onset OD faster than in the wells with less evaporation. Because of the decrease in onset time observed in the outer wells likely due to liquid evaporation throughout incubation, placement of samples and standards in the outer wells of the plates should be avoided.

3.5.3. ChromoLAL vs. Pyrochrome Reagent

After the first several experiments using ChromoLAL reagent, a different type of reagent, Pyrochrome, was received for all further experiments. Prior to use in the assay, the

comparability of results between Pyrochrome and ChromoLAL reagents was established. Three sets of standard curve samples were made from three different vials of CSE and each was tested with both types of reagents. The three standard curves for each reagent were very similar, so the curves were averaged and are shown in Figure 3.7.

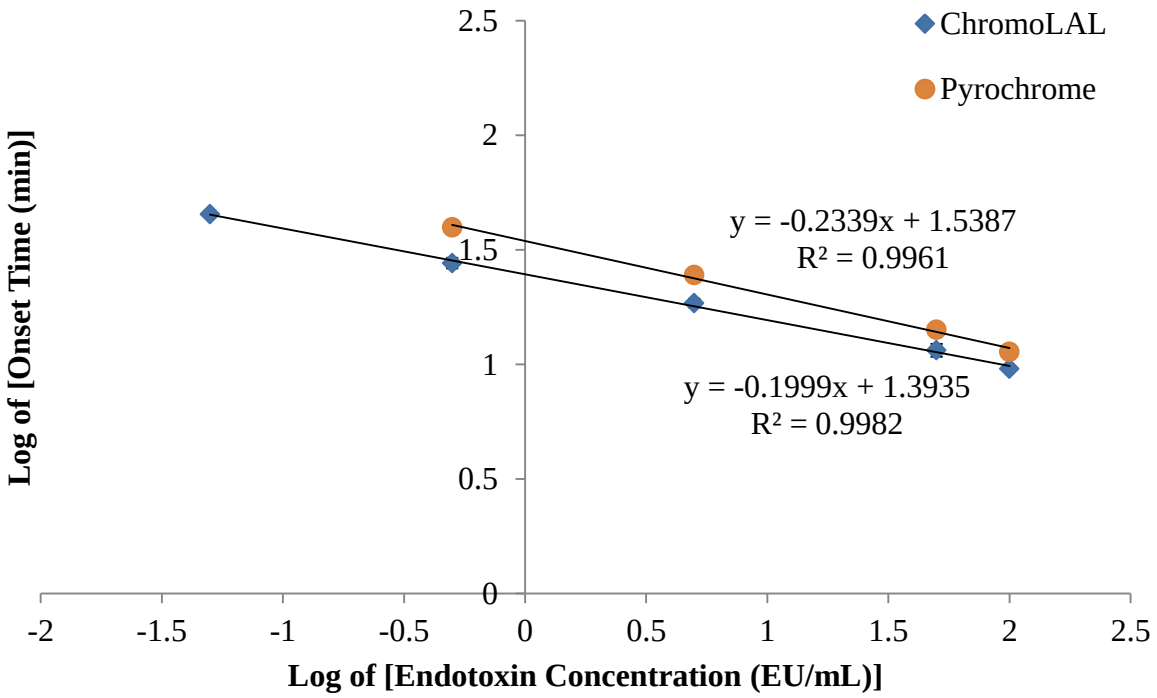

Figure 3.7. Comparison of the average of three standard curves using ChromoLAL reagent and three standard curves using Pyrochrome reagents.

As shown in Figure 3.7, the intercept for the standard curve mixed with the Pyrochrome reagent was higher than that of the ChromoLAL reagent. Additionally, the slope was steeper for the Pyrochrome standard curve. The magnitude of these differences can be assessed by observing all of the intercepts and slopes obtained from experiments with this assay. For the 72 standard curves that passed the specification for linearity, the standard curve slope was an average of -0.23 ± 0.03 and the intercept averaged 1.45 ± 0.09. Both intercepts and both slopes were within one standard deviation of the average of the parameter for every standard curve tested. This indicates that the difference between the reagents is reasonably small.

A spiking study was also included in this experiment, where 5 EU/mL from each vial was spiked into LRW and tested with both ChromoLAL and Pyrochrome reagents. The average amount of endotoxin measured in these samples was 8.07 ± 1.31 EU/mL (16% CoV) for the ChromoLAL reagent and 7.07 ± 0.71 EU/mL (10% CoV) for the Pyrochrome reagent. As both reagents were able to recover between 50 and 200% of the spiked endotoxin, these data suggest that both reagents produce accurate results. Considering that the Pyrochrome reagent recovered an amount closer to the spiked endotoxin concentration and had a smaller CoV, Pyrochrome reagent was used for all further experiments.

3.5.4. Volume of Sample and Reagent in Wells

Volumes of 100 µL of sample and 100 µL of LAL reagent were required in each well according to the procedure for use of the ChromoLAL reagent. The product insert for the Pyrochrome reagent states that either 100 µL or 50 µL of both sample and reagent could be used. To maintain consistency with previous experimental conditions, 100 µL of each was initially used with the Pyrochrome reagent. In order to save reagent, 50 µL of each was eventually tested for comparability in order to implement this variation of the assay. The same set of standards was tested with the 100 µL procedure as well as the 50 µL procedure, and the standard curves are graphed in Figure 3.8.

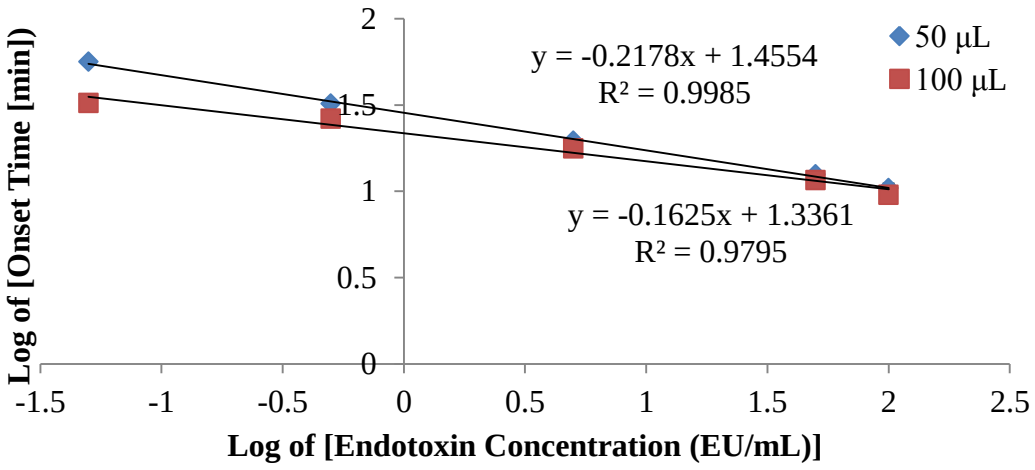

Figure 3.8. Comparison of standard curves using 100 µL or 50 µL per well of sample and Pyrochrome reagent.

The two standard curves in Figure 3.8 are fairly similar with the exception of their differing slopes. For this experiment, the slope of the 100 µL was less steep than previous curves, but the standard curve for 50 µL of sample and reagent was in the range of typical slopes observed, -0.23 ± 0.03. The 50 µL procedure was used for all further testing.

3.6. Matrix Effects

Samples produced throughout the GFP downstream process are expected to contain certain components such as salts, whose affect on the assay must be determined. Samples from AEC may contain up to 2 M NaCl while samples from HIC may contain up to 2 M $(NH_4)_2SO_4$. However, these samples typically were diluted 1:10,000 in order for the concentration of endotoxin to fall within the standard curve, making the salt concentration in the diluted sample only 0.0002 M. For testing the interference of these components, standards containing 0.05, 0.5, 5, 50, and 100 EU/mL were prepared in concentrations of 0.0002 M, 1 M, and 2 M NaCl or $(NH_4)_2SO_4$. These standards were tested for endotoxin concentration along with a normal standard curve containing no salts in order to check for any inhibition or enhancement of the assay with the salts.

3.6.1. Sodium Chloride

The standard curves containing sodium chloride are shown in Figure 3.9.

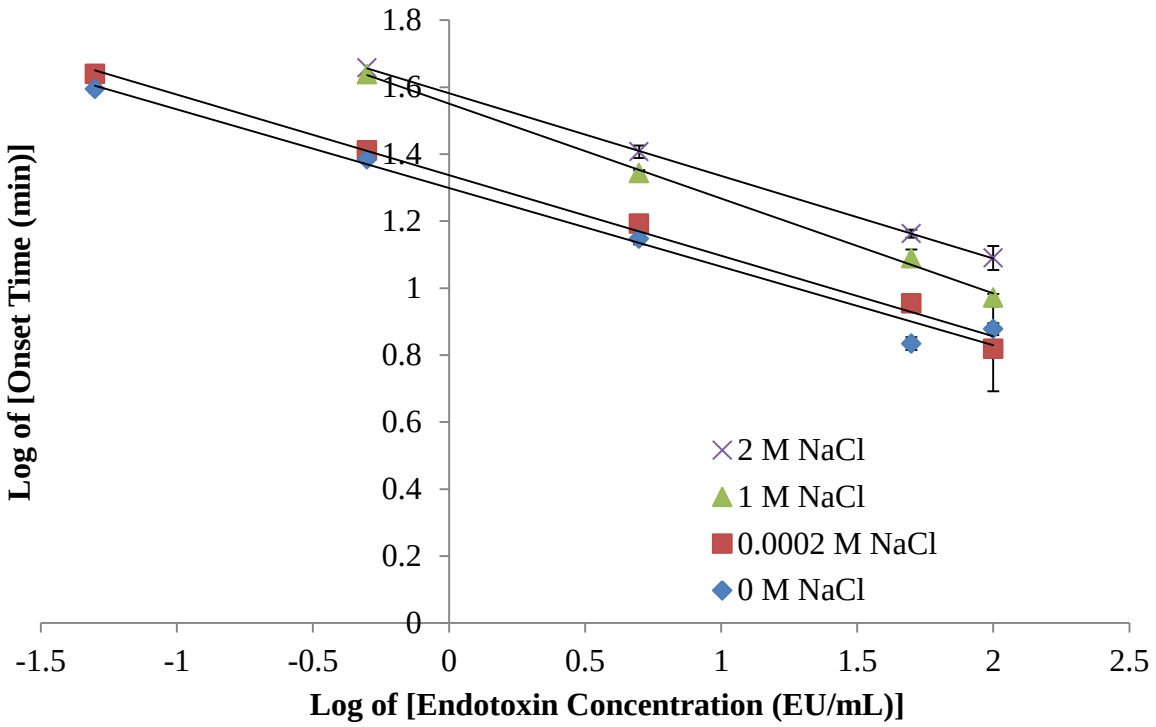

Figure 3.9. Endotoxin standard curves containing various concentrations of sodium chloride. Error bars represent ±1 standard deviation of onset time detected in triplicate wells for each sample.

Figure 3.9 shows that the standard curves shift to higher onset times when the standards contain 1 or 2 M NaCl. For the lowest concentration standard, 0.05 EU/mL, containing either 1 or 2 M NaCl, the onset time exceeded the incubation time of 60 minutes and was therefore not graphed in Figure 3.9. Because higher onset time typically implies that there is a less endotoxin in the sample, these samples appear to contain less endotoxin than the known amount that was spiked into the standard. Thus, high concentrations of NaCl can be considered to inhibit the assay.

The impact of the inhibition can be determined by comparing these standard curves to all standard curves obtained with the assay. For the 72 standard curves that passed the specification for linearity, the standard curve slope was an average of -0.23 ± 0.03 and the intercept averaged 1.45 ± 0.09. The slope of the standard curve containing 1 M NaCl was slightly lower than the average at -0.28, but the 2 M NaCl became relatively parallel to the typical standard curve with a slope of -0.25. The increase in standard curve intercept from no

or low concentration of NaCl (1.30 and 1.34, respectively) to the 1 and 2 M NaCl standard curves (1.55 and 1.58, respectively) spanned over two times the standard deviation of all of the standard curve intercepts. Although some standard curves without salt also had intercepts in this range due to some other variations in the assay procedure, the direct comparison of standard curve intercepts with and without salt indicates assay inhibition. Thus, samples anticipated to have high NaCl concentration (e.g. regeneration sample from AEC) should be diluted prior to endotoxin testing in order to prevent assay inhibition.

3.6.2. Ammonium Sulfate

The standard curves containing ammonium sulfate are shown in Figure 3.10 with the exception of 2 M $(NH_4)_2SO_4$ as all of these standards had an initial A_{405} greater than the onset OD.

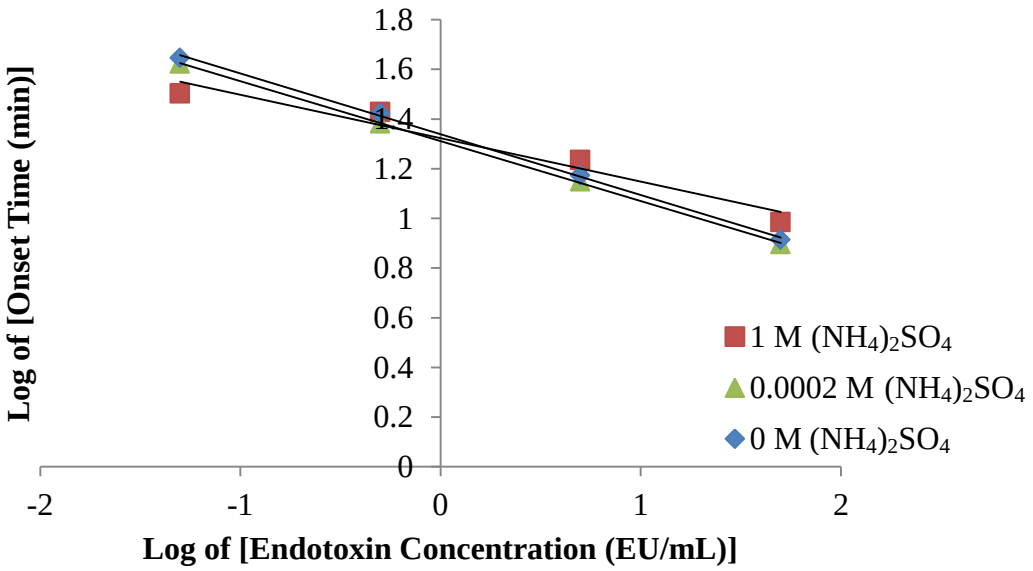

Figure 3.10. Endotoxin standard curves containing various concentrations of ammonium sulfate. Error bars represent ±1 standard deviation of onset time detected in triplicate wells for each sample.

Since the 2 M $(NH_4)_2SO_4$ clearly interferes with the assay, such high concentrations should not be tested. Additionally, the 1 M $(NH_4)_2SO_4$ has a shallower slope compared to the no and low

$(NH_4)_2SO_4$ standard curves. Its slope, -0.17, is two standard deviations away from the average slope of all standard curves, and thus not ideal for use in this assay. Samples containing these high concentrations of $(NH_4)_2SO_4$ (e.g. HIC load flowthrough, wash, and elution fractions) should be diluted with LRW prior to testing.

3.6.3. GFP Interference

A concern for this assay format was interference of GFP, which shows significant absorbance at 405 nm. Since most process samples had to be diluted significantly in order to obtain an endotoxin concentration within the standard curve, any interference was diluted out as well, and the presence of GFP did not affect the assay. However, when testing the endotoxin concentration in the final product, it was anticipated that dilution may not be necessary. To determine the effect of GFP concentration on A_{405} and subsequently define a maximum allowable GFP concentration to prevent assay interference, 100 µL of 2-fold serial dilutions of the 1 g/L GFP standard were plated on the same microplate used for chromogenic kinetic LAL testing. The absorbance is graphed in Figure 3.11 along with the onset OD of 0.15.

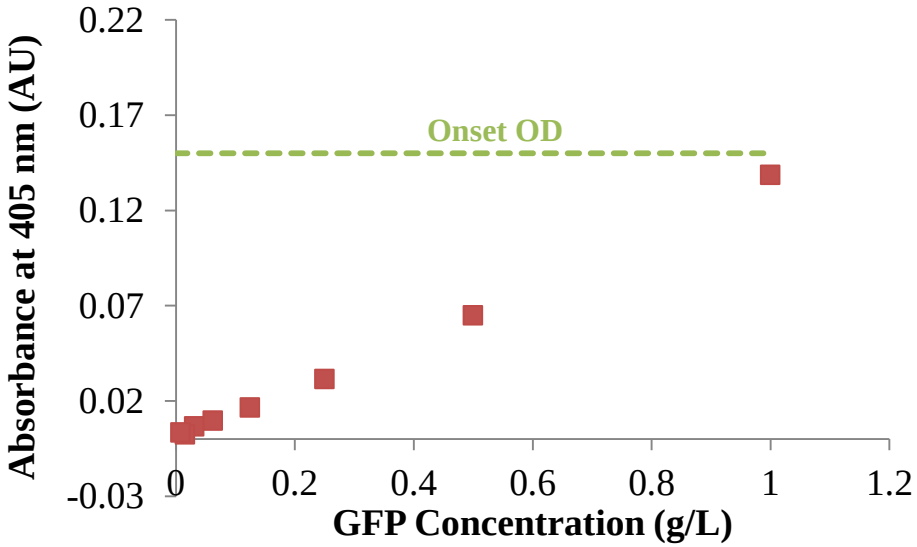

Figure 3.11. GFP interference with the chromogenic kinetic LAL assay.

Given that the initial absorbance for blank wells are between 0.05 and 0.06 AU, the concentration in the sample tested with the chromogenic kinetic assay should contain less than 0.25 g/L of GFP in order to prevent significant contribution to the absorbance due to the pNA released in the assay.

CHAPTER 4: Endotoxin Profile in the Current Intermediate-scale Process

4.1. Release of Endotoxin in Homogenization

The endotoxin concentration throughout the intermediate-scale downstream process was characterized for the current process beginning with endotoxin release during homogenization. The current intermediate-scale process uses two passes, but to explore endotoxin release in this step, the endotoxin and GFP concentrations were measured for samples homogenized at 300, 600, and 900 bar from one to five passes as described in section 2.3.1, and the results are shown in Figure 4.1.

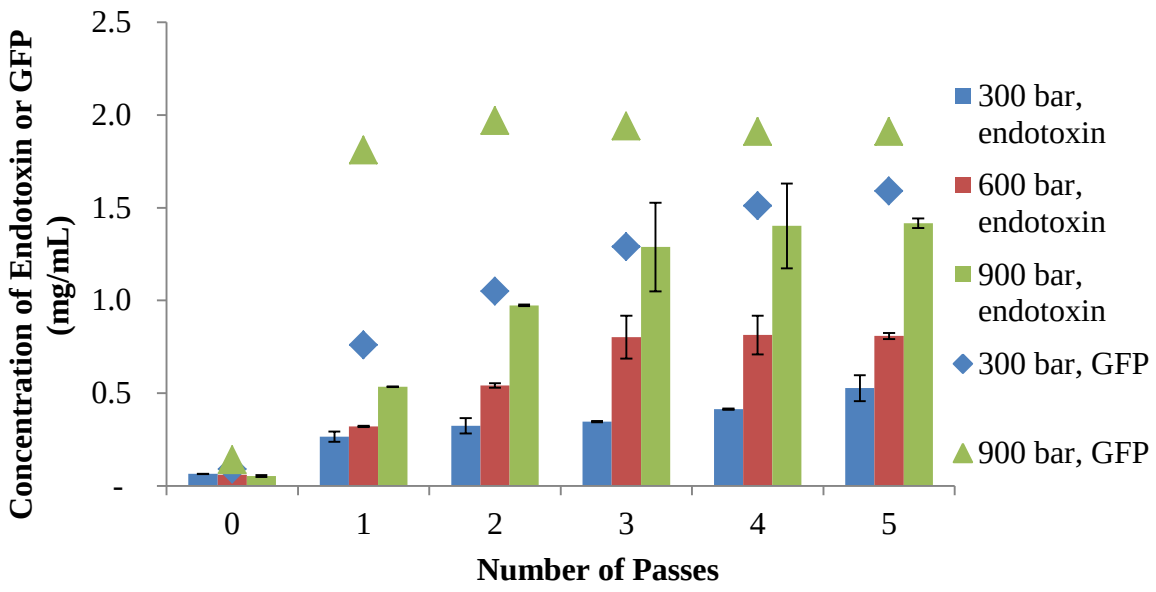

Figure 4.1. Release of endotoxin and GFP in intermediate-scale homogenization. Error bars represent ±1 standard deviation of endotoxin concentration detected in triplicate wells for each sample.

As shown in Figure 4.1, the amount of endotoxin is on the same order of magnitude as the concentration of GFP in the clarified lysate for most homogenization conditions,

illustrating the high level of the impurity that will need to be removed in the downstream process. The current process uses two passes at 900 bar because these conditions release the most GFP of the conditions tested. However, other homogenization conditions shown in Figure 4.1 release similar amounts of GFP. Only 12% higher GFP yield was obtained by using a second pass at 900 bar according to an average of 10 sets of data collected over 4 years (data not shown). However, the data in Figure 4.1 show that 82% more endotoxin is also released into the product stream under these conditions. Replicates of this process with the true intermediate-scale process have shown that 44%, 63%, or 107% more endotoxin is released with a second pass at 900 bar. To help evaluate the optimum set of parameters, the endotoxin/product ratio was calculated for each pass at 300 and 900 bar, and the data are graphed in Figure 4.2.

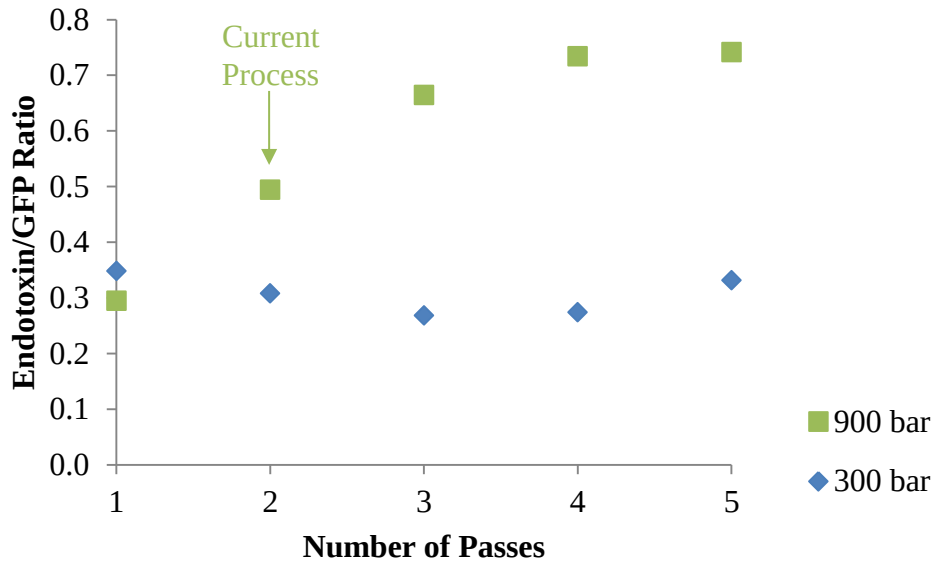

Figure 4.2. Endotoxin to GFP mass ratio in clarified lysate for different homogenization conditions.

All clarified lysate samples homogenized at 300 bar as well as clarified lysate homogenized with one pass at 900 bar have lower endotoxin/GFP mass ratios compared to the current process. The conditions with the highest GFP concentration and lowest endotoxin to GFP ratio, one pass at 900 bar or five passes at 300 bar, could be considered as options for

reducing endotoxin load to the subsequent steps while maintaining similar GFP recovery during homogenization with two passes.

4.2. Removal of Endotoxin in Intermediate-scale Lysate Clarification

The clarification steps of centrifugation and filtration could remove endotoxin if large portions of cell membrane were left after homogenization or if endotoxin aggregates are large enough that they could settle in the centrifuge or not permeate the filter membrane. While running the intermediate-scale process to generate material for chromatography studies, homogenization and clarification samples were tested to determine the effect of the current process centrifugation and subsequent 0.45 μm filtration steps on endotoxin concentration. The results are shown in Figure 4.3.

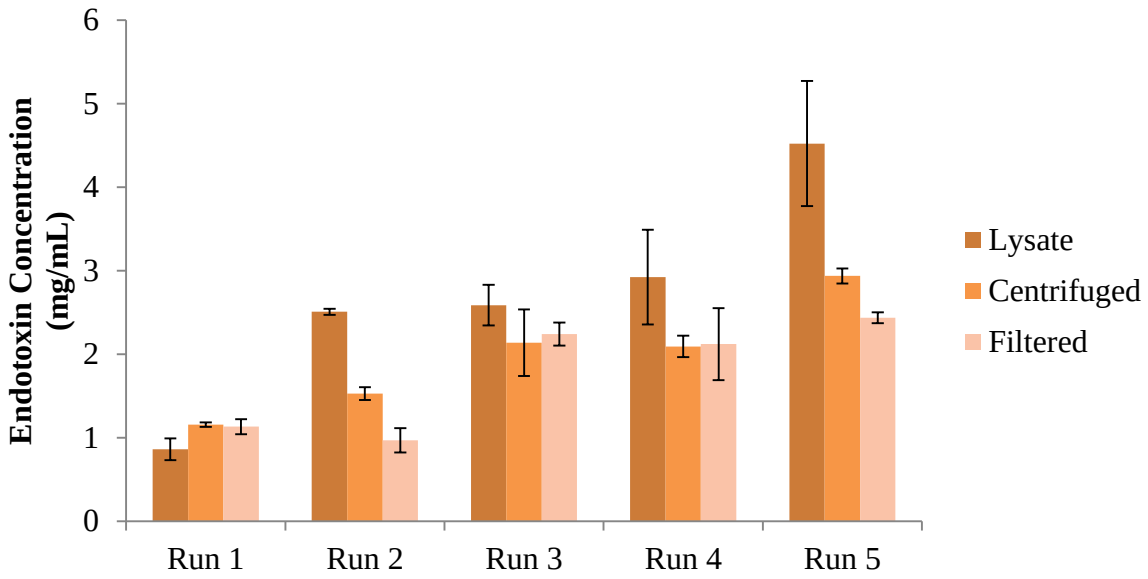

Figure 4.3. Endotoxin concentration in intermediate-scale lysate (900 bar, 2 passes), centrifuged lysate, and fully clarified (centrifuged and filtered) samples produced from five runs. Error bars represent ±1 standard deviation of endotoxin concentration detected in triplicate wells for each sample.

As shown in Figure 4.3, either the effect of centrifugation on endotoxin concentration is within the assay variability (runs 1 and 3) or centrifugation decreases the endotoxin concentration by 28%, 35%, or 39% in runs 2, 4, and 5, respectively. Figure 4.3 also shows

that for three out of five experiments (runs 1,3, and 4), the difference in endotoxin concentration between the centrifuged and filtered lysate is within the assay variability. However, endotoxin concentration decreased from the centrifuged lysate to the filtered sample for run 2 (37% removal) and run 5 (17% removal). These data alone are insufficient for elucidating the effect of centrifugation or filtration on endotoxin removal.

Additional samples were taken during the homogenization study and clarified as described in section 2.3.2 to help better understand the filtration effect. The endotoxin concentration before and after filtration for these samples are shown in Figure 4.4 and Figure 4.5.

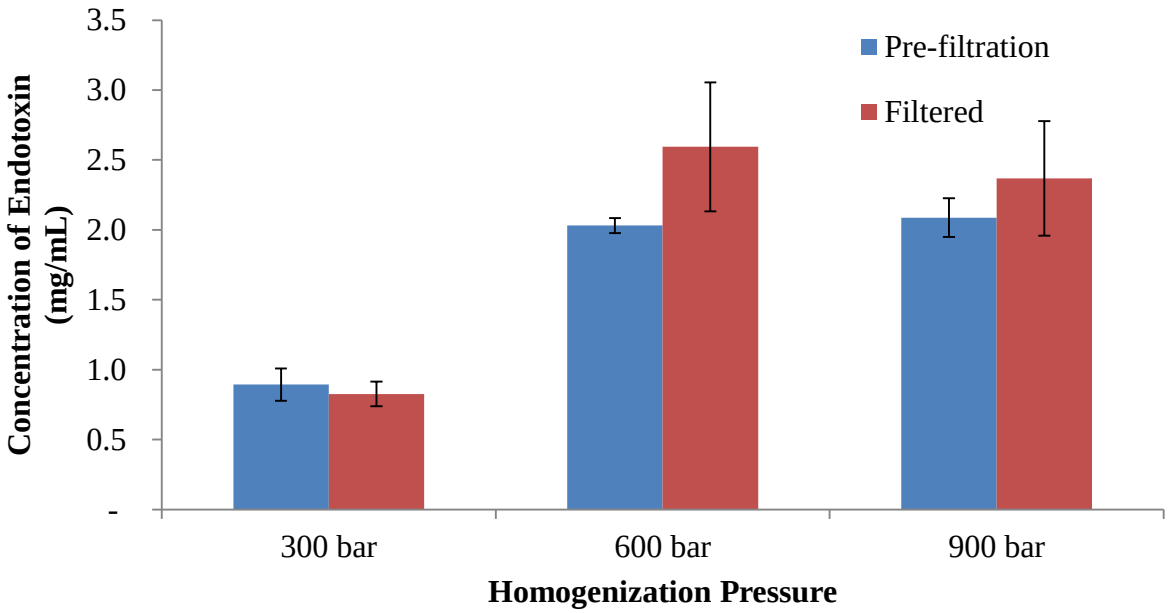

Figure 4.4. Effect of 0.45 µm capsule filtration on endotoxin concentration in centrifuged lysate homogenized with five passes. Error bars represent ±1 standard deviation of endotoxin concentration detected in triplicate wells for each sample.

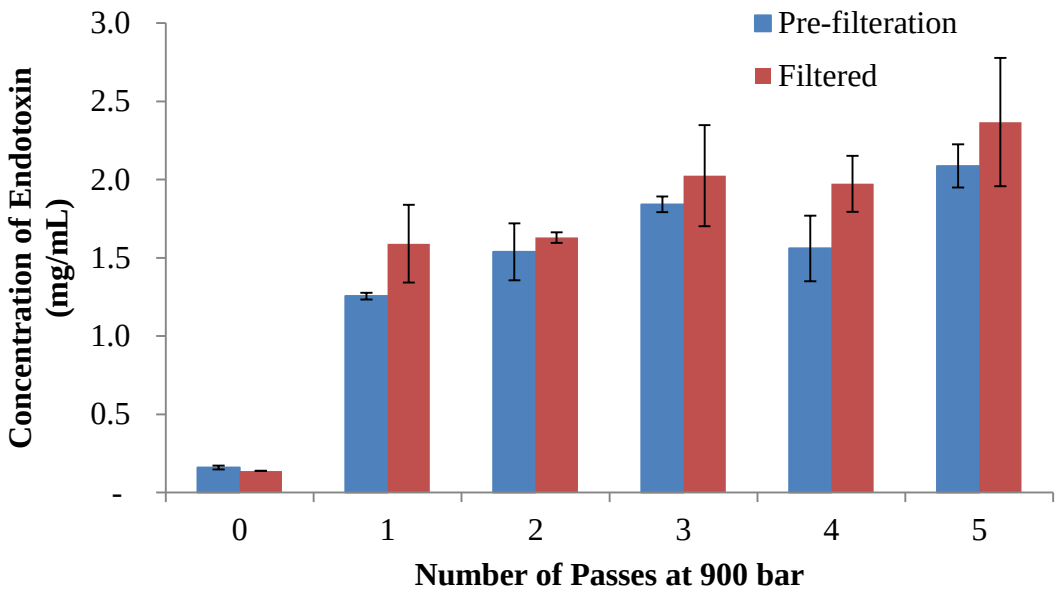

Figure 4.5. Effect of 0.45 µm syringe filtration on endotoxin concentration of centrifuged lysate homogenized at 900 bar. Error bars represent ±1 standard deviation of endotoxin concentration detected in triplicate wells for each sample.

For most of the samples in Figure 4.4 and Figure 4.5, the change in endotoxin concentration after filtration was within the variability of the assay. However, when endotoxin concentration was significant, it appeared to be higher after filtration than before. While the product specification for the capsule filters used for Figure 4.4 indicates that they are nonpyrogenic with <0.18 EU/mL[34] (<0.0216 ng/mL), there is a possibility that glucans from the cellulose acetate filter material contributed to the detected endotoxin concentration. Some glucans are known to interfere with the LAL assay because they can react with the reagent similarly to endotoxins.[35] Because these are the same filters normally used for lysate clarification, the glucan interference is of concern for endotoxin testing in these samples. The Glucashield buffer used to reconstitute the LAL reagent in most of these experiments is meant to block up to 100 ng/mL of β-(1,3)-glucans.[36] To determine if the amount of glucan released from the cellulosic filter is enough to overcome the Glucashield buffer inhibition and cause the observed increase in response from the LAL assay, 50 mM Tris buffer at pH 8.0 was filtered through a 0.45 µm capsule filter and samples of the filtrate were taken for endotoxin testing. The results indicate that the maximum increase is less than 0.24 ng/mL, which is negligible

when testing endotoxin levels in intermediate-scale clarified lysate, typically on the order of 1 mg/mL.

Although the syringe filters used in Figure 4.5 are Nylon and thus do not have the concern of glucan contamination, they are specified as nonsterile and have no indication of endotoxin levels. To determine if this increase in endotoxin was a result of endotoxin on the syringe filters, approximately 10 mL of 50 mM Tris buffer at pH 8.0 was filtered through a 0.45 μm syringe filter, and undiluted samples from before and after filtration were tested for endotoxin concentration. For this experiment, the endotoxin concentration in the buffer decreased from 8.45 ng/mL to 7.22 ng/mL after filtration. This indicates that the increase in endotoxin concentration seen in Figure 4.5 cannot be attributed to endotoxin on the syringe filters. As the possibilities of the filters introducing interfering glucans or endotoxins have been eliminated, the small increases seen in a few of the samples are likely attributed to assay variability, and the amount of endotoxin removed because of centrifuged lysate filtration can be considered negligible.

4.3. Removal of Endotoxin in AEC

Similar AEC columns were loaded with intermediate-scale clarified lysate from six different fermentation batches over the course of one year and yielded very consistent endotoxin distribution results as shown in Figure 4.6.

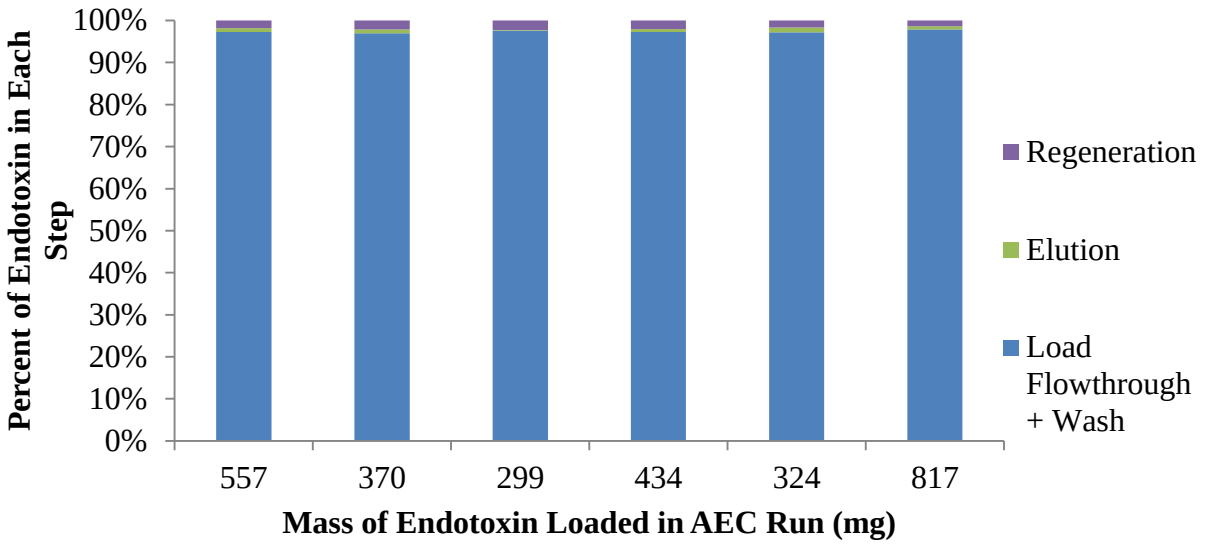

Figure 4.6. Distribution of endotoxin in AEC steps for the six runs of the current intermediate-scale process.

For these six runs, an average of 97.33 ± 0.33% of the endotoxin exiting the column was found in the load flowthrough and wash samples. The total endotoxin from all the fractions collected during the elution step made up only 0.78 ± 0.35% of the endotoxin. The remaining 1.87 ± 0.33% of the endotoxin remained bound to the resin during elution and was removed from the column during the regeneration step. When the sanitization samples were collected tested, they contained less than 0.1% of the total amount of endotoxin exiting the column.

These percentages were contrary to expected results for AEC at pH 8.0. With a pI of approximately 2, the expectation was that endotoxin would bind with higher affinity to the positively-charged Q Sepharose FF resin than GFP, which has a pI of 5.78. These data suggest that most of the endotoxin did not bind to the resin at all. An explanation for the lack of endotoxin binding is that the binding capacity of the resin was significantly exceeded, which resulted in 97% of the endotoxin flowing through without binding to the resin. This hypothesis is supported by the findings of a study by Chen et al., which estimated the binding capacity of endotoxin on Q Sepharose XL, a similar resin to Q Separose FF, to be 900,000 EU/mL resin,[9] which is approximately 0.108 mg endotoxin/mL resin. Comparing this binding capacity with the amount of endotoxin loaded to the AEC column in these intermediate-scale runs, between 8

and 18 mg endotoxin/mL of resin, it is clear that the total amount of endotoxin loaded to the column was well over its binding capacity.

However, if the total binding capacity of the resin is exceeded, endotoxin might be expected to displace GFP. It was evident from the visual presence of GFP in the column as well as the chromatogram (see Figure 2.2) that the GFP remained bound to the resin until the elution step. This effect was likely due to the anion exchange resin also exhibiting size exclusion properties. Although endotoxin monomers are typically 10-20 kDa, when in aqueous solutions, they typically arrange themselves into aggregates, which can have molecular weights up to 1,000 or even 8,000 kDa.[6] The exclusion limit for Q Sepharose Fast Flow pores is 4,000 kDa,[37] and it has been suggested that pore size should be more than five to ten times the size of the binding molecule to avoid mass transfer limitations.[6] Thus, it is likely that most of the endotoxin was unable to access the vast network of ligands inside the pores and could only bind to the outer surface of the bead, which accounts for only 1% of the total binding sites available on a Sepharose resin bead.[6] Since the molecular weight of GFP is 27 kDa, it could easily fit into the pores and occupy ligands that were inaccessible to the endotoxin.

Because the AEC resin in all of the intermediate-scale AEC runs using the existing process seemed to be saturated with endotoxin due to the fact that most of the endotoxin was present in the load flowthrough, it was assumed that the amount of endotoxin that bound during these runs was the maximum amount of endotoxin that could bind to the resin. To estimate the binding capacity of the endotoxin on the Q Sepharose Fast Flow resin, the sum of the endotoxin from the elution, regeneration, and sanitization steps (when applicable) for each of these intermediate-scale runs was divided by the column volume. An average binding capacity of 0.26 ± 0.07 mg endotoxin/mL resin (11.64 ± 3.30 mg endotoxin for the 45.4 mL column) was obtained, which was comparable to the 0.108 mg endotoxin/mL resin found for the Q Sepharose XL study.[9] However, the amount of endotoxin that bound to the resin may not have been constant for all runs. As stated at the beginning of this section, a relatively constant *percentage* of endotoxin was contained in the elution pool and regeneration fractions. This suggests that the amount of endotoxin that bound and eluted may also depend on the total amount of endotoxin loaded to the column. For the six intermediate-scale AEC runs using the

current process, the mass of endotoxin bound to the column (sum of endotoxin in elution, regeneration, and sanitization steps when applicable) as well as the mass of endotoxin in the elution pool are graphed as a function of the mass of endotoxin loaded in Figure 4.7.

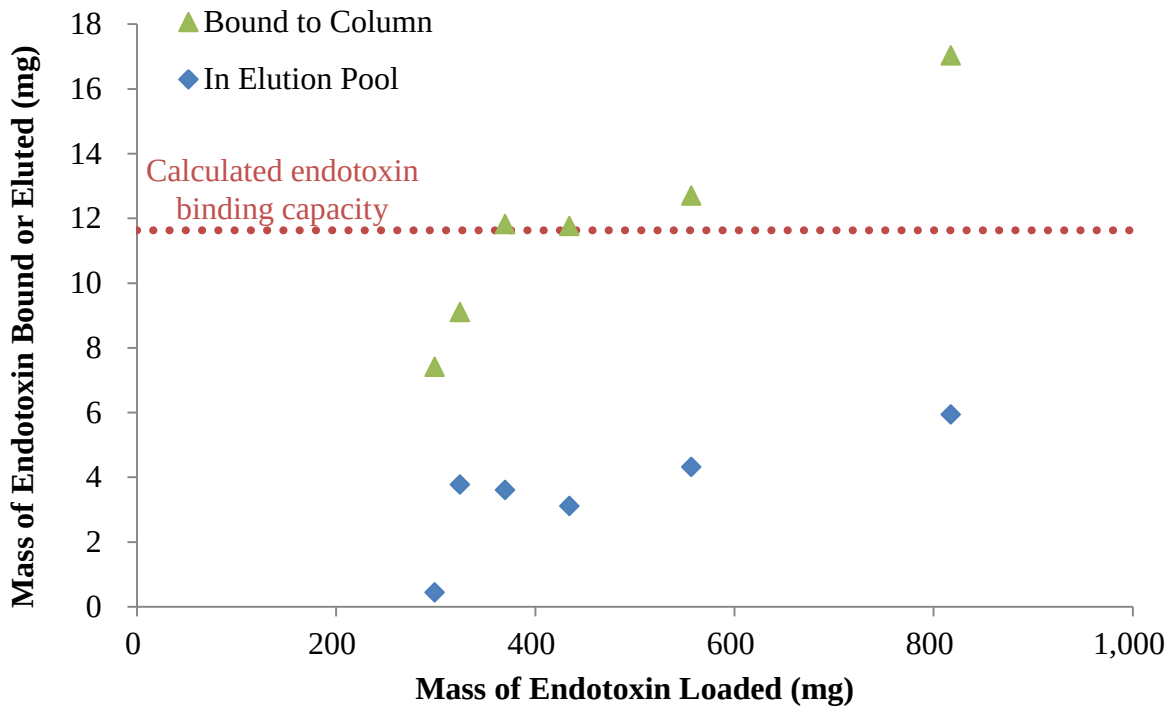

Figure 4.7. Dependence of the amount of endotoxin binding and eluting on the mass of endotoxin loaded for the six current intermediate-scale AEC runs. Mass of endotoxin bound was calculated using the sum of the endotoxin eluting during the elution, regeneration, and sanitization (when applicable) steps.

As observed in Figure 4.7, the amount of endotoxin bound to the column seemed to increase with increasing endotoxin load. A possible explanation for this observation is that with more endotoxin mass, more endotoxin monomers and small aggregates existed in the load. These lower molecular weight molecules were able to diffuse more easily into the pores of the resin beads, which allowed more endotoxin mass to bind. While the mass of endotoxin loaded during these six AEC runs ranged hundreds of milligrams, the amount of endotoxin bound ranged only 10 mg, indicating that the average of the total endotoxin bound may be an

adequate estimate of endotoxin binding capacity.

The amount of endotoxin in the elution pool also appeared to increase with increasing endotoxin load, likely due to the salt being able to only release a certain percentage of the bound endotoxin. Between 0.6 and 5.9 mg of endotoxin was contained in the entire elution pool for these six current intermediate-scale AEC runs. However, only part of the effluent during the elution step (the nine fractions with the most GFP) was taken for continued processing through the HIC step. For five of the six AEC runs, this eluate product pool sample was tested for endotoxin concentration and an average of only 17% ± 8% of the endotoxin in the total elution pool was in the product pool. To determine if the GFP and endotoxin could be better resolved during the AEC elution step, thereby decreasing the amount of endotoxin in the GFP fractions that were pooled for the HIC step, the concentration of endotoxin in each fraction was measured. The elution profiles of GFP and endotoxin for the first AEC run (557 mg endotoxin loaded) are shown in Figure 4.8.

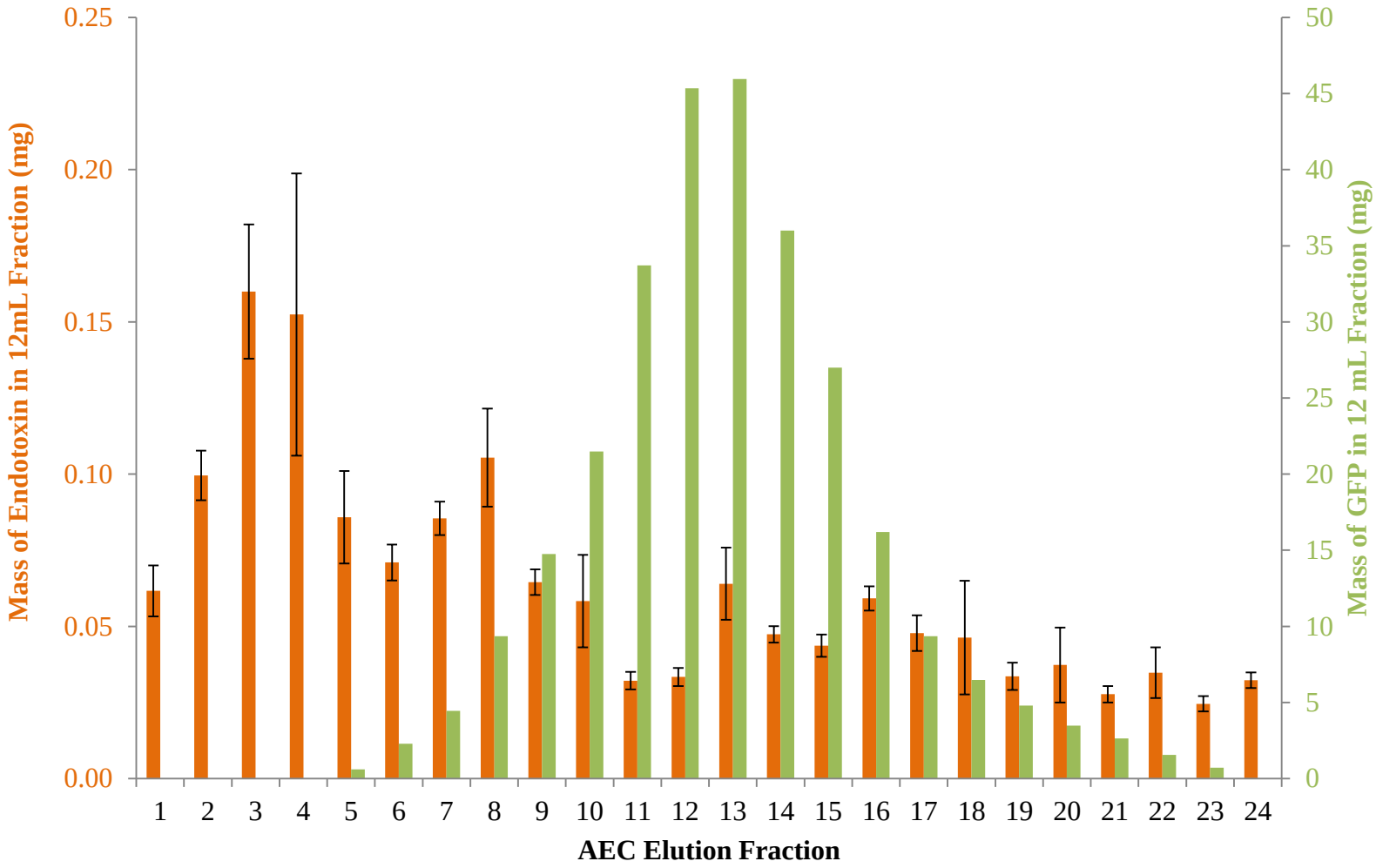

Figure 4.8. Endotoxin and GFP elution profiles for the first intermediate-scale AEC run with the current process. Error bars represent ±1 standard deviation of endotoxin concentration detected in triplicate wells for each sample.

Figure 4.8 shows that the endotoxin concentration was higher in the first several fractions compared to later in the elution step. This trend was consistent for all three AEC runs for which every fraction was tested for endotoxin concentration. The nine fractions containing the most GFP, fractions 9-17 in Figure 4.8, are mostly in the region containing less endotoxin, so the AEC elution does not offer an opportunity for significantly reducing the endotoxin concentration. With only 1-2 mg endotoxin differences in elution pools and little opportunity for improvement in the resolution between GFP and endotoxin, significant improvement in endotoxin removal with AEC may prove difficult as long as the amount of endotoxin loaded to the column exceeds the endotoxin binding capacity of the resin. Despite AEC removing over 99% of the loaded endotoxin, the product eluates from these runs still contained tens of millions of EUs and less than one gram of product. Consequently, the endotoxin removal in the next purification step, HIC, was studied.

4.4. Removal of Endotoxin in HIC

Three HIC runs were performed using the current intermediate-scale process. For each run, fractions were pooled from a different intermediate-scale AEC run, causing variation in the amount of endotoxin loaded. Results are shown in Figure 4.9. For the two runs that had higher endotoxin loading, more endotoxin did not bind to the resin (34% or 44% present in the load flowthrough and wash samples combined) as compared to the lower endotoxin load run (4%). This was a similar phenomenon to that observed in the intermediate-scale AEC runs, which was attributed to reaching maximum endotoxin binding capacity due to inaccessibility of endotoxin to the resin pores.

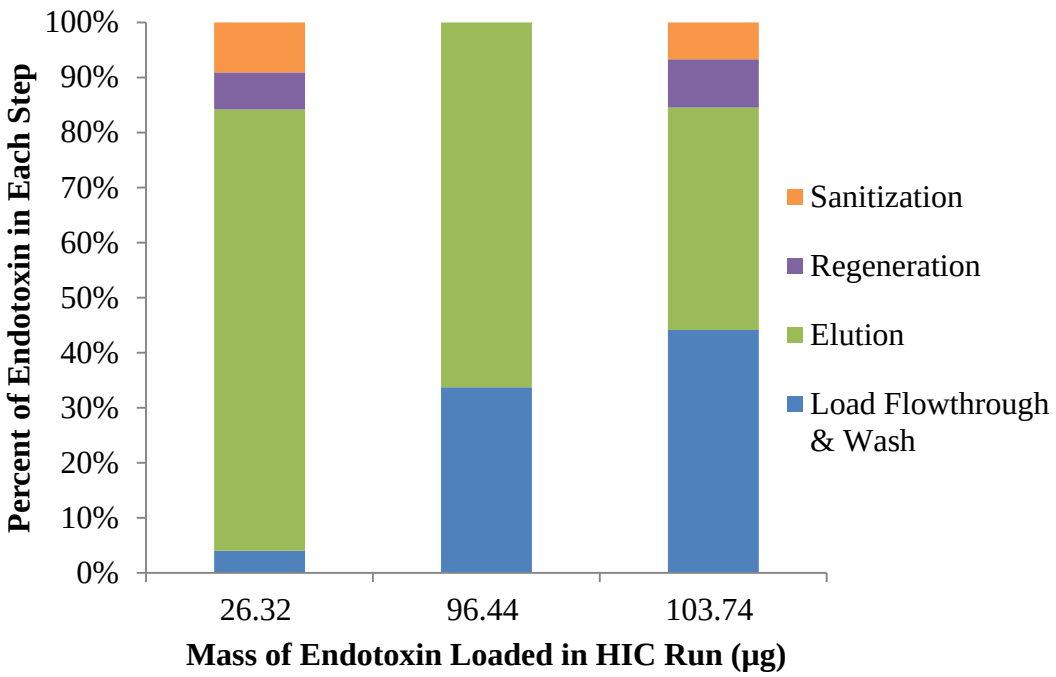

Figure 4.9. Distribution of endotoxin in HIC steps for the current intermediate-scale process. Note that the regeneration and sanitization samples were not collected and tested for the HIC run with 96.44 µg endotoxin load.

As expected because of its hydrophobic lipid A component, most of the endotoxin bound to the HIC resin, and between 40 and 80% of the endotoxin came out of the column during the elution step as shown in Figure 4.9. Despite the variation in endotoxin load among the three runs, when endotoxin concentration in each elution fraction was normalized by the amount of endotoxin loaded, comparable endotoxin profiles resulted as shown in Figure 4.10.

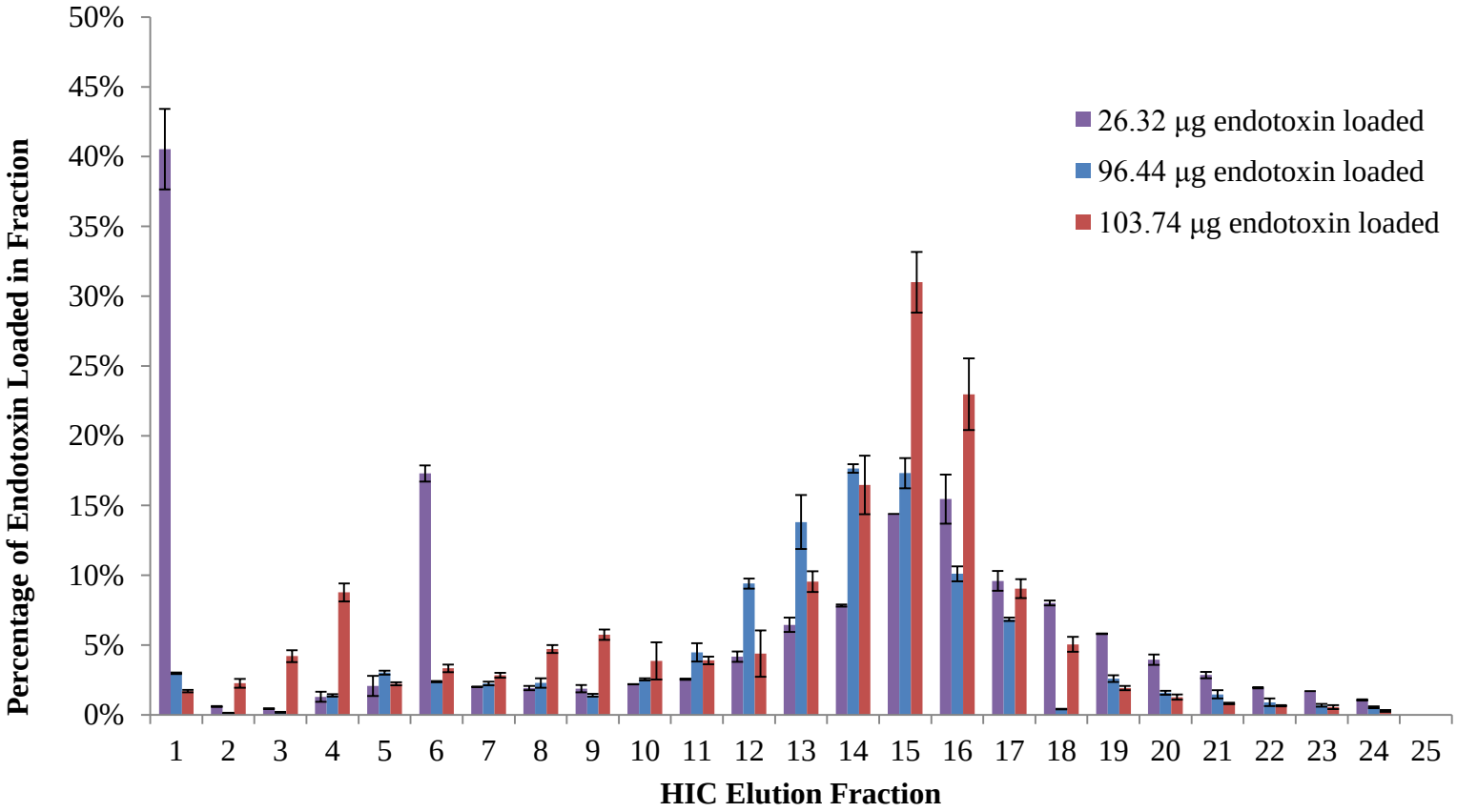

Figure 4.10. Endotoxin elution profiles normalized by loaded endotoxin for three current intermediate-scale HIC runs. The abnormally high endotoxin in fraction #1 is likely attributed to a contamination in the fraction collection line. Error bars represent ±1 standard deviation of endotoxin concentration detected in triplicate wells for each sample.

Since such a high percentage of the loaded endotoxin came out of the column during the elution step, knowing the profile of endotoxin compared to GFP in elution fractions was essential to understanding the extent of endotoxin removal during this step. The elution profile of endotoxin and GFP during the elution step remained fairly consistent; a representative profile is shown in Figure 4.11. When pooling fractions that resulted in 99% GFP recovery, between 48% and 73% removal was achieved for these three endotoxin runs. It is clear from the profile in Figure 4.11 that the endotoxin and GFP peaks overlap significantly. If these peaks were more resolved, endotoxin removal over this step could be improved.

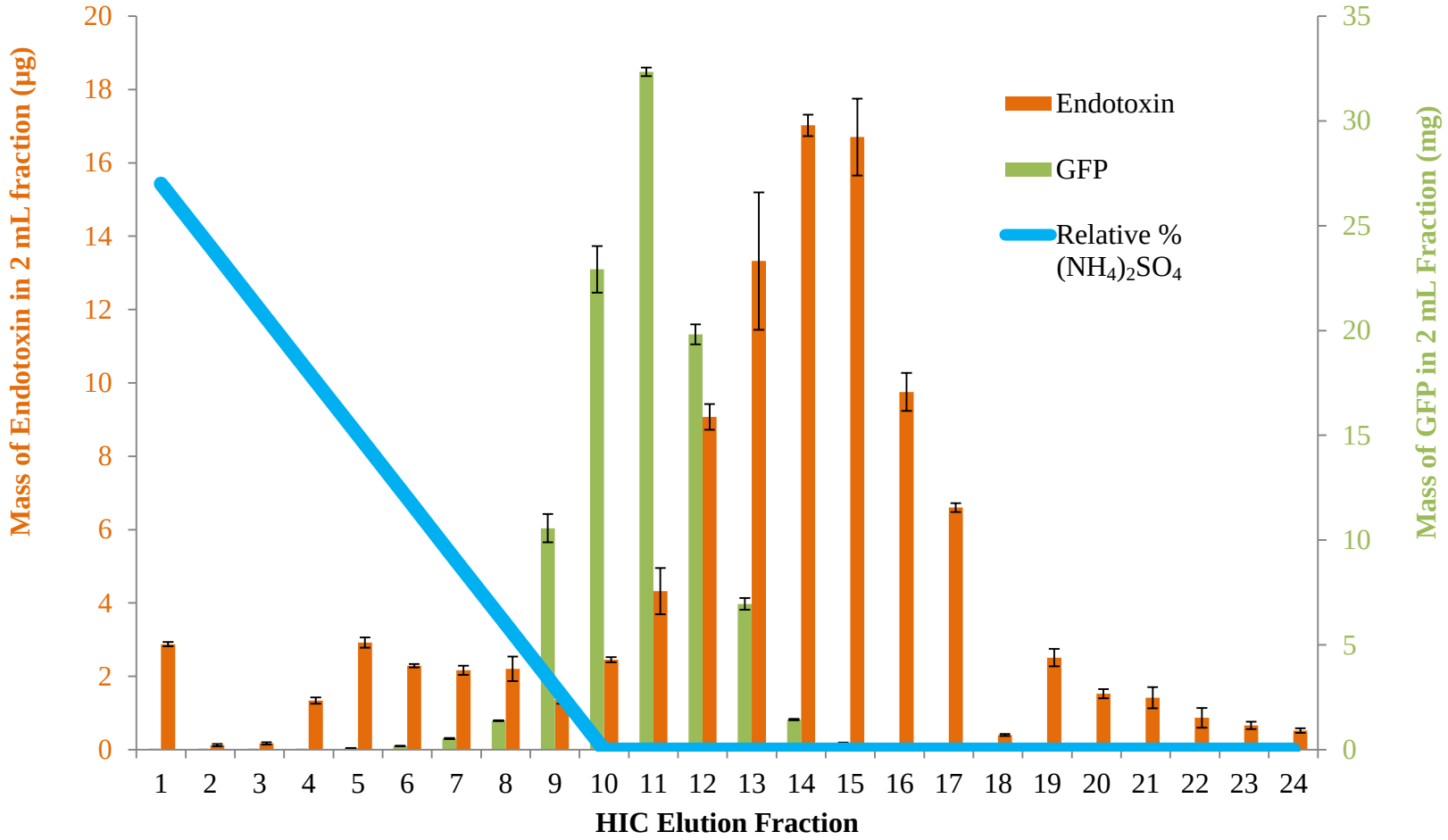

Figure 4.11. Endotoxin and GFP elution profiles for one intermediate-scale HIC run with the current process. Note that the axis for endotoxin mass is in units of micrograms while the units of GFP mass is milligrams. Salt concentration ranges from 2 M to 0 M ammonium sulfate. Endotoxin error bars represent ±1 standard deviation of endotoxin concentration detected in triplicate wells for each sample.

4.5. Final Product Characterization

To evaluate the effectiveness of the existing intermediate-scale process to remove endotoxin, the amount of endotoxin in GFP "drug substance" was compared to the FDA specification for endotoxin – less than 5 EU/kg body weight/hour. To make this comparison, several assumptions were required. First, the average body weight of adults in the US according to the National Center for Health Statistics, 75.4 kg, was used as an estimate of patient body weight.[38] The amount of endotoxin and GFP present in the HIC eluate pool was assumed to be the same as that in the drug product because there are no further purification steps and product loss in the UF/DF step is negligible. Also, it was assumed that the dose of the final product is given in less than one hour. Finally, an assumption was made regarding how much product should be delivered to the patient in an hour. Since GFP is not used as a protein therapeutic, this estimate was made based on other biologic dosage regimens, which vary widely. Some approved protein products produced in *E. coli* have dosages of 0.120 mg (Nivestim),[39] 0.546 mg (Lantus),[40] 6 mg (Neulasta),[41] and 8 mg (Krystexxa).[42] A moderate product dosage of 0.546 mg was chosen for initial calculations for comparison.

Using the aforementioned assumptions, the following equation was used to calculate the final amount of endotoxin in the product with units of EU/kg body weight/hour.

$$\frac{EU}{kg\ body\ weight * hr} = \frac{\sum_{f=i}^{j} EU}{(75.4\ kg) * \left(\sum_{f=i}^{j} mg_{GFP}\right) * \left(\frac{dose}{0.546\ mg\ GFP}\right) * \left(\frac{hr}{1\ dose}\right)}$$

As was apparent from the HIC profile in Figure 4.11, with more GFP-containing fractions pooled as the final product, more endotoxin will be present, especially when pooling the later fractions (11-14). Thus, it is expected that as more GFP is recovered in the HIC step as final product, the EU/kg body weight/hr increases. This relationship is shown for the three current intermediate-scale HIC runs in Figure 4.12. The HIC step yield was calculated by dividing the mass of GFP recovered in the corresponding pooled fractions by the total mass of GFP eluting from the column.

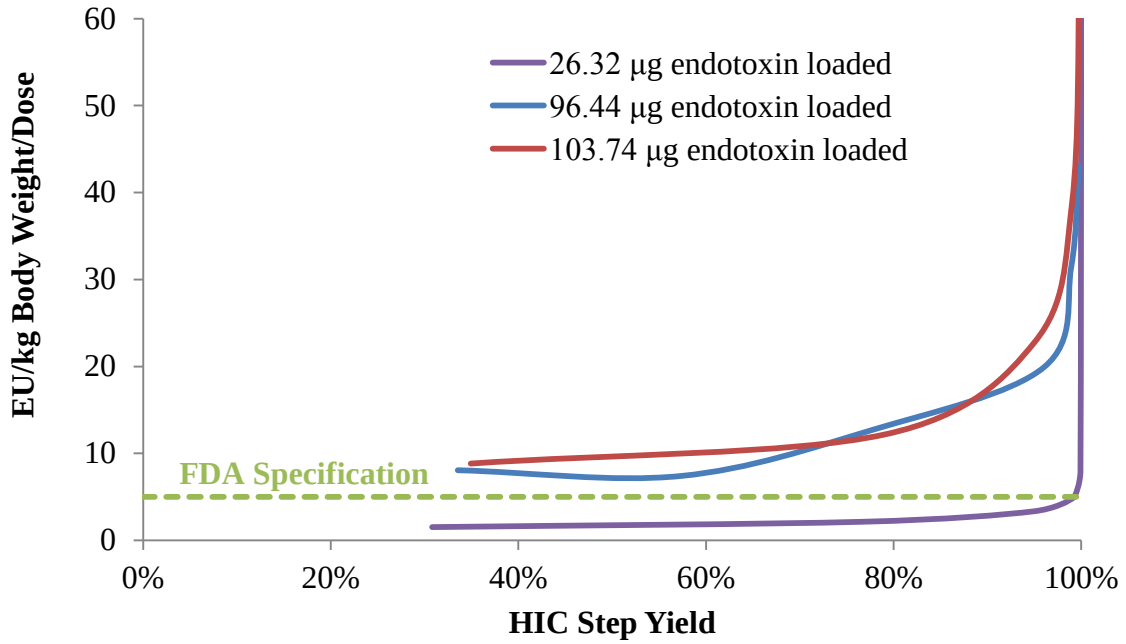

Figure 4.12. Endotoxin in the final product from the current process for an assumed product dosage of 0.546 mg/mL compared to the FDA endotoxin specification.

The calculated values for two of these runs failed to meet the FDA specification limit for maximum allowable endotoxin independent of GFP recovery, but the run with lowest endotoxin load to the HIC step (26.32 µg, purple line in Figure 4.12) produced product below 5 EU/kg body weight/dose when 99% or less of the GFP was recovered from the HIC step. These results suggest that the process was not consistently capable of meeting endotoxin specifications.

As this specification is highly dependent on product dosage, and an assumption of 0.546 mg/mL may not be fully representative, the maximum dosage that could be injected according to the FDA specification of containing 5 EU/kg body weight/hr was calculated according to the following equation:

$$maximum\ dose, \frac{mg\ GFP}{dose} = \frac{\left(\frac{5\ EU}{kg\ body\ weight * hr}\right) * (75.4\ kg) * \left(\sum_{f=i}^{j} mg_{GFP}\right) * \left(\frac{hr}{1\ dose}\right)}{\sum_{f=i}^{j} EU}$$

Figure 4.13 shows the effect of GFP recovery for these three current process runs on the maximum protein dose.

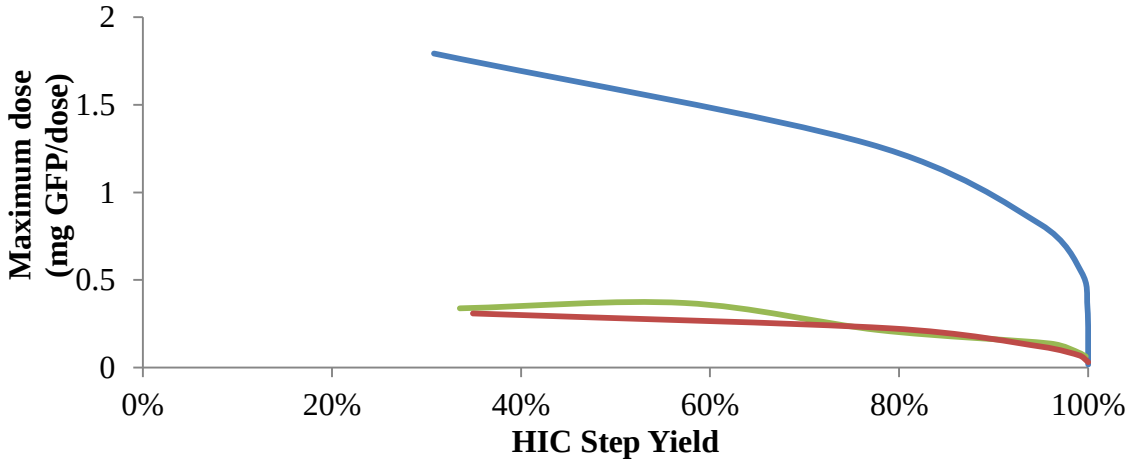

Figure 4.13. Maximum allowable dosage per hour versus HIC step yield for three runs of the current process to meet FDA endotoxin specification of 5 EU/kg body weight/hour.

Assuming that the process performs comparably for all products, the endotoxin removal in this process would only be sufficient for protein therapeutics with dosages of less than 0.2 mg protein/hour (with 80% product recovery). Although the low endotoxin HIC load could support a product with less than 1.2 mg product/hour, the process has proven to not produce product with consistent endotoxin levels. Since some of the runs with the current process had a final product that failed FDA specifications for reasonable dosage levels, improvement of endotoxin removal in the process is necessary.

CHAPTER 5: Improving Endotoxin Removal

5.1. AEC with Large-scale Clarified Lysate

GFP downstream processing with the large-scale equipment resulted in clarified lysate that appeared more transparent than its intermediate-scale equivalent as shown in Figure 5.1. Given the significant visual difference, this large-scale clarified lysate was loaded onto the intermediate-scale AEC column in order to characterize endotoxin removal. The results of this experiment showed the following: the majority of the endotoxin (97.5%) was present in the regeneration fraction; only 0.1% was in the elution pool; and 2.4% did not bind and was found in the load flowthrough and wash samples. This was in contrast to the results obtained in AEC experiments with clarified lysate generated at intermediate-scale, in which 97% of the endotoxin did not bind and was found in the load flowthrough and wash samples.

Figure 5.1. Photograph illustrating the difference in appearance between intermediate and large-scale clarified lysates.

The clarified lysate from large-scale had only 0.0078 mg endotoxin/mg GFP as opposed to 0.5 – 1 mg endotoxin/mg GFP in intermediate-scale clarified lysate. As described in section 4.3, when loading the AEC column with intermediate-scale clarified lysate, most of the endotoxin did not bind because 25 to 70 times the endotoxin binding capacity on the resin

was loaded. Loading the large-scale clarified lysate on the AEC column had such a different endotoxin profile because the load contained significantly less endotoxin, and thus did not exceed the endotoxin binding capacity. Only 5.7 mg of endotoxin (0.13 mg endotoxin/mL resin) was loaded onto the column from the large-scale clarified lysate, which was less than half of the endotoxin binding capacity estimated from the six intermediate-scale AEC experiments. Thus, the fact that most of the endotoxin eluted during the regeneration step can be explained by the resin having sufficient capacity to bind almost all of the endotoxin from large-scale clarified lysate as well as the endotoxin having a more negative charge and therefore binding to the resin with greater affinity relative to GFP.

To confirm these conclusions, AEC was performed with a second batch of large-scale clarified lysate. This batch had slightly higher endotoxin content with 0.0604 mg endotoxin/mg GFP, corresponding to loading 42.24 mg endotoxin, over 3.5 times the average endotoxin binding capacity of the resin. For this run, the endotoxin eluting from the column was more evenly distributed through the chromatography steps: 39% of the endotoxin did not bind to the resin and was accounted for in the load flowthrough and wash samples, 3% was found in the pool of all elution fractions, and 58% was in the regeneration and sanitization samples. Although a higher percentage (3%) of endotoxin in the elution pool was found for this run compared to the percentage of endotoxin in the elution pool when loading the current intermediate-scale process (1%), the actual amount of endotoxin present was significantly less. There was approximately one-tenth of the endotoxin in the elution pool for the 0.0604 mg endotoxin/mg GFP load and one-thousandth of the endotoxin in the elution pool when loading the 0.0078 mg endotoxin/mg GFP material. This follows the trend mentioned in section 4.3, which found that the amount of endotoxin in the elution pool decreased with decreasing endotoxin loading. Without any further purification, the entire elution pool from the lowest endotoxin load AEC run could meet the FDA endotoxin specification for drug products with dose requirements as high as 10 mg. This shows the importance of lysate clarification steps in endotoxin removal from the process.

5.2. Intermediate-scale Lysate Clarification Improvement

Three potentially impactful processing differences were identified and studied for the

purpose of understanding the contribution of clarification steps to endotoxin removal so that improvements in endotoxin removal could be made at intermediate-scale:

1. The large-scale clarification process did not include a centrifugation step prior to filtration.
2. In large-scale, there were long (weeks) and inconsistent hold times between homogenization pass 1 and pass 2 (the final pass) as well as between pass 2 and filtration. Intermediate-scale centrifugation and filtration occurred the same day as both homogenization passes.
3. The large-scale process used filters with 0.2 μm pores rather than 0.45 μm pores.

The effect of filtration pore size on the concentration of endotoxin in intermediate-scale centrifuged lysate was determined in a study with several syringe filters of different pore sizes described in section 2.3.3. The results are shown in Figure 5.2 along with the large-scale clarified lysate results as benchmarks of low endotoxin-to-GFP ratio.

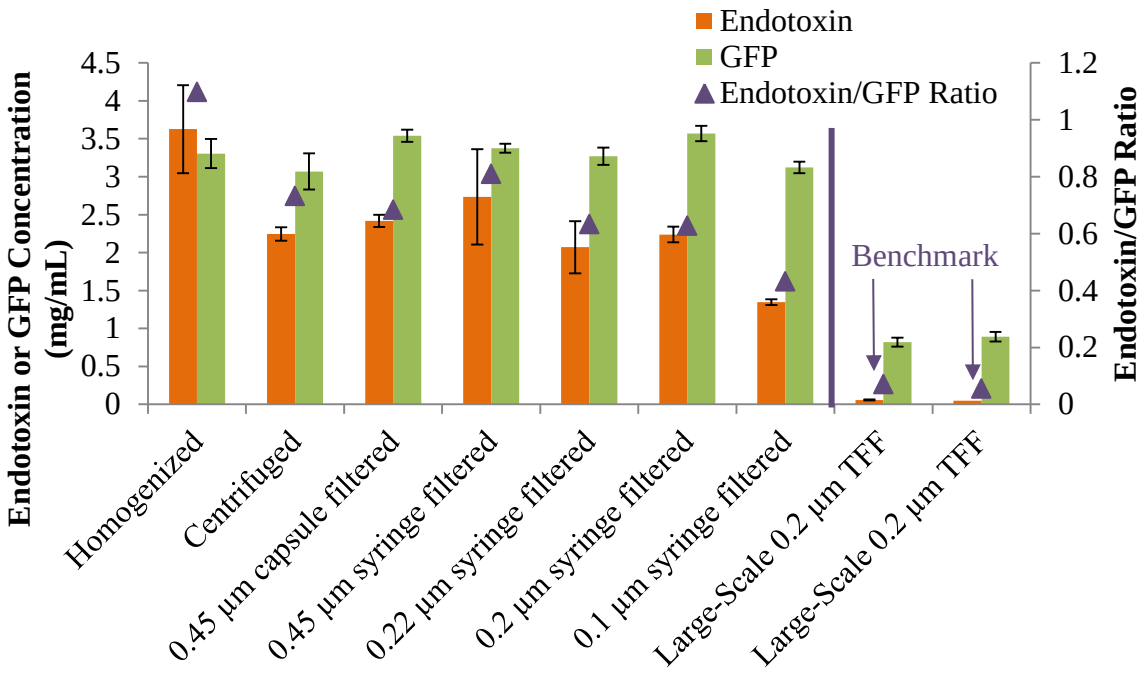

Figure 5.2. Effect of filter pore size on endotoxin removal from centrifuged intermediate-scale lysate as compared to the low endotoxin large-scale clarified lysates. Endotoxin error bars represent ±1 standard deviation of endotoxin concentration detected in triplicate wells for each sample.

As shown in the Figure 5.2, decreasing filter pore size did not significantly affect the endotoxin concentration in the filtrate until a pore size of 0.1 µm. This change in filter pore size was able to decrease the endotoxin to GFP ratio from 0.73 in the centrifuged lysate to 0.43 in the 0.1 µm filtrate, but was not sufficient to decrease the ratio to be comparable to that of the two large-scale clarified lysates, 0.071 or 0.056.

To explore the effects that hold time and centrifugation have on endotoxin concentration of clarified lysate, a hold time study was performed as described in section 2.3.3. Figure 5.3 and Figure 5.4 show the results of these studies for centrifuged and non-centrifuged lysates and their filtrate samples.

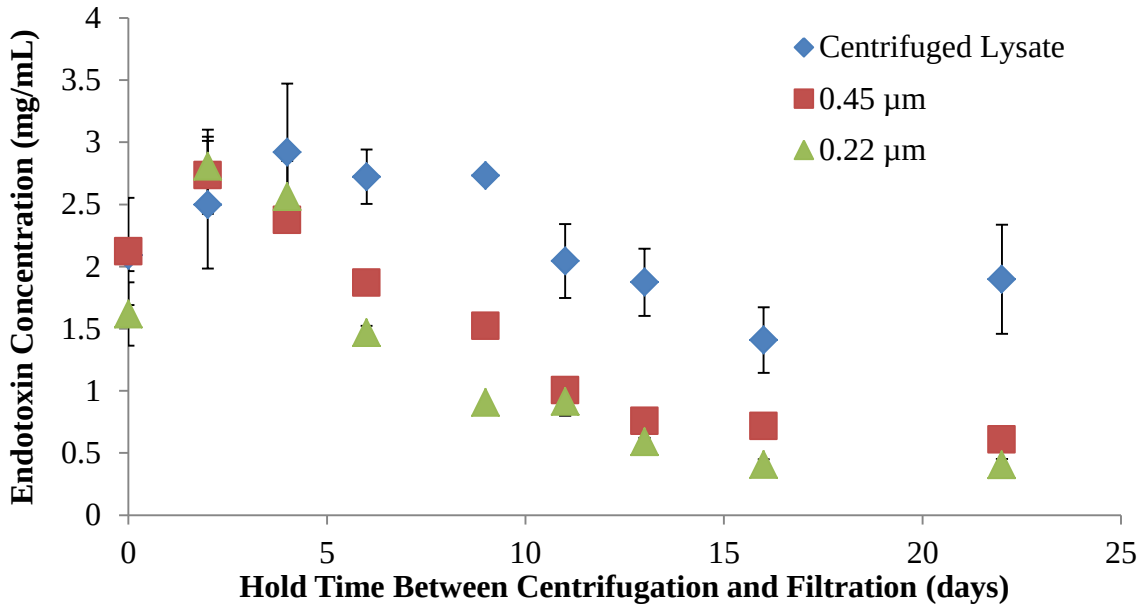

Figure 5.3. Effect of hold time prior to syringe filtration with centrifuged intermediate-scale lysate. Error bars represent ±1 standard deviation of endotoxin concentration detected in triplicate wells for each sample.

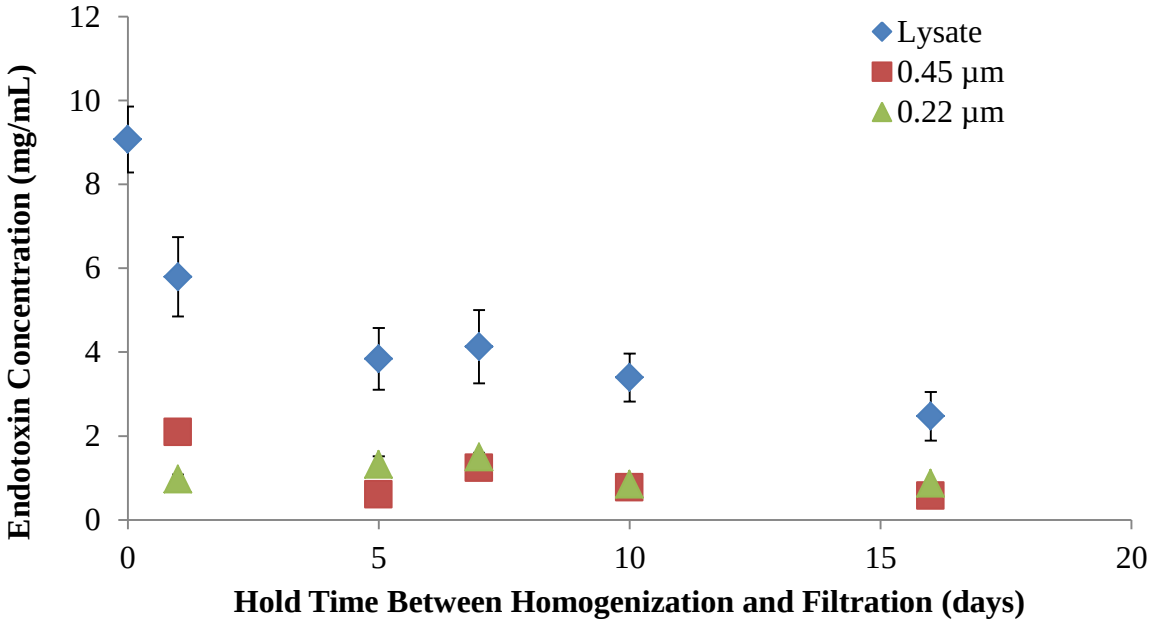

Figure 5.4. Effect of hold time prior to capsule filtration with non-centrifuged intermediate-scale lysate. Error bars represent ±1 standard deviation of endotoxin concentration detected in triplicate wells for each sample.

The immediate filtration of centrifuged lysate shown in Figure 5.3 was consistent with the initial clarification studies (Figure 4.3) as well as the pore size study (Figure 5.2), which showed little or no decrease in endotoxin concentration. Over time, precipitate settled at the bottom of the container. The lysate samples simultaneously decreased in endotoxin concentration over time, suggesting that endotoxin may be precipitating. Once significant precipitation was observed, the centrifuged lysate was not mixed prior to filtration or testing. The non-centrifuged lysate, however, was mixed prior to each filtration. Figure 5.3 shows that a significant difference in endotoxin concentration upon filtration does not occur until the centrifuged lysate had been held for approximately 6 days. The endotoxin concentration in the filtered centrifuged lysate gradually decreased over time until reaching a low of 0.4 mg/mL with the 0.2 μm filter after 16 days. Compared to the centrifuged lysate, the non-centrifuged lysate had approximately 5 times more endotoxin likely due to fermentation and cell paste variability as well as lack of a centrifugation step. Despite the high initial endotoxin concentration, direct filtration of the lysate was still able to significantly decrease endotoxin levels to values as low as the centrifuged and filtered clarified lysate. The percent removal was calculated for each condition using the starting endotoxin concentration of lysate or centrifuged lysate at that time point. Figure 5.5 shows the percent of endotoxin removed after 0.2 μm filtration of both centrifuged and non-centrifuged lysate over time.

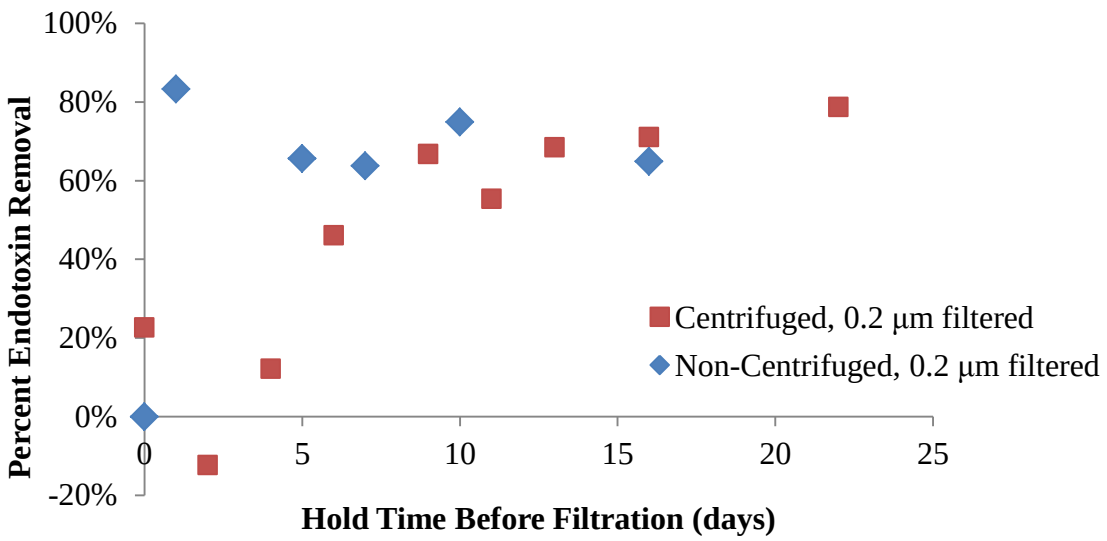

Figure 5.5. Comparison of endotoxin removal for 0.2 µm filtration of centrifuged and non-centrifuged intermediate-scale lysate after various hold times

Most importantly, the endotoxin decrease observed with the direct filtration clarification process occurred on day 1 after homogenization. This suggests that having large particulates, which were typically removed during centrifugation, in the material to be filtered aided in the removal of additional endotoxin, which otherwise would permeate the membrane. It is hypothesized that the large aggregated particles are likely to form a cake on the membrane, which could act as a filter aid to catch smaller endotoxin aggregates.

Although the GFP concentration determined by the fluorescence assay remained relatively constant for all of these filtered samples (data not shown), other product quality attributes such as amino acid truncation, oxidation, or isomerization were not studied. In biopharmaceutical development, the impact of extended hold times on the critical quality attributes of the product require thorough assessment in order to implement a hold time in a validated process. In general, it is not recommended or efficient to have a 16 day hold time of very impure product in a biopharmaceutical manufacturing process. Thus, for the intermediate-scale process, immediate filtration of lysate to decrease endotoxin levels in the AEC load was preferred.

5.3. Improved Lysate Clarification Confirmation Run

In order to confirm the effect of directly filtering the lysate on the endotoxin profile in the intermediate-scale downstream process, 6 L of fresh intermediate-scale lysate was prepared. Enough lysate was filtered to load the AEC column, and some of the lysate was clarified using the steps for the current process for direct comparison. Figure 5.6 shows how the intermediate-scale lysate clarified by not centrifuging and directly 0.22 µm capsule filtering was able to achieve a similar clarity and color to that seen at large-scale.

Figure 5.6. Photograph illustrating the visual difference in the same intermediate-scale lysate prepared using the current clarification process (right) and the direct 0.22 µm filtration process mimicking large scale (left) prepared on the same day.

This lysate contained 4.52 mg/mL of endotoxin, which is almost 2-fold higher than lysate produced in most of the previous intermediate-scale runs. The current clarification process decreased endotoxin concentration to 2.94 mg/mL. This step was followed by 0.45 µm filtration, which decreased the endotoxin concentration in the clarified lysate to 2.44 mg/mL, for an overall 46% removal in endotoxin for the current clarification process. Filtering the lysate through the 0.22 µm capsule filter without centrifugation decreased the endotoxin

concentration to 0.26 mg/mL, removing 94% of the endotoxin from the lysate. This was consistent with direct filtration of lysate results described in the previous section.

In order to load the typical 700 mg of GFP from the 0.22 µm-direct-filtered lysate onto the AEC column, 6.8 times more than the average endotoxin binding capacity (6.8 x BC) of the column was loaded. The profile of the endotoxin for this run followed the trend of increasing endotoxin in the load flowthrough and wash with increasing endotoxin load. A comparison of where the endotoxin elutes for these significantly different clarified lysates is shown in Figure 5.7 in order of increasing endotoxin load.

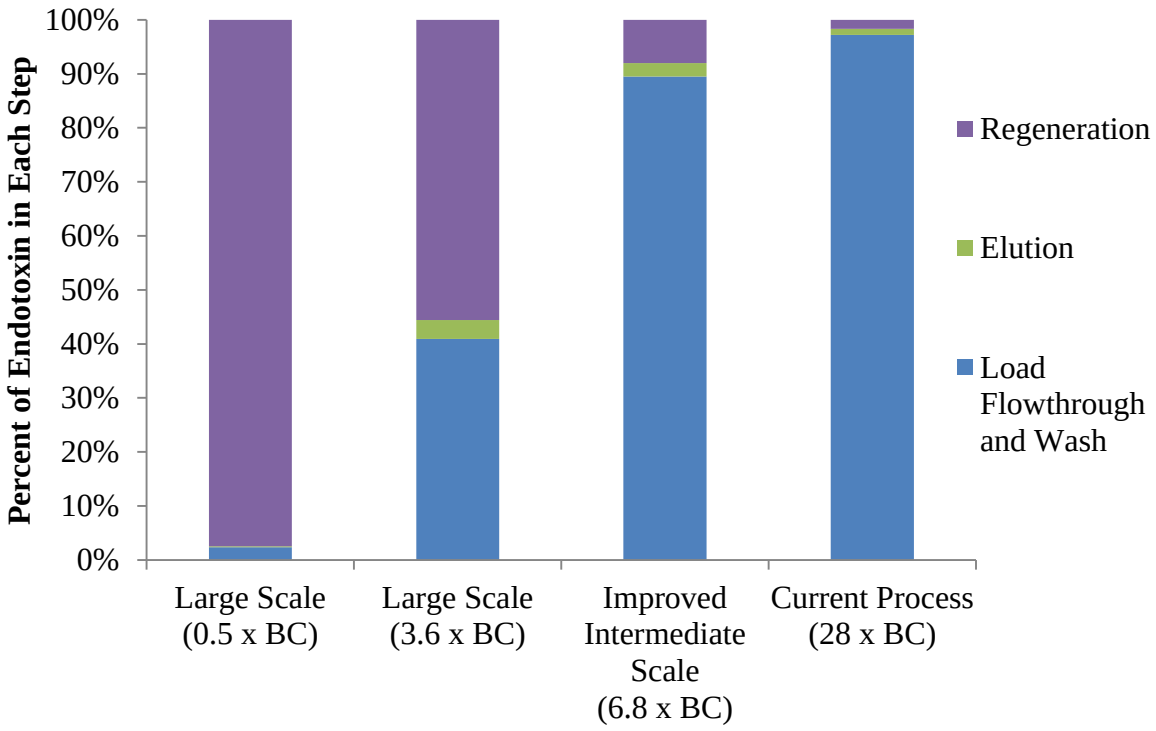

Figure 5.7. AEC endotoxin profile trend with increasing endotoxin loading.

While the AEC elution pools from the current intermediate-scale process contained an average of 3.5 mg of endotoxin, the improved clarified lysate run had 1.31 mg of endotoxin in the total elution step pool. This observation fit with the trend of decreasing endotoxin in elution pool with decreasing endotoxin load, which is shown with all AEC runs in Figure 5.8.

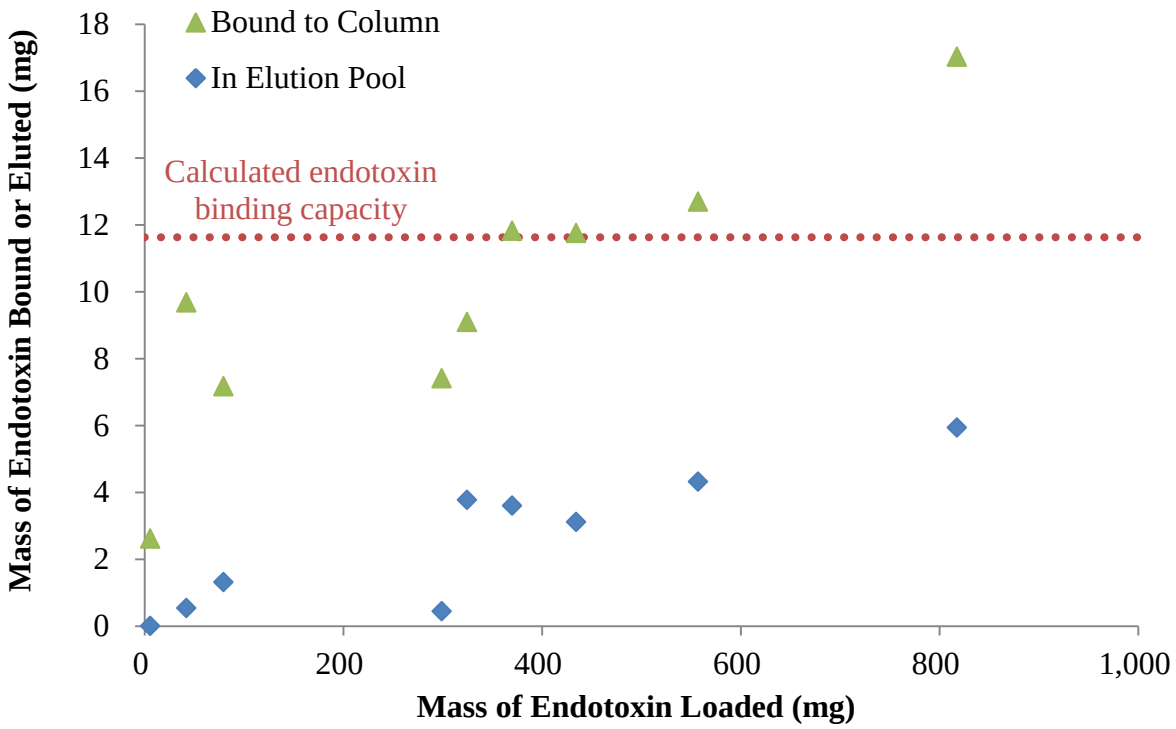

Figure 5.8. Dependence of the amount of endotoxin binding and eluting on the mass of endotoxin loaded to AEC for the two large-scale clarified lysate, improved intermediate-scale clarified lysate, and six current intermediate-scale clarified lysate loads. Mass of endotoxin bound was calculated using the sum of the endotoxin eluting during the elution, regeneration, and sanitization (when applicable) steps.

The amount of endotoxin present in the nine fractions that contained the most GFP was approximately 0.22 mg, 17% of the total pooled eluate. Although the improved clarification process was capable of producing AEC load material with one-tenth of the endotoxin, the improvement was not reflected to this extent in the AEC eluate, which still contained almost 11 million EUs for less than 1 g of GFP product. As predicted in section 4.3, significant increase in AEC endotoxin removal was most easily accomplished when lysate clarification was capable of reducing endotoxin levels to below the endotoxin binding capacity of the resin.

While this clarified lysate had one-tenth of the endotoxin as the same lysate clarified with the current processing steps, it was still almost 10-fold higher than the large-scale clarified lysate with the higher endotoxin load. The hold time experiments showed that endotoxin concentration in the filtrate decreased if the lysate was held for several days prior to filtration.

Thus the lack of hold time for the improved intermediate-scale lysate clarification process is a likely cause for the higher endotoxin concentration. After five days of hold time for the 5 L of lysate, a significant amount of precipitate was observed, as shown in Figure 5.9.

Figure 5.9. Photograph illustrating precipitate in intermediate-scale lysate five days after cell lysis.

To determine the effect of holding the lysate on endotoxin concentration in the clarified lysate, the material in Figure 5.9 was filtered and tested for endotoxin concentration. First, several milliliters of only the liquid portion of the lysate in Figure 5.9 was pumped through a 0.22 μm capsule filter. Then, the precipitate was mixed with the liquid portion using a magnetic stirrer for several minutes, and the mixture was filtered through a 0.22 μm capsule filter. The concentration of endotoxin in clarified lysate for this experiment using each of the described methods is shown in Figure 5.10.

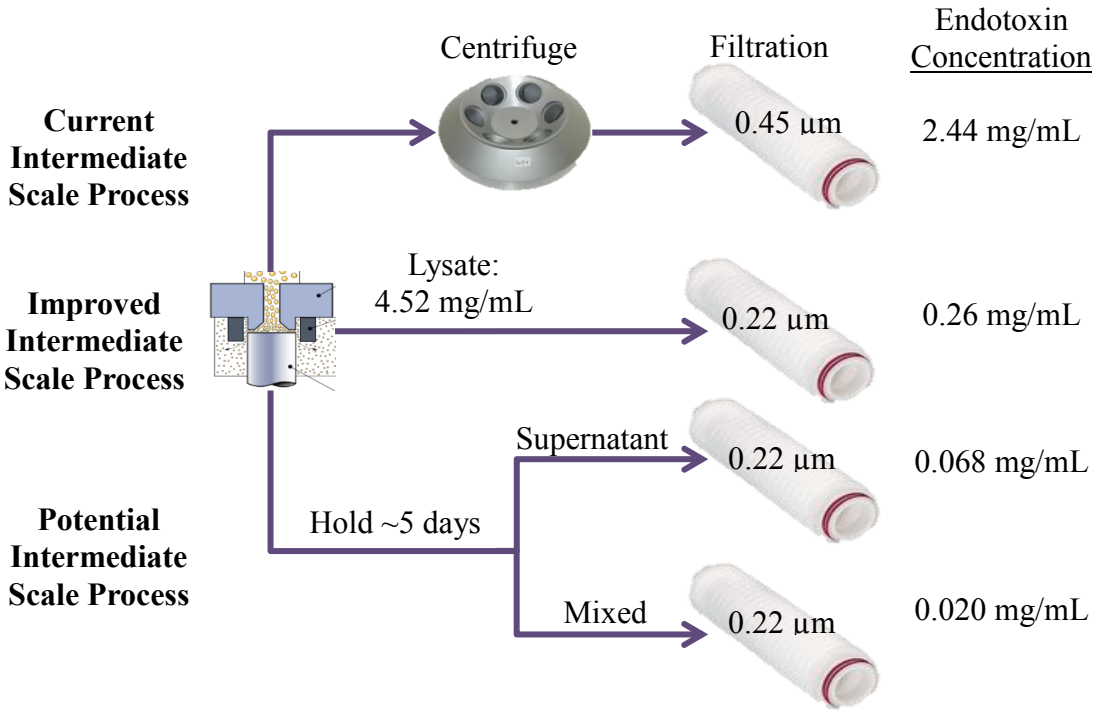

Figure 5.10. Endotoxin levels in clarified lysate using various clarification steps.

Figure 5.10 shows that removing the centrifugation step produces a filtrate with approximately one-tenth of the endotoxin. The endotoxin concentration of clarified lysate was further reduced by one-tenth by holding the lysate for five days and filtering the mixed held lysate. Additionally, the endotoxin concentration in the filtrate of the mixed lysate was less than one-third of that in the filtrate of the lysate supernatant. The non-centrifuged lysate contained relatively large cell debris, and the mixed held lysate contained the cell debris as well as relatively large particulates formed over the hold time. As both of the filtrates that contained less endotoxin had more particulates prior to filtration, these observations supported the hypothesis developed in section 5.2 that the particulates aid in the filtration of endotoxin. Filtering the held lysate decreased endotoxin levels of intermediate-scale lysate so low that when loading 700 mg of GFP on the AEC column, only 0.75 times the endotoxin binding capacity would be loaded. With this clarified lysate, the AEC step would have likely behaved similarly to the lowest endotoxin load from large-scale, which loaded 0.5 times the endotoxin binding capacity and decreased the endotoxin levels from 5.77 mg endotoxin loaded to only

3.6 μg endotoxin (approximately 30,000 EUs) in the total elution pool. The AEC eluate and subsequent HIC fractions would likely have significantly lower endotoxin, which would allow for the final product to meet the FDA endotoxin specification. However, having these long hold times is not practical, and its impact on product quality is not well understood. Since filtration without centrifugation was not capable of producing sufficiently low endotoxin in the AEC eluate without significant hold time in the process, improvement of the HIC step was explored.

5.4. HIC Resolution Improvement

From the HIC elution profile in Figure 4.11, it is clear that better resolving the endotoxin and GFP peaks would decrease the endotoxin concentration in the final product. Resolution of a chromatography step is dependent on elution buffer pH and conductivity gradient slope, bead size, ligand density on the bead, flow rate, and protein load.[43] In order to minimize significant changes to the current process, improvement focused on the gradient slope of the elution buffer conductivity. Ammonium sulfate load concentration and elution gradients were varied in order to develop a shallower gradient in an attempt to better resolve the endotoxin from the GFP product. It is well known that decreasing the slope of the elution gradient generally helps to improve resolution between proteins in chromatography.[44] However, making the gradient shallower while maintaining the same ammonium sulfate concentration range for the linear gradient would cause the processing time to increase. Thus, to maintain a consistent processing time, methods to narrow the ammonium sulfate linear gradient concentration range were explored.

As the GFP seemed to elute in the latter half of the normal linear gradient for the current process, equilibration of the column and loading the material at only 1 M $(NH_4)_2SO_4$ was considered. Equilibrating, loading, and consequently starting the elution at a lower salt concentration would allow for the gradient to be shallower while maintaining the same processing time. In this experiment, over half of the GFP flowed through the column during the load and wash steps, demonstrating that 1 M $(NH_4)_2SO_4$ was not enough to bind all of the GFP to the resin. However, immediately decreasing the concentration to 1 M $(NH_4)_2SO_4$ at the start of the elution step after equilibrating, loading, and washing at 2 M $(NH_4)_2SO_4$ allowed the GFP

to fully bind to the resin but elute closer to the beginning of the elution step. This allowed time to make the elution gradient shallower to better resolve the later-eluting endotoxin peak from the GFP peak. Along with starting at the lower salt concentration, the gradient was also made shallower by increasing the gradient portion of the elution to 30 mL (6 CVs) as opposed to the 20 mL (4 CVs) of the current process. To maintain processing time, the hold at 0 M $(NH_4)_2SO_4$ after the gradient was shortened. Figure 5.11 shows the elution salt gradient methods for both the current process as well as the shallower gradient process.

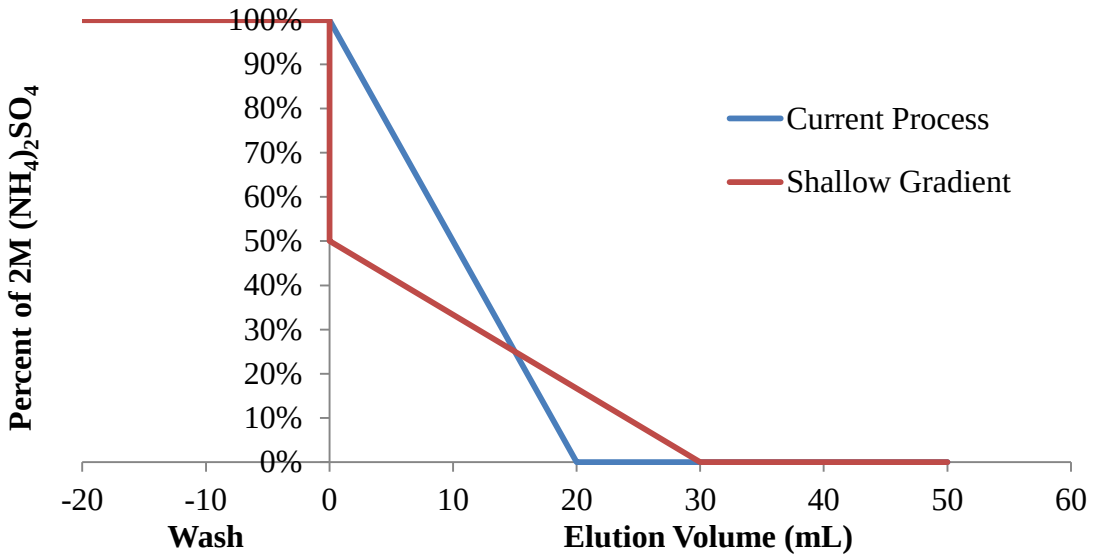

Figure 5.11. Shallow gradient HIC elution method compared to the current elution method. Note that for both processes, total elution volume was maintained at 50 mL, or 10 CVs.

AEC eluate from the current process was used to load the HIC column for this experiment in order to be more comparable to the current process and assess the effect of only the HIC method change. This run contained 61% of the endotoxin in the elution pool, which is comparable to the current process runs. However, observing the elution profile of GFP and endotoxin in each elution fraction as shown in Figure 5.12, it was clear that making the gradient shallower was successful in improving the resolution between GFP and endotoxin. Because the initial ammonium sulfate concentration was immediately decreased to 1 M for this method, the endotoxin that eluted in the first several fractions of Figure 4.11 likely all eluted at

once in fractions 3-5 of Figure 5.12. All four subsequent HIC runs used this elution gradient method in order to decrease endotoxin levels in the final product. Although the endotoxin loads for these HIC runs spanned about 4 orders of magnitude, their elution profiles all showed very similar trends compared to Figure 5.12, though the later-eluting endotoxin peak was typically higher than the endotoxin peak eluting before GFP. The HIC elution profile when loading the AEC eluate from the two improved clarified lysate runs are shown in Figure 5.13 and Figure 5.14 for comparison. Figure 5.13 load material originated from the intermediate-scale lysate that was directly 0.22 μm filtered after generation, and with 98% step HIC step yield (corresponding to pooling fractions 7-15) was able to remove 91% of the loaded endotoxin. Figure 5.14 was from the lowest endotoxin clarified lysate from large-scale, but represents a HIC run that would be comparable to intermediate-scale lysate held for five days prior to 0.22 μm filtration. This HIC run removed 66% of the endotoxin loaded when recovering 98% of the GFP (corresponding to fractions 6-15). These runs showed the more typical elution profile as well as the significantly decreased concentration of endotoxin in the HIC fractions with lower endotoxin load. By decreasing the amount of endotoxin coeluting with GFP, this method has consistently shown improvement compared to the current elution gradient method while maintaining processing time.

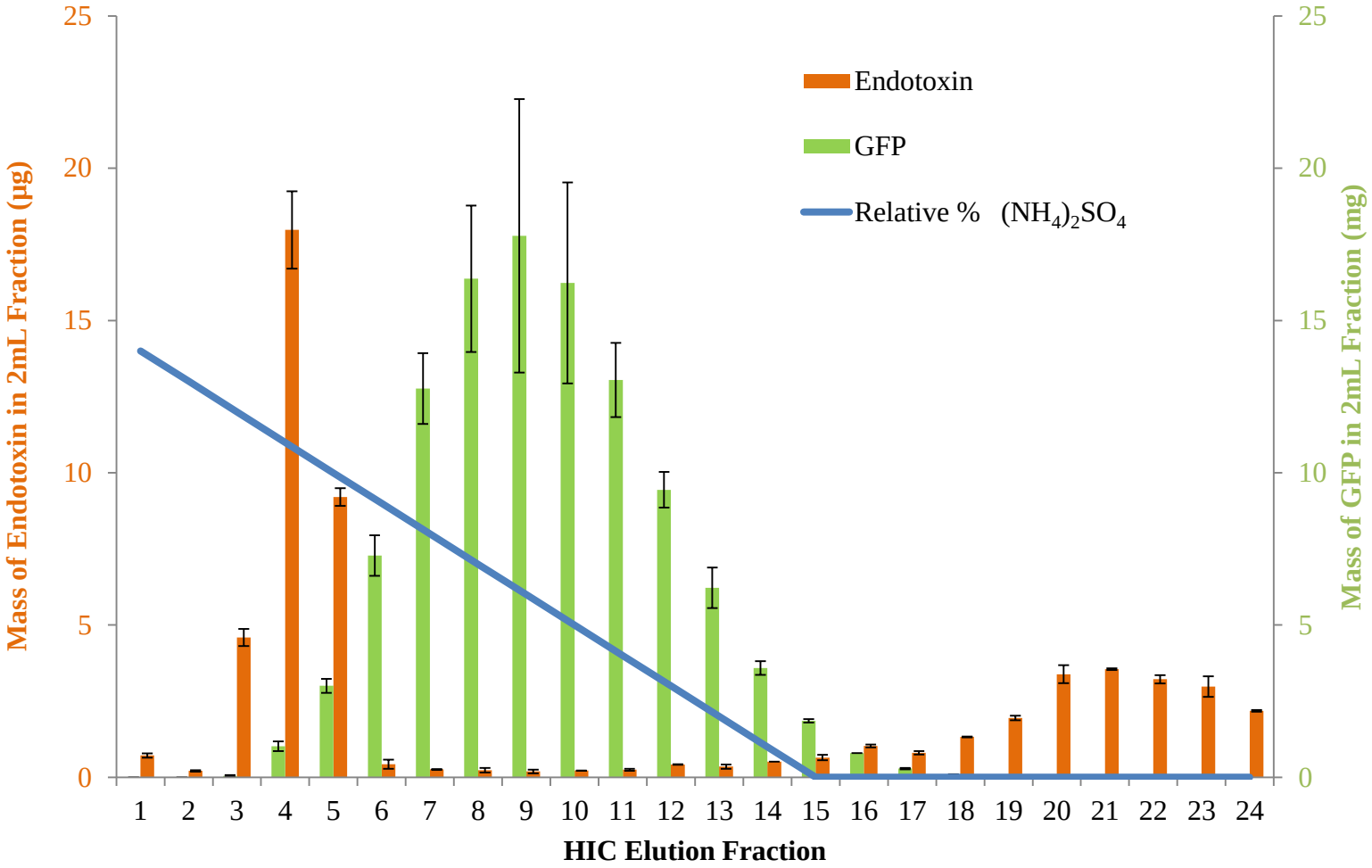

Figure 5.12. Endotoxin and GFP elution profiles with the shallow gradient HIC method for a HIC column loaded with AEC eluate from the current process. Salt concentration ranges from 1 M to 0 M ammonium sulfate. Endotoxin error bars represent ±1 standard deviation of endotoxin concentration detected in triplicate wells for each sample.

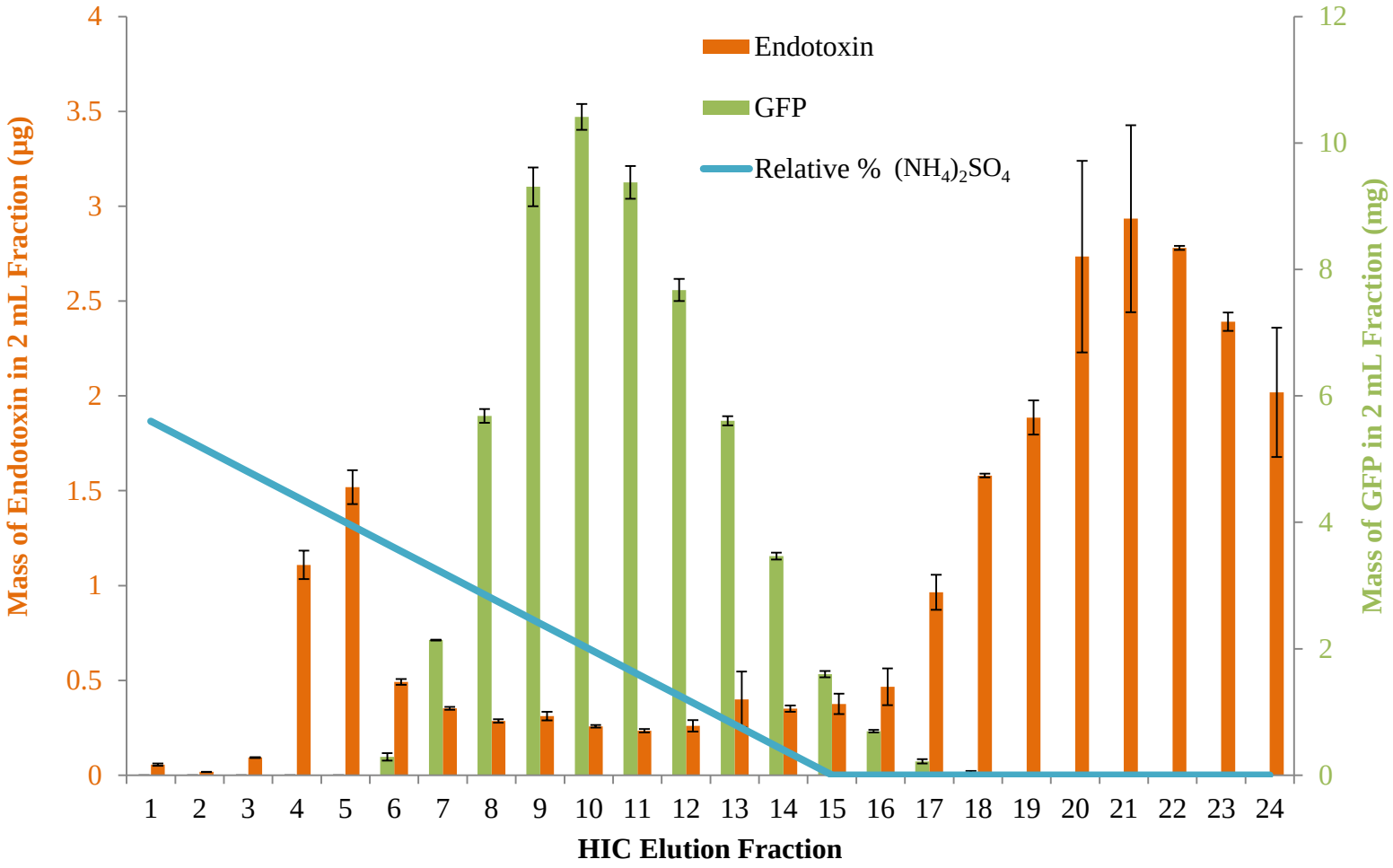

Figure 5.13. Endotoxin and GFP elution profiles with the shallow gradient HIC method for a HIC column loaded with eluate from AEC, which was loaded with directly 0.22 µm filtered intermediate-scale lysate. Salt concentration ranges from 1 M to 0 M ammonium sulfate. Endotoxin error bars represent ±1 standard deviation of endotoxin concentration detected in triplicate wells for each sample.

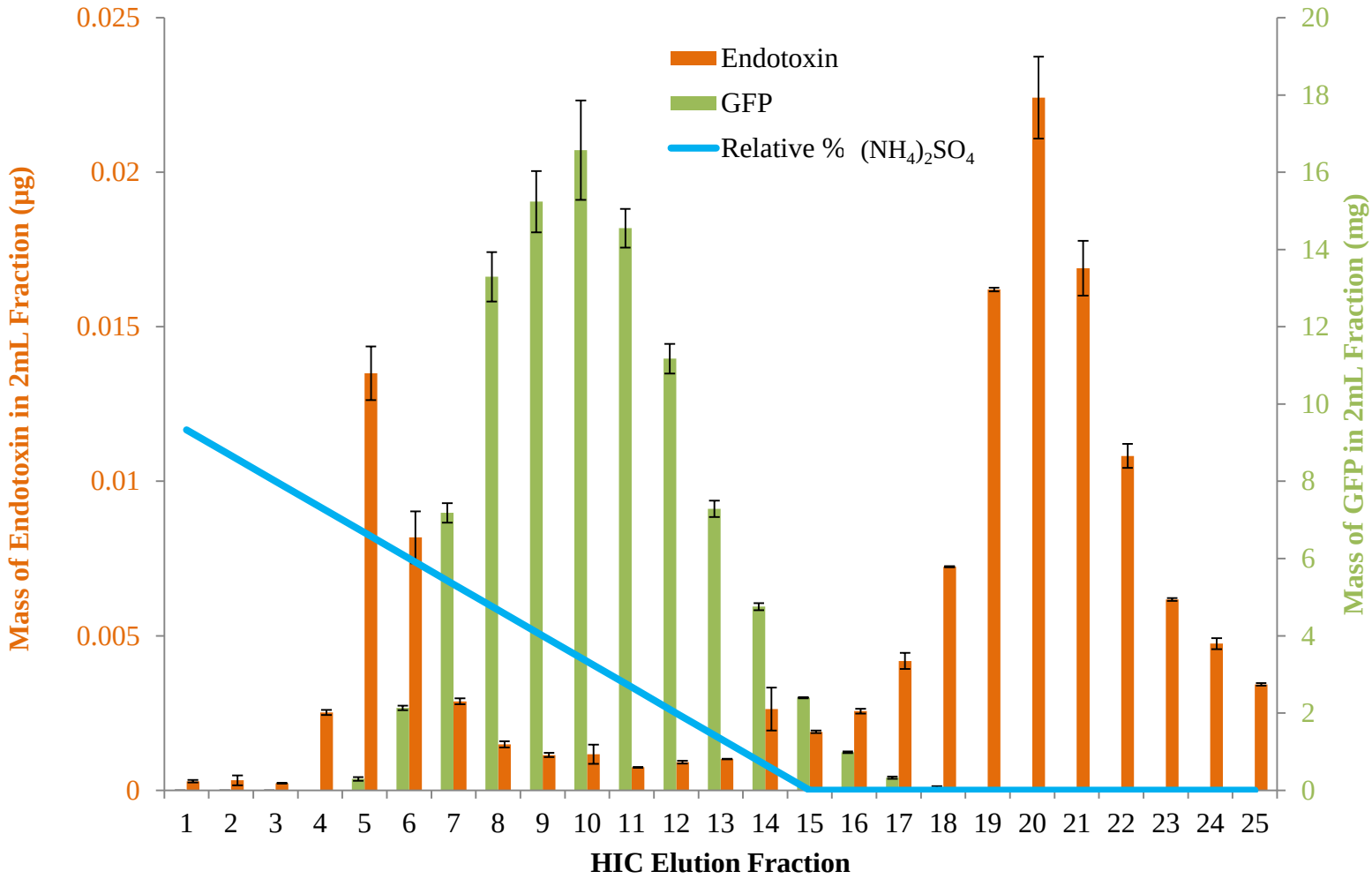

Figure 5.14. Endotoxin and GFP elution profiles with the shallow gradient HIC method for a HIC column loaded with eluate from AEC, which was loaded with low endotoxin large-scale clarified lysate. Salt concentration ranges from 1 M to 0 M ammonium sulfate. Endotoxin error bars represent ±1 standard deviation of endotoxin concentration detected in triplicate wells for each sample.

5.5. Final Product Evaluation

The endotoxin concentration in the final product was determined for the three dosage levels as described in section 4.5 for the current intermediate-scale process with only the HIC shallow gradient method improvement. The EU/kg/dose was graphed versus product recovery from the HIC step as shown in Figure 5.15.

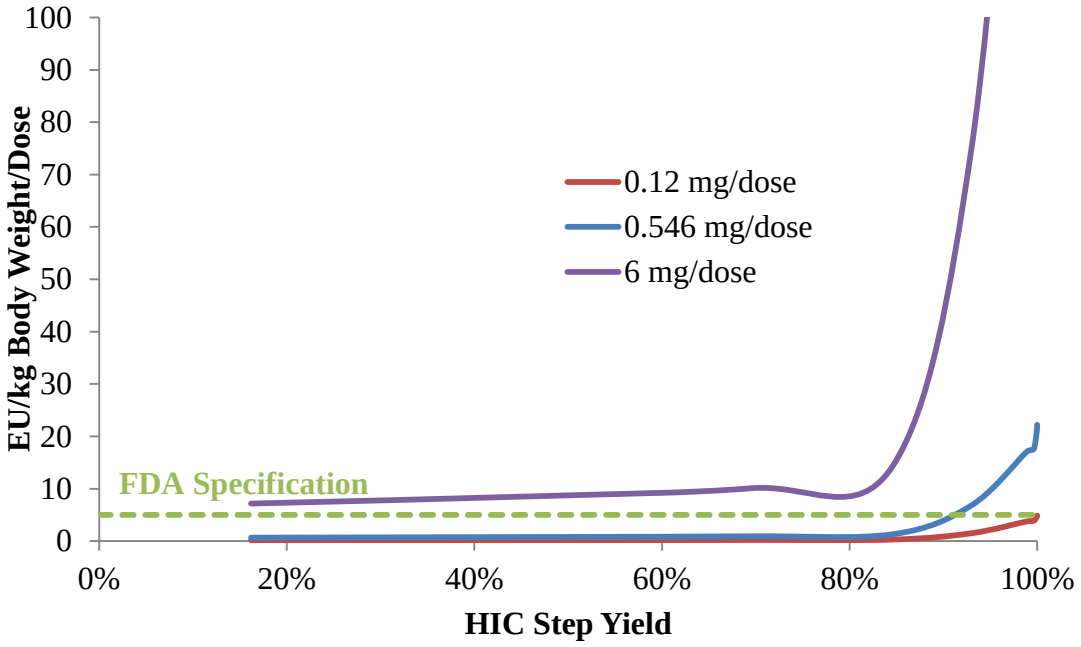

Figure 5.15. Evaluation of endotoxin in final product for current intermediate-scale process AEC eluate with shallow HIC gradient (corresponding to elution profiles in Figure 5.12).

Figure 5.15 shows that by just improving the HIC gradient, the current process was capable of meeting endotoxin specifications for dosages of 0.12 mg and 0.546 mg but was out of specification for the 6 mg/dose. Figure 5.16 and Figure 5.17 show the same graph for the shallow gradient HIC runs performed with eluate from AEC loaded with direct filtered intermediate-scale lysate and low endotoxin large-scale clarified lysate, respectively. The latter is likely comparable to the intermediate-scale process with lysate held for 5 days prior to direct filtration and improved HIC method. It is clear from Figure 5.17 that this process

was capable of producing a final product with significantly less than the FDA specification of 5 EU/kg/dose, even for high dosages of 6 mg product/dose.

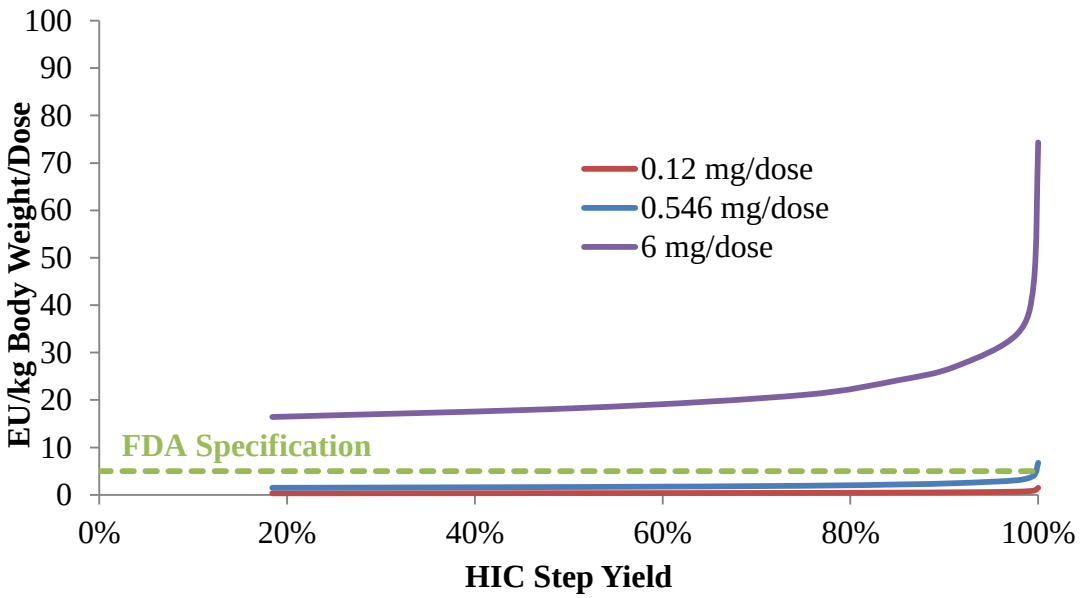

Figure 5.16. Evaluation of endotoxin in final product for direct filtered intermediate-scale lysate loaded onto intermediate-scale AEC followed by shallow HIC gradient (corresponding to profiles in Figure 5.13).

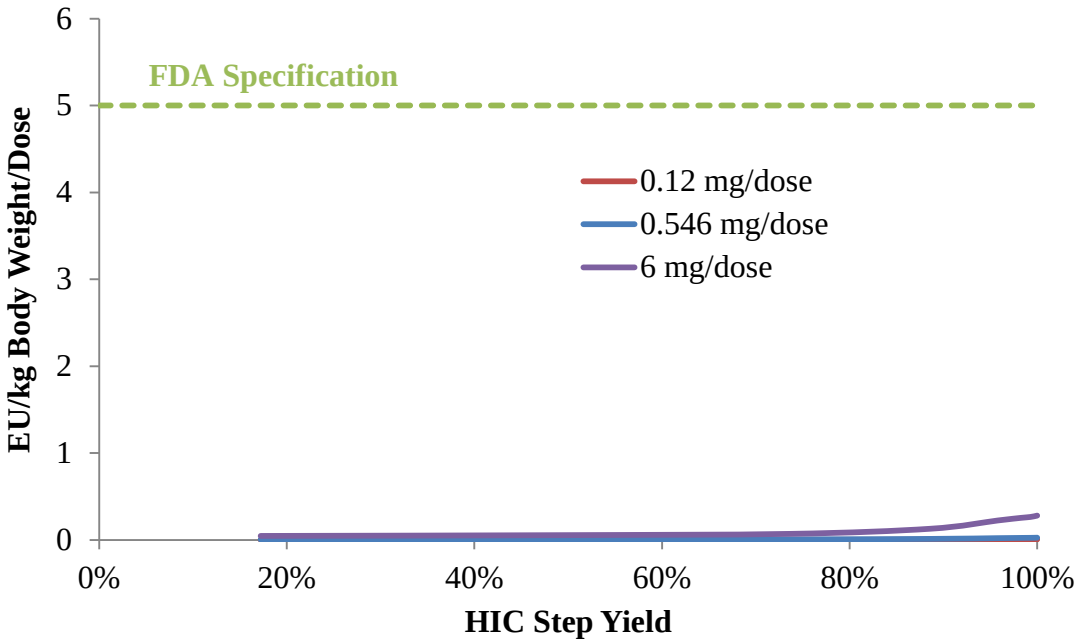

Figure 5.17. Evaluation of endotoxin in final product for large-scale clarified lysate loaded onto intermediate-scale AEC followed by shallow HIC gradient (corresponding to profiles in Figure 5.14).

CHAPTER 6: Conclusions and Future Work

The current GFP downstream process at BTEC does not remove enough endotoxin for a reasonable dose of drug product to consistently meet the FDA required endotoxin specification for parenteral drugs of 5 EU/kg body weight/hour. Homogenization of the *E. coli* cells released almost the same mass of endotoxin as GFP, making it one of the most prevalent impurities in the process. Little endotoxin removal was detected across the current intermediate-scale lysate clarification steps – centrifugation and filtration. Endotoxin removal in AEC was significant but dependent on the amount of endotoxin loaded. At high endotoxin loading, the binding capacity for endotoxin was exceeded. Because endotoxin aggregates are of comparable size to the resin pores, binding capacity of endotoxin on Sepharose beads is low. Over 97% of the endotoxin does not bind to the resin and is therefore separated from the product. Endotoxin decreases from roughly 500 mg loaded to less than 4 mg in all AEC elution fractions, with even less in the GFP-containing fractions that make up the product pool. The current HIC method removed approximately 58% of endotoxin, and the elution profile showed overlapping GFP and endotoxin peaks, presenting an opportunity for improvement. By making the salt elution gradient shallower, the endotoxin and GFP peaks were more resolved and endotoxin removal from final product was increased to as high as 91%.

This work also uncovered differences in endotoxin clearance between large- and intermediate-scale lysate clarification processes. Omission of the centrifugation step that is part of the intermediate-scale process and directly filtering the lysate using a 0.22 μm filter removed 96% of the endotoxin and contained less than one-thirteenth of the endotoxin as the clarified lysate produced with the current clarification process. When 5 L of the lysate was held for five days prior to 0.22 μm filtering, endotoxin removal was further increased to 99.87%, and the clarified lysate contained approximately one-four hundredth of the endotoxin as compared to the current process.

When the clarified lysate with the lowest endotoxin (representative of five day lysate hold prior to 0.22 μm filtration) was processed with HIC using the shallow elution gradient,

the final product easily met the FDA endotoxin specification with dosages up to 100 mg. Although holding lysate may reduce endotoxin, it is not ideal for product quality or processing logistics. Implementing direct filtration without the hold time as well as the shallow HIC gradient, the endotoxin removal in this process would be sufficient to produce drugs with dosages of 1 mg or less.

This work has consistently shown that reduction of endotoxin improves when large particulate are present in the material to be filtered during the lysate clarification steps. More experiments are needed to better understand why this occurs. Once this is well understood, methods to encourage precipitation, flocculation, or aggregation in the lysate prior to filtration could be studied. For example, the addition of divalent cations to encourage endotoxin vesicle formation could be used, though the ionic strength must be carefully considered so as not to interfere with binding of GFP onto the anion exchange resin in the subsequent purification step. This could allow products with higher dosages to meet the FDA endotoxin specification with this process without implementation of a five-day hold time.

Rather than encouraging endotoxin aggregation prior to clarification, methods of encouraging endotoxin disaggregation could be studied for use in the final tangential flow filtration step. In the presence of detergents such as 1% deoxycholate or a solution of 2% sodium cholate and 5 mM EDTA, the structure of endotoxin micelles have been shown to break down such that most of the endotoxin can be recovered in the filtrate of a 10 kDa MWCO membrane.[14] If the added components could be efficiently and sufficiently removed in diafiltration, adding these detergents prior to the final ultrafiltration step could remove the majority of the remaining endotoxin from the final product.

However, when changing the physical properties of the endotoxin, the accuracy of the LAL assay is compromised. Since endotoxin aggregates are the biologically active form, the same mass of endotoxin broken into monomers would likely have much less activity in the assay. In order to explore these methods, thorough correlation of endotoxin aggregate size with assay activity may be required.

If constraints to maintain the current process unit operations were not in place, more options would be available for redesigning the GFP downstream process to improve

endotoxin removal. For example, a cation exchange chromatography (CEC) column could be considered as a replacement for AEC or as a third purification step. If the cells were resuspended in a buffer around pH 5, GFP would be positively-charged and bind to the resin, while endotoxin would remain negatively-charged and not be able to bind. However, many have tried this and noticed that because of the opposite charges as well as other interactions, a significant amount of endotoxin binds to the positively-charged proteins, causing them to be copurified.[45] The interaction between endotoxin and positively-charged proteins has been shown to be disrupted by alkanediols,[8] which could be introduced during the wash phase of CEC in order to further reduce endotoxin levels after the capture step. Experiments with CEC should be performed to determine how the amount of endotoxin that would bind and copurify on a CEC column compares to the amount of endotoxin that coelutes with the GFP in the AEC column in the current process. Although alkanediol washes are more effective with CEC, they have been shown to also reduce endotoxin levels in AEC eluate by up to 70% if the protein is eluted with low pH buffer.[46] This wash method could also be explored as an endotoxin reduction method incorporated into the current AEC process.

REFERENCES

1. Organization, W. H. Requirements for the use of animal cells as in vitro substrates for the production of biologicals. *WHO Tech. Rep. Ser.* **878,** (1998).

2. Research., U. S. D. of H. and H. S. F. and D. A. C. for B. E. and. Points to consider in the manufacture and testing of monoclonal antibody products for human use (1997). U.S. Food and Drug Administration Center for Biologics Evaluation and Research. (1997).

3. Anicetti, V. Purity analysis of protein pharmaceuticals produced by recombinant DNA technology. *Trends Biotechnol.* **7,** 342–349 (1989).

4. Magalhães, P. & Pessoa, A. J. Lipopolysaccharide, LPS Removal, Depyrogenation. *Encyclopedia of Industrial Biotechnology: Bioprocess, Bioseparation, and Cell Technology* (2009).

5. United States Department of Health, Education, and W. P. H. S. F. and D. A. Bacterial Endotoxins/Pyrogens. *FDA Insp. Tech. Guid.* **40,** (1985).

6. Petsch, D. & Anspach, F. B. Endotoxin removal from protein solutions. *J. Biotechnol.* **76,** 97–119 (2000).

7. Ferrer-Miralles, N., Domingo-Espín, J., Corchero, J. L., Vázquez, E. & Villaverde, A. Microbial factories for recombinant pharmaceuticals. *Microb. Cell Fact.* **8,** 17 (2009).

8. Magalhães, P. & Lopes, A. Methods of endotoxin removal from biological preparations: a review. *J. Pharm. Pharm. Sci.* **10,** 388–404 (2007).

9. Chen, R. H. *et al.* Factors affecting endotoxin removal from recombinant therapeutic proteins by anion exchange chromatography. *Protein Expr. Purif.* **64,** 76–81 (2009).

10. Jang, H. *et al.* Effects of protein concentration and detergent on endotoxin reduction by ultrafiltration. *BMB Rep.* **42,** 462–466 (2009).

11. Seydel, U., Labischinski, H., Katowsky, M. & Brandenburg, K. Phase Behavior, Supramolecular Structure, and Molecular Conformation of Lipopolysaccharide. *Immunobiology* **187,** 191–211 (1993).

12. Ongkudon, C. M., Chew, J. H., Liu, B. & Danquah, M. K. Chromatographic Removal of Endotoxins: A Bioprocess Engineer's Perspective. *ISRN Chromatogr.* 1–9 (2012). doi:10.5402/2012/649746

13. Hirayama, C., Ihara, H. & Li, X. Removal of endotoxins using macroporous spherical poly(γ-methyl l-glutamate) beads and their derivatives. *J. Chromatogr. B Biomed. Sci. Appl.* **530,** 148–153 (1990).

14. Sweadner, K. J., Forte, M. & Nelsen, L. L. Filtration removal of endotoxin (pyrogens) in solution in different states of aggregation. *Appl. Environ. Microbiol.* **34,** 382–5 (1977).

15. Ong, K. G. *et al.* A rapid highly-sensitive endotoxin detection system. *Biosens. Bioelectron.* **21,** 2270–4 (2006).

16. Martin, W. J. & Marcus, S. Studies on Bacterial Pyrogenicity, III. Specificity of the United States Pharmacopeia Rabbit Pyrogen Test. *Appl. Microbiol.* **12,** 483–6 (1964).

17. Santos-Oliveira, R. Comparison of Limulus amebocyte lysates with the United States pharmacopeial pyrogen test and the portable test system for radiopharmaceuticals. *J. AOAC Int.* **93,** 1458–61

18. Associates of Cape Cod, I. Limulus Amebocyte Lysate, Pyrochrome Product Insert. (2011).

19. Nakamura, S., Morita, T., Iwanaga, S., Niwa, M. & Takahashi, K. A sensitive substrate for the clotting enzyme in horseshoe crab hemocytes. *J. Biochem.* **81,** 1567–9 (1977).

20. Tsien, R. Y. The green fluorescent protein. *Annu. Rev. Biochem.* **67,** 509–544 (1998).

21. Huss, E. & Moberk, A. Press Release. *Royal Swedish Academy of Sciences* http://www.nobelprize.org/nobel_prizes/chemistry/l (2008).

22. Encyclopedia, W. T. F. Green fluorescent Protein. http://en.wikipedia.org/wiki/Green_fluorescent_pro

23. Ray, M. GFP, UV Media for 300 L Vessel. *MR-013 Revis. 2* (2009).

24. Kostyukovskaya, M. Production of Robust BL21(DE3) with IPTG in 300L Bioreactor. *BTEC Stand. Oper. Proced.* **BR-018,** (2013).

25. Gilleskie, G. Introduction to Downstream Processing: BEC 436/536 Course Pack.

26. Gedeon, A., Massiani, P. & Babonneau, F. *Zeolites and Related Materials: Trends Targets and Challenges(SET)*. (Elsevier, 2008). at <https://books.google.com/books?id=DM8SSGkqxmkC&pgis=1>

27. Healthcare, G. E. Hydrophobic Interaction Chromatography and Reversed Phase Chromatography: Principles and Methods. (2006).

28. Gilleskie, G. Operation and Cleaning of the Alfa Laval LAPX 404 Disc Stack Centrifuge. *BTEC Stand. Oper. Proced.* **BP-006,** (2012).

29. Taylor, J. Operation and Use of the GEA Niro Inc. Homogenizer (HOM-2050). *BTEC Stand. Oper. Proced.* **BP-003,** (2013).

30. Semcer, R. L. Direct Quantification of Green Fluorescent Protein (GFPuv). *BTEC Stand. Oper. Proced.* **AN-003,** (2010).

31. ICH. Validation of analytical Procedures: text and methodology Q2(R1). *Guidance* **1994,** 17 (2005).

32. USP. ⟨ 85 ⟩ Bacterial Endotoxins Test.

33. Mueller, M. *et al.* Aggregates are the biologically active units of endotoxin. *J. Biol. Chem.* **279,** 26307–26313 (2004).

34. Sartorius. Sartobran P MidiCaps: Specifications. http://www.sartorius.com/en/product/product–detail

35. Roslansky, P. F. & Novitsky, T. J. Sensitivity of Limulus amebocyte lysate (LAL) to LAL-reactive glucans. *J. Clin. Microbiol.* **29,** 2477–83 (1991).

36. Associates of Cape Cod, I. *Glucashield: Glucan Inhibiting Buffer*. (2013).

37. Sigma-Aldrich. Product Information: Sepharose Ion Exchange Media. (2012).

38. U.S. Department of Health and Human Services, Centers for Disease Control and Prevention, N. C. for H. S. Anthropometric Reference Data for Children and Adults: United States, 2007-2010. *Vital Heal. Stat.* **11,** (2012).

39. B.V., H. E. Summary of Product Characteristics: Nivestim. http://www.ema.europa.eu/docs/en_GB/document_libra

40. Inc., R. Lantus. http://www.rxlist.com/lantus–drug.htm (2013).

41. Inc., R. Neulasta: Dosage and Administration. http://www.rxlist.com/neulasta–drug/indications–do (2015).

42. Drugs.com. Krystexxa Dosage. http://www.drugs.com/dosage/krystexxa.html (2015).

43. Dudás, F. Ö. Analytical Techniques for Studying Environmental and Geologic Samples: Ion Exchange Chromatography. *MIT OpenCourseWare* (2011).

44. Joshi, V., Kumar, V., Rathore, A. & Krull, I. The Role of Elution Gradient Shape in the Separation of Protein Therapeutics. *LCGC North Am.* **32,** 736–741 (2014).

45. Petsch, D., Rantze, E. & Anspach, F. B. Selective adsorption of endotoxin inside a polycationic network of flat-sheet microfiltration membranes. *J. Mol. Recognit.* **11,** 222–30 (1998).

46. Lin, M.-F., Williams, C., Murray, M. V & Ropp, P. A. Removal of lipopolysaccharides from protein-lipopolysaccharide complexes by nonflammable solvents. *J. Chromatogr. B. Analyt. Technol. Biomed. Life Sci.* **816,** 167–74 (2005).

APPENDIX

Appendix A- *Standard Operating Procedure for Chromogenic Kinetic Pyrochrome Assay*

1. PURPOSE

1.1. This method is used for the detection and quantification of bacterial endotoxin, which elicit a strong response from the human immune system resulting in severe illness or endotoxic shock.

2. SCOPE

2.1. This assay is performed on water samples, buffers, and samples from BTEC's green fluorescent protein downstream process.

3. PRINCIPLE

3.1. This assay utilizes a cell lysate from the horseshoe crab (*Limulus polyphemus*), which contains a pathway of enzymes that are activated in the presence of low levels of endotoxin. The reagent also contains a synthetic peptide ((α-N-benzoyl)-Ile-Glu-Gly-Arg-) that is bound to p-nitroanilide (PNA), which is cleaved upon activation of the enzymatic pathway. The peptide-PNA molecule is colorless, but after cleavage with the peptide, PNA alone is yellow, allowing the extent of the reaction to be measured using the absorbance at 405 nm.

3.2. The time required to reach a certain absorbance is calculated for known endotoxin concentration standards and used to construct a standard curve to quantify endotoxin in unknown samples.

4. DEFINITIONS

4.1. Endotoxin / lipopolysaccharide (LPS) – an integral part of the outer cell membrane of Gram-negative bacteria. Endotoxin consists of a lipid component, Lipid A, a core region, and a long oligosaccharide chain. Lipid A is the most conserved part of endotoxin and is responsible for most of the biological activities of endotoxin.

4.2. *Limulus* Amebocyte Lysate – an aqueous extract of horseshoe blood, which contains enzymes that are activated in the presence of endotoxin.

5. REFERENCES

5.1. Associates of Cape Cod, I. Limulus Amebocyte Lysate, Pyrochrome Product Insert. (2011).

5.2. Nakamura, S., Morita, T., Iwanaga, S., Niwa, M. & Takahashi, K. A sensitive substrate for the clotting enzyme in horseshoe crab hemocytes. *J. Biochem.* **81,** 1567–9 (1977).

5.3. USP 34, Chapter 85, Bacterial Endotoxins Test (2011).
5.4. BTEC SOP AN-020. Endotoxin Testing Using the LAL Gel Clot Method Limit Test in Accordance with USP 34 Chapter 85.

6. SAFETY

6.1. Wear area-specific personal protective equipment (refer to GL-002: Gowning Requirements for the BTEC Facility).

7. EQUIPMENT & MATERIALS

7.1. Solutions/Reagents
- 7.1.1. Sample(s) to be tested
- 7.1.2. LAL Reagent Water (LRW); Associates of Cape Cod P/N W020P, stored at room temperature
- 7.1.3. Control Standard Endotoxin (CSE); Associates of Cape Cod P/N EC010, stored at 2 – 8 °C
- 7.1.4. Pyrochrome® LAL Reagent; Associates of Cape Cod P/N CG1500, stored at 2 – 8 °C
- 7.1.5. Glucashield® Buffer; Associates of Cape Cod comes with Pyrochrome Reagent, stored at 2 – 8 °C

7.2. Lab Equipment
- 7.2.1. Pyroplate® depyrogenated and glucan-free 96-well microplate, Associates of Cape Cod P/N CA961
- 7.2.2. BioTek Instruments Synergy4 plate reader
- 7.2.3. Pipettes and tips, including 50 µL multi-channel pipette
- 7.2.4. Reagent reservoir
- 7.2.5. 1.5 mL Eppendorf tubes
- 7.2.6. Parafilm
- 7.2.7. Vortex mixer

8. PROCEDURE

8.1. Set up the plate reader.
- 8.1.1.1. Turn on the plate reader and corresponding laptop. When the equipment is finished with its initiation sequence, close the plate drawer.
- 8.1.1.2. Click on Gen5 1.10 icon located on the computer desktop.
- 8.1.1.3. Under Create a New Item, select Experiment.
- 8.1.1.4. For the protocol, select PyrochromeLAL2pathlength.prt located in C:\Program Files (x86)\Bio Tek\Gen 5 1.10\Protocols
- 8.1.1.5. Select the icon on the far right of the toolbar that shows the temperature.

8.1.1.6. In the window that pops up, click the "Pre-Heating" tab, ensure the requested temperature reads 37°C, and click the check box next to "On" and click on the "Close" button.

8.2. Control Standard Endotoxin (CSE) Preparation

8.2.1. Remove a vial of CSE from refrigeration and allow it to come to room temperature. Record the lot number used.

8.2.2. Gently tap the bottom of the vial on the countertop to collect all of the endotoxin powder away from the stopper cap.

8.2.3. Remove the crimp seal from the vial and remove the stopper.

8.2.4. Reconstitute the CSE with LRW to a concentration of 100 EU/ml in accordance with the certificate of analysis provided with the CSE.

Note: The certificate of analysis typically states that dilution of the CSE with 2 ml of LRW yields a concentration of 100 EU/ml, so reconstitute to that concentration and vortex 30-60 seconds.

8.2.4.1. Label the vial with the reconstitution date and concentration.

Note: The reconstituted CSE has not been validated to be stable for use in this assay on days other than the day it was reconstituted. A fresh vial should be reconstituted for each day of testing.

8.2.5. Dilute the CSE further to create a standard curve. Vortex each solution for 10-20 seconds prior to use. A suggested dilution scheme is tabulated in Table 1.

Table 1. Suggested CSE Dilution Scheme

Standard	Endotoxin	Water	Concentration
Vial	10 ng in CSE vial	2 mL LRW	100 EU/mL
A	500 µL vial	500 µL LRW	50 EU/mL
B	100 µL Standard A	900 µL LRW	5 EU/mL
C	100 µL Standard B	900 µL LRW	0.5 EU/mL
D	100 µL Standard C	900 µL LRW	0.05 EU/mL

8.3. Negative Control Preparation

8.3.1. The negative control is LRW.

8.4. Sample Preparation

8.4.1. Samples must typically be diluted with LRW in order to fall within the standard curve and/or to avoid matrix effects from high salt or GFP concentrations. The amount of dilution is highly dependent on the sample. 100-fold serial dilutions are recommended (990 µL LRW with 10 µL sample).

8.4.1.1. For intermediate-scale process samples of reconstituted cell paste, lysate, clarified lysate, of anion exchange load flowthrough a dilution of 1:1,000,000 is recommended. For all other anion exchange samples and samples collected downstream of this in the intermediate-scale process, a dilution of 1:10,000 is recommended.

Note: Clarified lysate from the large-scale process and all samples downstream may contain significantly less endotoxin. If an approximate endotoxin concentration is unknown, 2-3 dilutions of the same sample may be tested in order to avoid retesting on a new plate.

8.4.1.2. Vortex each sample or dilution for 10-20 seconds prior to use.

Note: If the plate setup in Figure 1 is used, only 12 samples can be tested per plate.

8.5. Reagent Preparation

8.5.1. Calculate the required volume of reagent required for testing of all samples according to the following equation:

$V_{reagent}$=0.05 mL * 3 *(# of samples + # of standards + 1)

Note: For the dilution scheme in Table 1, # of standards is 5. The one extra is for the negative control.

8.5.1.1. Determine the number of Pyrochrome vials required for testing all samples. If the reagent volume is less than 3 mL, only one vial is required.

Note: When testing only 12 samples and the standard curve, one vial is sufficient.

8.5.2. For each vial of Pyrochrome® LAL reagent needed, a vial of Glucashield® Buffer is also required. Remove required reagents from refrigeration and allow them to come to room temperature. Record the lot number(s) used.

8.5.3. Tap the LAL vial to ensure that the LAL powder is collected at the bottom of the vial.

8.5.4. Remove the aluminum caps covering both vials and discard.

8.5.5. Dispense 3.2 ml of Glucashield® Buffer into the LAL vial and gently swirl the vial until all of the powder is dissolved. Cover with Parafilm.

8.5.6. Label the vial with the reconstitution date and preparer's initials.

8.5.7. Place vial in 2 – 8°C refrigerator and wait at least 5 minutes to allow the reagent to fully dissolve.

8.6. Sample Preparation and Assay Setup

8.6.1. Add 50 µL of each sample, standard, and negative control in triplicate wells on the Pyroplate. A suggested plate setup for use with the analysis template is shown in Figure 1.

	1	2	3	4	5	6	7	8	9	10	11	12
A												
B		Sample 1			Sample 2			Sample 3			Sample 13	
C		Sample 4			Sample 5			Sample 6				
D		Sample 7			Sample 8			Sample 9				
E		Sample 10			Sample 11			Sample 12			Sample 14	
F		Negative Control			0.05 EU/mL			0.5 EU/mL				
G		5 EU/mL			50 EU/mL			100 EU/mL				
H												

Figure 1. Suggested plate setup. Green boxes represent sample wells, red boxes represent standard wells, and white boxes represent wells containing no liquid.

Note: Placement of samples in the outside wells of the plate is not recommended as the long incubation time of the assay causes excess evaporation in these wells, which increases assay variability.

Note: Four additional samples could be tested in wells B11-D11, E11-G11, B12-D12, and E12-G12. However, care must be taken in step 8.6.3 that triplicate wells of each of these samples are mixed with the reagent simultaneously in order to avoid increasing assay variability.

Note: Anticipated samples with higher endotoxin concentration should be placed toward the bottom of the plate as these will likely react faster and should be mixed with the reagent closer to the time that data collection begins.

8.6.2. Prepare plate reader

8.6.2.1. Ensure the temperature has reached 37°C.

8.6.2.2. Select the Read Plate icon in the toolbar.

8.6.2.3. Enter a plate ID and in the comments section enter any details you wish to include. Then click "Read."

8.6.2.4. Browse for the computer location that you want your data saved in and enter a file name that includes the date and your initials. **Do not press save at this point.**

8.6.3. Dispense the LAL reagent.

8.6.3.1. Pour the reconstituted Pyrochrome® reagent into the reagent reservoir.

8.6.3.2. Quickly dispense 50 µL of reagent into each well using a multi-channel pipette such that triplicate wells of the same sample are mixed with the reagent simultaneously. Aspirate and dispense the well contents 2-3 times to mix. Take care to

only dispense to the first stop on the pipette so as not to introduce bubbles, which will interfere with absorbance readings. Use a new set of pipette tips for mixing reagent with each set of samples.

Note: For the plate setup in Figure 1, a 12-channel pipette should be used to mix all 9 wells in Row B followed by Row C, etc.

8.6.4. As soon as all of the reagent has been dispensed, quickly open the plate reader drawer, put the plate in, and click the "Save" button on the software to start the experiment.

8.6.5. The plate reader first shakes the plate for 15 seconds to ensure proper mixing. Following a pathlength reading for each well, the absorbance at 405 nm in each well is measured every minute for 75 minutes. A final pathlength is measured before the plate reader ejects the plate.

8.6.6. Remove the plate and discard when done.

8.6.7. Close the plate drawer and turn off plate reader.

9. RESULTS

9.1. Export results to excel

9.1.1. In the "Data:" dropdown menu of the plate results window, select "Read 1:Pathlength."

9.1.2. Click the excel export icon next to the dropdown menu. An excel spreadsheet will automatically be created with the data from the first pathlength reading.

9.1.3. Select "Read 3:Pathlength" and click the excel export. The data will automatically be added to the first excel sheet below the first set of data.

9.1.4. Select "OnsetOD 0.15: Onset Time [Read 2:405]" and click the excel export icon. The data will automatically be added to the same excel sheet below the second set of data.

9.1.5. Save the excel spreadsheet with a name including the date and your initials.

9.2. Copy results into template

9.2.1. Open the file "Chromogenic Kinetic Endotoxin Assay Analysis Template" located in C:\Users\264 Lab\Desktop\Report Forms.

9.2.2. Select "File" and "Save As" to save the file in another location under a different name containing the date and your initials.

9.2.3. Copy the values in the Read 1:Pathlength table from the raw data file. Click cell B5 in the analysis template and paste the copied values.

9.2.4. Copy the values in the Read 3:Pathlength table from the raw data file. Click cell B15 in the analysis template and paste the copied values.

9.2.5. Copy the values in the OnsetOD 0.15: Onset Time [Read 2:405] table

from the raw data file. Click cell R15 in the analysis template and paste the copied values.

9.2.6. Rename the samples in the plate setup that begins in cell R5 and type in dilution factors used for each sample into column AV.

9.3. Analysis

9.3.1. Ensure that the onset times for all three negative control wells (cells S-U20) are greater than 75 minutes.

9.3.2. Ensure that the coefficient of variation for each standard (cells T61-65) is less than 10% and that of each sample (cells AT4-17) is less than 20%. If variation is high for one standard or sample, check if one onset time is significantly different from the other two. Attempt to determine a source of variability and evaluate if the outlier could be removed.

9.3.3. Ensure that the standard curve appears linear and the correlation coefficient, r, (cell AM2) is greater than 0.98.

9.3.4. Ensure that all sample onset times fall within the standard curve range. Cells containing onset times outside the standard curve range will be highlighted in red in column AI. Data from samples that fall outside of this range cannot be used, and an alternative dilution will need to be tested.

9.3.5. If the above conditions are met, the average and standard deviation of endotoxin concentration for each sample can be reported.